THE UNIVERSITY OF CALGARY

Chloride Movement During Calcium Uptake into the Sarcoplasmic Reticulum of Cardiac and Smooth Muscle

by

Natashka S. Pollock

A THESIS

SUBMITTED TO THE FACULTY OF GRADUATE STUDIES

IN PARTIAL FULFILMENT OF THE REQUIREMENT FOR THE

DEGREE OF MASTER OF SCIENCE

DEPARTMENT OF CARDIOVASCULAR/RESPIRATORY SCIENCES

CALGARY, ALBERTA

JUNE, 1997

THE UNIVERSITY OF CALGARY

FACULTY OF GRADUATE STUDIES

The undersigned certify that they have read, and recommend to the Faculty of Graduate Studies for acceptance, a thesis entitled "Chloride Movement During Calcium Uptake into the Sarcoplasmic Reticulum of Cardiac and Smooth Muscle" submitted by Natashka S. Pollock in partial fulfilment of the requirements for the degree of Master of Science.

Supervisor, Dr. Gary J. Kargacin
Department of Cardiovascular/Respiratory Sciences

Dr. Rodger Loutzenhiser
Department of Cardiovascular/Respiratory Sciences

Dr. Michael P. Walsh
Department of Biochemistry and Molecular Biology

Dr. Wayne Giles
Department of Cardiovascular/Respiratory Sciences

Dr. David Severson
Department of Medical Science

9/23/97
Date

ABSTRACT

In muscle, contraction is triggered by a rapid increase of Ca^{2+} in the cytoplasm. Relaxation occurs when intracellular Ca^{2+} is resequestered into the sarcoplasmic reticulum (SR). Since the SR does not sustain a membrane potential, counter-ion movement must occur during Ca^{2+} uptake to alleviate the charge buildup. To examine the role of Cl^- as a co-ion, SR Ca^{2+} uptake was examined in the presence of Cl^- channel blockers (NPPB and (R)-IAA-94) and other anions in isolated, saponin-permeabilized smooth muscle cells (SMCs) and cardiac SR vesicles.

In SMCs, NPPB and (R)-IAA-94 decreased Ca^{2+} uptake but uptake was unaltered when I^-, Br^-, or methanesulphonate were substituted for Cl^-. In cardiac SR, NPPB and (R)-IAA-94 had no significant effect on Ca^{2+} uptake although uptake was reduced by I^-. We conclude that Cl^- conductance influences the rate of Ca^{2+} uptake in both muscle types, but operates differently in the two.

ACKNOWLEDGEMENTS

I was extremely fortunate to work with a wonderful group of people over the past three years. I want to specifically thank Dr. Gary Kargacin for giving me the opportunity to work in his lab and for always being available to help me. A sincere thank-you to my office-mate Dr. Meg Kargacin, who assisted in all aspects of my work and did everything with a great sense of humour. A special thanks to Erwin Wirch for performing the SDS-PAGE and Western blotting experiments and to Kathy Loutzenhiser for developing the protocol for isolation of the rabbit stomach cells. I also wish to acknowledge Gisele and Zenobia who created an enjoyable lab atmosphere.

I especially wish to thank Dr. R. Loutzenhiser for his guidance and encouragement as well as his involvement as a committee member. Thanks to Dr. Walsh, Dr. D. Severson and Dr. W. Giles who comprised my examining committee. I am also grateful to Dr. W. Cole for his support and for critical reading of my manuscript.

Aside from the learning experiences in graduate school, I also looked forward to participating in weekly "TG" meetings, and the activities with everyone in the MSGSA. I especially want to acknowledge Sarah Warden, Mirna Nahas and Martina Reslerova for their support and friendship. I was also fortunate to be a part of a collaborative and fun research group who expanded my horizons in many ways. Thanks, SMRGies!

Of course, I wish to thank my family for being supportive and interested in my progress. I love you Mom, Sonie, and Aaron. I also wish to thank Curtis whose patience and understanding has been a source of strength and stability throughout the program.

The financial support of Medical Research Council is gratefully acknowledged.

for Dad

with love and remembrance

TABLE OF CONTENTS

LIST OF FIGURES

LIST OF TABLES

ABBREVIATIONS

ACA - anthracene-9-carboxylic acid

ADP - adenosine 5'-diphosphate

ATP - adenosine 5'-triphosphate

ATPase - degrades ATP to ADP

BCl - Big chloride channel

$Ca_{50\%}$ - $[Ca^{2+}]$ at 50% V_{max} (see below)

cAMP - cyclic adenosine 3'-5'-monophosphate

CP - creatine phosphate

CPK - creatinine phosphokinase

cps - counts per second

DAC - diphenylamine-2-carboxylate

DAG - diacylglycerol

DCCD - dicyclohexylcarbodiimide

DIDS - 4,4'-diisothiocyanatostilbene-2,2'-disulfonic acid

DNase - enzyme which degrades DNA

DNDS - 4,4'-dinitrostilbene-2,2'-disulfonic acid

DTT - dithiothreitol

EGTA - ethylene glycol bis(β-aminoethylether)-N,N,N'N'-tetraacetic acid

FCCP - carbonyl cyanide p-trifluoromethoxyphenylhydrazone

GMP - guanosine 5'-monophospate

GTP - guanosine 5'-triphosphate

HBSS - Hank's balanced salt solution

HEPES - 4-(2-hydroxyethyl)piperazine-1-ethanesulfonic acid

IC_{50} - 50% inhibitory concentration

IP_3 - inositol-1,4,5-trisphosphate

K_d - dissociation constant

kDa - kiloDalton

K_i - inhibitory constant

MeS - methanesulfonate

*n*H - Hill coefficient

NPPB - nitrophenylpropylamine benzoate

O.D. - optical density

P_i - inorganic phosphate

PIP_2 - phosphatidylinositol 4,5- bisphosphate

PIPES - piperazine-N,N'-bis (2-ethanesulfonic acid)

PKA - protein kinase A

PKI - protein kinase inhibitor

PL - phospholamban

PMCA - plasma membrane Ca^{2+}-ATPase

PMT - photomultiplier tube

POD - peroxidase-conjugated

P_x - permeability of ion "x"

(R)-IAA-94 - indanyloxyacetic acid

SCl - small chloride channel

SD - standard deviation

SDS-PAGE - sodium dodecylsulfate polyacrylamide gel electrophoresis

SERCA - sarco/endoplasmic reticulum Ca^{2+}-ATPase

SITS - 4-acetoamido-4'-isothiocyanostilbene-2-2'-disulfonic acid

SPQ - 6-methoxy-N-(3-sulfopropyl) quinolinium

SR - sarcoplasmic reticulum

TBS - Tris-HCl buffered saline

TppMnIII - tetraphenyl-21H, 23H-porphinemanganese (III) chloride

V_p - potential difference established by Ca^{2+} pump

VDAC - voltage-dependent anion channel

V_{max} - maximal velocity of Ca^{2+} uptake

INTRODUCTION

Smooth muscle cell morphology

Smooth muscle cells are morphologically distinct from both skeletal and cardiac muscle cells. They are elongated, vermiform cells with tapered ends and no visible striations (Gabella, 1983). The plasma membranes of smooth muscle cells possess inpocketings, or caveolae, which are also present in skeletal and cardiac muscle as well as endothelial cells (Gabella, 1983). Smooth muscle cells do not possess a transverse tubule network (as is present in cardiac and skeletal muscle cells) to bring plasma membranes into closer proximity with central SR membranes. However, smooth muscle cells have a large surface area to volume ratio, which allows Ca^{2+} to quickly diffuse into central regions of the cell. It has been proposed that in smooth muscle, peripheral SR interacts with the plasma membrane, possibly forming surface couplings similar to those found in cardiac muscle (Devine et al., 1972; Somlyo and Franzini-Armstrong, 1985). Cole and Garfield (1989) suggested that a large proportion of the SR in uterine smooth muscle may lie just beneath the plasma membrane. In 1972, Devine et al. determined that the distance between the apposing membranes may be as little as 8-12 nm. However, it has been established that the SR membrane is not continuous with the sarcolemma (Kowarski et al., 1985; Somlyo and Franzini-Armstrong, 1985). Kowarski et al. (1985) provided evidence for this by using electron probe X-ray microanalysis of

tissue cryosections to show that Na^+ and Cl^- concentrations were different between the SR and the extracellular fluid. Na^+ and Cl^- concentrations were the same in the SR and cytoplasm.

It appears that the close proximity of the superficial SR and the plasma membrane may have a functional role in Ca^{2+} homeostasis. Moore et al. (1993) showed that the Na^+/K^+ ATPase and the Na^+/Ca^{2+} exchanger co-localize in the caveolar region of the plasma membrane which is closely associated with the superficial SR. They utilized techniques of immunolabelling and digital imaging to localize the proteins and corresponding structures. They found that the co-localization of the labels for the Na^+/Ca^{2+} exchanger, the Na^+/K^+ ATPase and the SR (identified with an anti-calsequestrin antibody) was statistically greater than would be expected by chance ($p < 0.002$). This spatial organization suggests an interdependence between SR Ca^{2+} loading and the activity of the Na^+/Ca^{2+} exchanger. In theory, the activity of the Na^+/Ca^{2+} exchanger would accelerate upon increased Ca^{2+} release from the proximal SR. Moore et al. (1993) further proposed that these sarcolemmal transporters contribute to a high Ca^{2+} gradient between the plasma membrane and the SR, which could explain the physiological relevance of a Na^+/Ca^{2+} exchanger with a low reported Ca^{2+} affinity (Fay et al., 1992). Sturek et al., (1992) described an SR buffer-barrier in smooth muscle which divides the myoplasm into two major regions: a subsarcolemmal region and the bulk myoplasm. This SR buffer-barrier prevents Ca^{2+} from penetrating the central cytoplasm and activating contraction (Chen and van Breeman, 1992). According to the theory of Sturek et al. (1992), the level of Ca^{2+} loading in the SR also has an impact on

the $[Ca^{2+}]_{free}$ of the central myoplasm. When the SR is depleted of Ca^{2+}, it has a greater buffering capacity and therefore slows the increase in average myoplasmic $[Ca^{2+}]_{free}$ after Ca^{2+} influx (Sturek et al., 1992). Conversely, when the SR is incapable of resequestering Ca^{2+} (ie. after caffeine or ryanodine application), the rate at which myoplasmic $[Ca^{2+}]_{free}$ rises is accelerated (Sturek et al., 1992).

The SR of both cardiac and smooth muscle cells contain the Ca^{2+}-binding proteins calreticulin and calsequestrin. The purpose of these proteins is to reduce the Ca^{2+} gradient against which the Ca^{2+}-ATPase is pumping, and to prevent precipitation of Ca^{2+} salts within the SR (Tharin et al., 1992). Calreticulin is a low-capacity binding protein when compared to calsequestrin, which binds 40-50 mol Ca^{2+}/mol protein (MacLennan et al., 1983). Calreticulin binds 1 mol Ca^{2+}/mol with high affinity (K_d = 10 μM; Baksh and Michalak, 1991) and 18 mol Ca^{2+}/mol with low affinity (K_d = 2 mM; Baksh and Michalak, 1991). Calreticulin is the principal SR Ca^{2+}-binding protein in non-muscle and smooth muscle cells (Milner et al., 1991), and is a component of Ca^{2+}-binding proteins in cardiac and skeletal muscle (Tharin et al., 1992).

Calsequestrin was initially identified within smooth muscle SR as granular strands in deep-etched rotary shadow preparations labelled with tannic acid (Somlyo and Franzini-Armstrong, 1985). When present, smooth muscle calsequestrin closely resembles the cardiac form of calsequestrin, but is distinct from the fast-skeletal muscle isoform (Wuytack et al., 1987). Conformational changes of calsequestrin have been described (Cala and Jones, 1983), and have provided a means to differentiate between the skeletal and cardiac muscle forms of calsequestrin (Wuytack et al., 1987). In an

alkaline environment, skeletal and cardiac forms of calsequestrin separate electrophoretically into molecular weights of 63 000 (skeletal) and 55 000 (cardiac). In porcine uterine smooth muscle, calreticulin acts as the major Ca^{2+}-binding protein (Milner et al., 1991). Using the techniques of immunoblotting, $^{45}Ca^{2+}$ overlay and Stains-All staining (which are commonly used in the detection of calsequestrin), calsequestrin could not be identified in porcine uterine smooth muscle (Milner et al., 1991). However, small quantities were detected using a Mono Q FPLC column. Milner et al. (1991) concluded that calsequestrin is expressed in small amounts in porcine uterine smooth muscle, compared to cardiac and skeletal muscle tissues.

Ca^{2+} uptake in the sarcoplasmic reticulum

The sarcoplasmic reticulum (SR) is an intracellular organelle involved in the regulation of the cytosolic Ca^{2+} concentration in cardiac, skeletal and smooth muscle cells. Upon stimulation, much of the Ca^{2+} required for muscle contraction is released from the SR; this Ca^{2+} then diffuses into the proximity of the contractile apparatus. For relaxation to ensue, intracellular [Ca^{2+}] must be decreased. Ca^{2+} is either resequestered into the SR against a concentration gradient by an SR Ca^{2+} pump or extruded out of the cell by sarcolemmal Ca^{2+} pumps and Na^{+}/Ca^{2+} exchangers (Carafoli, 1987).

The SERCA pumps (sarcoplasmic or endoplasmic reticulum Ca^{2+}-ATPase family), which are exclusive to SR/ER membranes, have been cloned and are the products of three genes. The SERCA1 Ca^{2+} pump is present only in fast-twitch skeletal muscle (Lytton et al., 1992), whereas the SERCA3 pump protein can be found in cardiac,

smooth muscle and non-muscle tissue (Burk et al., 1989). There are two SERCA2 Ca^{2+}-ATPase isoforms which are products of alternative splicing of the same gene (Khan et al., 1990). The SERCA2a isoform is primarily found in cardiac muscle, but has been identified in smooth muscle as well. In pig stomach smooth muscle cells, approximately 70-80% of Ca^{2+} pump activity is due to the SERCA2b isoform (Eggermont et al., 1990). SERCA2b is the predominant isoform of smooth and non-muscle, but is not commonly expressed in cardiac muscle (Raemaekers and Wuytack, 1996). Khan et al. (1990) found that rabbit heart possessed transcripts for the smooth muscle isoform of the Ca^{2+} pump. However, they acknowledge the heterogeneity of muscle as a potential problem in determining the type(s) of mRNA present in a given tissue and suggest that cardiac nerves or blood vessels could account for the presence of the smooth muscle Ca^{2+} pump isoform in the rabbit heart preparation (Khan et al., 1990).

Burk et al. (1989) noted that the distribution of SERCA2b has a lower degree of tissue specificity compared with the SERCA3 and SERCA2a Ca^{2+}-pump isoforms. Lytton et al. (1988) did not detect any SERCA2a transcripts in rabbit myometrium and Khan et al. (1990) found that rabbit stomach smooth muscle did not contain any SERCA2a mRNA. This conflicts with the data of Gunteski-Hamblin et al. (1988), who found both the cardiac and smooth muscle isoforms present in whole stomach from rabbit.

The SERCA2b isoform differs from its splice variant by a stretch of 49 amino acids which replace the last four C-terminal amino acids of the SERCA2a product (Verboomen et al., 1994). The additional amino acids are largely hydrophobic and could

form an extra transmembrane domain, which would result in the C-terminus of SERCA2b residing on the opposite side of the SR membrane than the C-terminus of SERCA2a (Campbell et al., 1992). The SERCA2b pump isoform demonstrates a twofold higher Ca^{2+} affinity (Verboomen et al., 1992; Verboomen et al., 1994), a twofold lower Ca^{2+} uptake rate (Verboomen et al., 1994) and a lower ATP hydrolysis rate (Lytton et al., 1992) compared with the SERCA2a isoform. Verboomen et al. (1994) determined that these differences are due to the additional expanse of amino acids. They created SERCA2b mutants which lacked 12, 31 or 49 amino acids in the C-terminus, and found that all mutants acquired characteristics resembling those of the SERCA2a proteins (Verboomen et al., 1994).

The amount of pump protein also differs between cardiac and smooth muscle. Ca^{2+} pump protein relative to total crude membrane protein in cardiac myocytes is 70 $\pm$ 10 times greater than in stomach smooth muscle (Khan et al., 1990). This difference may partially explain why the Ca^{2+} uptake rate in smooth muscle SR vesicles is reported to be at least an order of magnitude lower than in cardiac SR vesicles (Raemaekers and Wuytack, 1996). Smooth muscle also has a lower density of Ca^{2+} pumps in the SR membrane which may also contribute to the slower rate of relaxation of smooth muscle when compared with cardiac muscle (Raemaekers and Wuytack, 1996).

Phospholamban (PL) is a homopentameric protein of 52 amino acids which resides on the SR membrane in cardiac and smooth muscle and regulates Ca^{2+} uptake by its interaction with the SERCA Ca^{2+} pump (Raemaekers and Jones, 1986). In its unphosphorylated state, phospholamban decreases the Ca^{2+}-sensitivity of the SERCA2

pump (Colyer and Wang, 1991), as well as the rate of Ca^{2+} binding (Tada et al., 1980). Phospholamban in the SR of smooth muscle can be phosphorylated by endogenous cyclic-AMP-dependent protein kinase, cyclic-GMP-dependent protein kinase (Raemaekers and Jones, 1996) or Ca^{2+}-calmodulin-dependent protein kinase II (Raeymaekers and Jones, 1986). Simmerman et al. (1986) determined the partial amino acid sequence of phospholamban and identified the phosphorylation sites of Ca^{2+}-calmodulin- and cAMP-dependent protein kinases to be the threonine[17] and serine[16] residues, respectively. The association between SERCA proteins and phospholamban has been examined in cardiac (Morris et al., 1991; James et al., 1989; Colyer et al., 1991) and smooth muscle SR (Eggermont, 1990). It was suggested that smooth muscle cells may have a lower ratio of phospholamban to SERCA2 molecules compared with cardiac SR membranes (Raemaekers and Wuytack, 1996). A relationship of two moles phospholamban per mole of SERCA2 protein was determined in cardiac SR (Colyer and Wang, 1991). However, Eggermont et al. (1990) found that PL and SERCA2 in smooth muscle were not consistently proportional to each other. The predicted amino acid sequence of phospholamban determined by cDNA sequencing was found to be identical between pig stomach smooth muscle and dog cardiac muscle (Verboomen et al., 1992). However, the level of phospholamban expression differs according to animal species as well as the tissue type (Missiaen et al., 1992): for example, it was undetectable in pig aorta at the protein level using both immunostaining and phosphorylation, but mRNA levels indicated $0.4 \pm 0.07 \times 10^{-18}$ mol of transcripts/μg of RNA. This was approximately 12-fold lower than mRNA levels in ileal smooth muscle and 122-fold lower than phospholamban

mRNAs in cardiac muscle, determined using the RNAase protection assay (Eggermont et al., 1990). It was also found that PL-antibody labelling and PKA-induced phosphorylation of PL in smooth muscle SR membranes was less than in cardiac SR (Raemaekers and Jones, 1986). Phospholamban is not found in fast skeletal muscle (Jorgensen and Jones, 1986), although the PL binding site is a unique characteristic of all members of the SERCA family, including the fast skeletal muscle isoform (James et al., 1989).

A Ca^{2+}-ATPase also exists on the plasma membrane of muscle cells and serves to extrude Ca^{2+} from the cell during relaxation, as well as counteracting the passive Ca^{2+} leak into the cell down its concentration gradient (Missiaen et al., 1992). The amino acid sequence of the sarcolemmal Ca^{2+} pump differs significantly from the SR pump (Carafoli, 1992), and it belongs to a different gene family, termed the plasma membrane Ca^{2+}-transporting ATPases (PMCA) (Raemaekers and Wuytack, 1996). The PMCA pumps, compared to the SERCA2 pumps, differ in molecular weight, and respond differently to phospholamban and calmodulin (Raemaekers and Wuytack, 1996). The plasmalemmal Ca^{2+} pump does not cross-react with SERCA antibodies, and is insensitive to thapsigargin, a known inhibitor of the SERCA family Ca^{2+} pumps (Lytton et al., 1993). Given the higher surface-to-volume ratio of smooth muscle vs. skeletal muscle cells, it is possible that the smooth muscle sarcolemmal Ca^{2+} pump, in conjunction with the Na^{+}/Ca^{2+} exchanger, plays a greater role in decreasing intracellular $[Ca^{2+}]$ in smooth muscle than it does in skeletal muscle (Raemaekers and Wuytack, 1996). However, Kargacin and Fay (1991) proposed that, in smooth muscle cells, the plasma membrane

Ca^{2+}-ATPase plays a greater role in long term Ca^{2+} regulation whereas the SR is more involved during Ca^{2+} transients. Kargacin and Kargacin (1995) determined that the rate of Ca^{2+} uptake by the SR is high enough for the SR to play a major role in removing Ca^{2+} during relaxation. They calculated that the SR of a single skinned smooth muscle cell could resequester 3.2×10^{-15} mol of Ca^{2+}, which exceeds the $[Ca^{2+}]$ required to elicit a single contraction by more than ten fold (Kargacin and Kargacin, 1995).

SR Ca^{2+} release

The SR membrane also contains Ca^{2+} release channels. All smooth muscle SR membranes contain inositol 1,4,5-trisphosphate (IP_3) receptors, which release Ca^{2+} upon binding IP_3 and are blocked by heparin (Ehrlich and Watras, 1988). IP_3 is produced endogenously as a product of a signal transduction cascade initiated by a GTP-binding protein (G protein) coupled receptor which, when activated, releases a G-protein to in turn activate phospholipase C, stimulating the conversion of phosphatidylinositol 4,5-bisphosphate (PIP_2) to diacylglycerol (DAG) and IP_3 (Somlyo and Himpens, 1989). The activity of the IP_3 receptor is modulated by both intravesicular and cytosolic $[Ca^{2+}]$ (Missiaen et al., 1992).

The ryanodine receptor is a second Ca^{2+} release channel which is found in some, but not all, smooth muscle SR membranes (Missiaen et al., 1992). It is traditionally thought of as the "Ca^{2+}-induced-Ca^{2+}-release" (CICR) channel, and can be activated following substantial Ca^{2+} influx across the plasma membrane (Berridge, 1993). The activity of this channel can be modulated by exogenous ryanodine. Application of 10 μM

or less of ryanodine will deplete SR Ca^{2+} stores by blocking the ryanodine receptor in an open state. Addition of ryanodine at concentrations 500 μM or greater will block the receptor in a permanently-closed state and prevent Ca^{2+} release (Herrmann-Frank et al., 1991). Species or tissue differences in the characteristics of Ca^{2+} uptake and release of smooth muscle cells may be accounted for by the differential localization and/or density of SR channels, including Ca^{2+} release sites (Somlyo and Himpens, 1989). Ikemoto et al. (1989) proposed that Ca^{2+}-dependent conformational changes in calsequestrin may have an impact on ryanodine receptor channel function in skeletal muscle SR.

SR ion channels and their functions

During uptake, Ca^{2+} concentrations within the SR can exceed that of the cytoplasm by a factor of 1000 or greater (Garcia and Miller, 1984). Since the SR membrane does not develop a sustained membrane potential (Garcia and Miller, 1984), compensatory ion movement must occur during Ca^{2+} uptake into the SR. The putative electroneutrality of the SR Ca^{2+} pump was initially examined by several investigators using rabbit skeletal muscle SR. Morimoto and Kasai (1986) separated non-leaky SR vesicles containing pump protein into four groups using KCl density gradient centrifugation: those with anion channels only, those with cation channels only, vesicles with both cation and anion channels, or those with no ion channels and only the Ca^{2+}-ATPase. They succeeded in separating the vesicles according to their differential weights by selectively permeabilizing the vesicle membranes with ionophores. For example, cation-only vesicles were made lighter with the addition of valinomycin, a K^+ ionophore,

which then allowed them to be separated from anion-only vesicles by centrifugation. They discovered that the vesicles which contained only pump protein were incapable of resequestering Ca^{2+} (Morimoto and Kasai, 1986). Experiments by Zimniak and Racker (1978) in which the Ca^{2+}-ATPase was incorporated into proteoliposomes showed that the K^+ ionophore, valinomycin, enhanced Ca^{2+} uptake when phosphate was present within the vesicles as a precipitating ion. However, Ca^{2+} accumulation also occurred in the absence of valinomycin, and therefore in the apparent absence of any compensatory ion flux. This appears to contradict the observations of Morimoto and Kasai (1986), who found that Ca^{2+} uptake could not occur without compensatory ion movement. However, Morimoto and Kasai (1986) suggested that Zimniak and Racker's proteoliposomes may have been leaky, allowing cations and anions to permeate the vesicular membrane. In a review on cardiac SR, Feher and Fabiato (1990) noted that the experimental electrical potential difference established by the Ca^{2+} pump (V_p) of ~50 mV (Zimniak and Racker, 1978; Morimoto and Kasai, 1986) is still far below what might be expected for the quantity of Ca^{2+} transported across the membrane. Given 2 moles of Ca^{2+} transport per mole of ATP hydrolysis and the experimental conditions employed, including: 0.1 mM extravesicular Ca^{2+}, 5 mM intravesicular Ca^{2+}, 0.5 mM ADP, 0.5 mM P_i, and 4.5 mM ATP, Feher and Fabiato (1990) calculated that the Ca^{2+} pump should be stopped at a potential of 120 mV. Even fairly large changes in the concentrations of reaction parameters would not alter their conclusion that the theoretical V_p is far greater than the measured V_p. One proposed explanation for the discrepancy between the calculated and observed V_p is that additional charge movement coupled with Ca^{2+} uptake may reduce

the theoretical V_p (Feher and Fabiato, 1990). In intact cells, it is likely that compensatory ion movement occurs to fully balance the accumulation of positive charge and to prevent the development of an SR membrane potential during Ca^{2+} uptake.

In proteoliposomes, it was found by Yu et al. (1993) that H^+ efflux occurred during Ca^{2+} uptake and that further uptake was eventually inhibited upon alkalinization of the liposome interior. This inhibition could be relieved by the H^+ ionophore FCCP. In SR vesicles, however, FCCP had no effect on Ca^{2+} uptake rate. This was likely due to the native permeability of the membrane to other ions which could offset charge build up (Yu et al., 1993). Feher and Fabiato (1990) further noted that in skeletal muscle SR, Ca^{2+} accumulation is only partially compensated by the countertransport of H^+. Somlyo et al. (1981) also argued that *in situ*, the free movement of Na^+, K^+ and Cl^- should diffuse the development of a potential difference across the membrane of the SR.

The Gibbs-Donnan equilibrium states that an unequal distribution of ions across a semi-permeable membrane generates osmotic pressure and an electrical potential difference across the membrane (Brown and Stubbs, 1983). For simplicity, we will only consider the movements of three principal ions: Ca^{2+}, K^+, and Cl^-. (Na^+ was not present in the experimental uptake buffers described below). Firstly, if it is assumed that both K^+ and Cl^- ions are freely permeable across the SR membrane and can passively diffuse to compensate the influx of positive charge during Ca^{2+} uptake, then a change in permeability of either Cl^- or K^+ would result in a concomitant change in the concentration of the remaining ion. To maintain electroneutrality, in the face of reduced Cl^- conductance, K^+ would have to be distributed across the SR membrane to compensate

for the influx of Ca^{2+}. The K^+ concentration within the SR required to compensate a membrane potential of 50 mV (based on the estimates of V_p of Feher and Fabiato, 1990) can be calculated if we assume that K^+ outside the SR is 100 mM. The Donnan equation (Brown and Stubbs, 1983) applies the Nernst equation to determine the ionic concentrations of a particular ion across the membrane:

$$E_{Ca2+} = RT/zF \ln [K^+]_{outside}/[K^+]_{inside}$$

where RT/zF is $\pm$ 58 (at 20°C), depending on the charge of the ion being considered. Using these parameters, the calculated K^+ concentration within the SR would be 13.8 mM. If Cl^- were the only permeable ion, the same Cl^- concentration within the SR (assuming a concentration of 100 mM outside the SR) would be 727 mM. If, on the other hand, two ions are not equally permeable across a membrane, changes in the ability of the more permeant ion to cross the membrane could alter SR Ca^{2+} uptake. For example, if Cl^- were more permeable than K^+, a blockage of Cl^- channels and the permeation of K^+ at a slower rate would reduce the rate of Ca^{2+} uptake. In situations where Ca^{2+} is rapidly released and resequestered, this could reduce the rate of loading of the SR.

The SR membrane in cardiac and skeletal muscle has been shown to be permeable to Cl^- as well as H^+, Na^+ and K^+ (Meissner and McKinley, 1982). Meissner and McKinley (1982) demonstrated monovalent cation (H^+, Na^+, K^+) conduction in both canine skeletal and cardiac SR using radioactive isotopes. Although they provided

evidence for cation conductance, they also showed that Cl^- permeability exceeds that of K^+, H^+, and Na^+ in native SR vesicles. They also compared the ion permeability of reconstituted SR and plasmalemmal membranes and noted that, whereas the majority of surface membrane vesicles are impermeable to Cl^-, vesicles created from endoplasmic and sarcoplasmic reticula consistently allow the passage of Cl^- ions. Only two thirds of the SR vesicles from skeletal muscle were permeable to K^+ or Na^+ although all were permeable to Cl^- and H^+. Ion permeability of the vesicles was determined by measuring isotope efflux rates. Millipore filters were used to isolate the vesicles, and radioactivity within the vesicles was quantitated. Given the consistency of Cl^- and H^+ permeability, it was concluded that both Cl^- and H^+ channels were present in higher density than Na^+ and K^+ channels in skeletal muscle SR membranes (Meissner & McKinley, 1982). It is also interesting to note that a greater proportion of the reconstituted cardiac SR contained K^+ or Na^+ permeable channels (>85%) compared with skeletal muscle SR (~70%) (Meissner & McKinley, 1982). Kasai and Kometani (1979) determined that skeletal muscle SR vesicles were fifty times more permeable to Cl^- than K^+. Toad skeletal muscle SR was studied by Fink and Stephenson (1987) who found that the capacity of the SR to load Ca^{2+} increased when voltage-dependent K^+ channels were blocked with tetraethylammonium, 4-aminopyridine, procaine or decamethonium. These investigators proposed that K^+ channel inhibition increased H^+ (or Mg^{2+}) efflux from the SR, therefore stimulating Ca^{2+} uptake. Ca^{2+} accumulation could be enhanced either due to counter-ion movement (cation efflux), or intravesicular alkalinization which could increase sensitivity of Ca^{2+} binding sites (Fink and Stephenson, 1987). Based on these

results, Kourie et al. (1996a) suggested that K^+ could not be a principal ion in charge compensation if K^+ channel inhibition enhanced, rather than diminished, Ca^{2+} uptake. This led them to conclude that Cl^- plays a predominant role in maintaining electroneutrality during Ca^{2+} uptake into the SR (Kourie et al., 1996a).

Soler et al. (1994) compared rates of Ca^{2+} uptake in rabbit skeletal muscle SR vesicles after substituting choline or gluconate for either K^+ or Cl^-, respectively. Ca^{2+} sequestration rates measured using a $^{45}Ca^{2+}$ tracer were lower in buffers containing choline chloride or potassium gluconate compared with a control KCl buffer. Uptake rates were higher in the choline chloride buffer than they were in the potassium gluconate buffer. Assuming equal and low permeation rates for choline and gluconate across a reconstituted SR membrane (Soler et al., 1994), these results suggest that Cl^- influx into the SR has a greater role than K^+ efflux during Ca^{2+} uptake since uptake rates were higher when Cl^- was the permeant ion species.

Confirmation of the involvement of Cl^- movement in the function of the SR of smooth muscle cells during Ca^{2+} uptake has been lacking to date. The purpose of the present study was to determine if Cl^- functions as a compensatory anion during Ca^{2+} uptake and to characterize the transport process involved in Cl^- flux across the SR membrane in both cardiac SR vesicles and smooth muscle SR.

SR Cl^- channels

The results presented above indicate that anions may play a role in maintaining electroneutrality across the SR. The properties of identified SR Cl^- channels are

summarized in Table 1 and described in detail below. The varied characteristics of Cl^- channels in cardiac and skeletal muscle SR membranes (Table 1) suggest that the pathways involved may differ between muscle types.

A 200 pS SR Cl^- channel from rabbit skeletal muscle was found to be non-selective for monovalent anions, but was competitively inhibited by 10-100 mM SO_4^{2-} on the cytoplasmic (cis) side of the SR membrane (Tanifuji et al., 1987). Kourie et al. (1996) recently identified two different types of Cl^- channels from rabbit skeletal muscle SR vesicles. The first Cl^- channel, termed BCl (analagous to the BK, or large conductance K^+ channel), is very similar to the 200 pS Cl^- channel initially described by Tanifuji et al. (1987). Kourie reported a conductance of 250 pS for the BCl, in an asymmetrical solution of CsCl (50 mM on the intravesicular side of the SR membrane and 250 mM on the cytoplasmic side of the membrane). BCl was Ca^{2+}-sensitive, and highly Cl^- selective with a Cs^+ permeability: Cl^- permeability ratio (P_{Cs}/P_{Cl}) of 0.03. Cl^- conductance was inhibited in 80 μM 4,4'-diisothiocyanatostilbene 2,2'-disulfonic acid (DIDS), applied to either side of the membrane, but was unaffected by 8 μM DIDS. 30-70 mM Li_2SO_4 decreased BCl current when present on the cytoplasmic side of the membrane, but was without effect when applied to the lumenal side of the membrane. The second, small conductance Cl^- channel from the skeletal muscle SR membrane (SCl) is a potentially novel, Cl^--selective channel of 70 pS (in 50 mM CsCl cytoplasmic: 250 mM lumenal CsCl) with a low Cs^+ permeability, P_{Cs}/P_{Cl}, of 0.04-0.08 (Kourie et al., 1996). Li_2SO_4 had no effect when administered to either side of the SR membrane,

Table 1. Cl^- channels have been described above in Table 1 according to their conductance in the indicated solution. Concentrations are noted for both the cytoplasmic and intravesicular sides of the SR membrane (ie. 250/50 Cl^- would mean that conductance was determined with 250 mM Cl^- on the *cytoplasmic* side of the membrane, and 50 mM Cl^- on the *lumenal* side). Voltage and Ca^{2+}-dependence information are also described if available from the literature. Dashes mean that the specific characteristic was not tested. Voltage dependence is indicated on the left, Ca^{2+} dependence is indicated on the right. Cl^- channel inhibitors are described in the last column on the right. The inhibitor concentration is indicated (in μM) as well as the side of the membrane to which the inhibitor was added.

Investigator, Year	Muscle Type	Conductance, cytoplasmic/lumenal [Cl^-](mM)	Voltage/Ca^{2+} dependence	Inhibitors
Tanifuji et al., 1987	Rabbit skeletal SR	200 pS 100/100 Cl^-	Y/-	Cytoplasmic SO_4^{2-} 10-100 mM
Kourie et al., 1996(b)	Rabbit skeletal SR	250 pS 50/250 Cl^-	-/Y	80 μM DIDS (either side), Cytoplasmic SO_4^{2-} 30-70 mM
Kourie et al., 1996(b)	Rabbit skeletal SR	70 pS 50/250 Cl^-	-/Y	8 μM DIDS (either)
Rousseau et al., 1989	Canine cardiac SR bilayers	55 pS 260/260 Cl^-	Y/N	10 mM DIDS, 15 mM SO_4^{2-} (cytoplasmic)
Kawano et al., 1992	Porcine cardiac SR	116 pS 500/50 Cl^-	N/N	20 μM PKI, 200 μM DNDS (cytoplasmic)
Decrouy et al., 1996	Human atrial SR	67 pS 250/50 Cl^-	low/-	1-100 μM SITS, anti-PL antibody 0.6 μg/ml (both cytoplasmic)
Decrouy et al., 1995	Canine/sheep ventricular SR	92 pS 250/50 Cl^-	low/-	Anti-PL Ab
Shoshan-Barmatz et al, 1996	Rabbit skeletal SR	-Not determined-	Y/-	100 μM DIDS, 300 μM DCCD (cytoplasmic)
Townsend and Rosenberg, 1995	Porcine cardiac SR (lipid bilayers)	130 pS 250/250 Cl^-	Y/N	pH>7, stilbenes, NPPB (Ki=53 μM, trans only) 1 mM Zn/Cd (both)

indicating that SCl is equally permeable to Cl^- and SO_4^{2-}. DIDS, however, was a more potent inhibitor of the SCl than the BCl channel and decreased P_o significantly at a concentration of 8 μM. The SCl has qualities which closely resemble a Ca^{2+}-activated-Cl^--channel in endosomes from rat kidney cortex (Reeves and Gurich, 1994). The rat kidney cortex Cl^- channel has a conductance of 90 pS, is voltage-dependent and inhibited by DIDS at micromolar concentrations. The channel is anion-specific with a P_K/P_{Cl} of 0.08 and selectivity sequence of $NO_3^- > F^- > Br^- > Cl^- >> I^-$ (Reeves and Gurich, 1994).

Rousseau (1989) characterized a voltage-dependent SR Cl^- channel from canine cardiac myocytes with a 55 pS conductance. The open probability of Cl^- channels from canine cardiac SR incorporated into bilayers was not lowered upon addition of sulphate, although Cl^- current amplitude was reduced. An SR Cl^- channel isolated from porcine cardiac myocytes was found to be both Ca^{2+} and voltage-independent (Kawano et al., 1992). This 116 pS Cl^- channel (in 500 mM CsCl (cytoplasmic) / 50 mM CsCl (lumenal)) was regulated by protein kinase A (PKA). The channel spontaneously inactivated upon incorporation into the lipid bilayers unless the catalytic subunit of PKA was added to the cytoplasmic face of the Cl^- channel. This activation could be reversed by a protein kinase inhibitor specific to PKA (Kawano et al., 1992). Kawano and Hiraoka (1993) later found that the 116 pS channel was inhibited by the Ca^{2+}-calmodulin complex. Another cardiac SR Cl^- channel was described in human atrial myocytes (Decrouy et al., 1996). It had characteristics similar to the SR Cl^- channel from ventricular cells described by Decrouy et al. (1995): low voltage sensitivity and a

conductance of 67 pS (250 mM cytoplasmic CsCl : 50 mM lumenal CsCl) or 103 pS in symmetrical solution (250/250 mM CsCl). This Cl^- channel was activated only when it was closely associated with phospholamban on the cytoplasmic side of the SR membrane, and was inhibited by application of 1-100 μM SITS on either side of the membrane (Decrouy et al., 1996). Townsend and Rosenberg (1995) looked at the characteristics of a Cl^- channel from porcine cardiac SR which was reconstituted into phospholipid bilayers. This channel was found to be sensitive to several stilbene derivatives applied to the lumenal side of the membrane: DNDS reduced the conductance with a K_i of 570 μM, and both DIDS and SITS also blocked the Cl^- channel; nitrophenylpropylamino benzoate (NPPB) had a K_i of 52.6 μM on the lumenal side of the membrane, and anthracene-9-carboxylic acid (ACA; K_i=1500 μM) and diphenylamine-2-carboxylate (DAC; K_i=707 μM) also inhibited the Cl^- channel. The divalent cations, Zn^{2+} and Cd^{2+}, both inhibited the Cl^- channel in concentrations of 1 mM applied to either side of the membrane. Townsend and Rosenberg (1995) looked at the effect of changing pH on the activity of the Cl^- channel. Although they found no effect when pH was altered on the cytoplasmic face of the membrane (pH 5.5-9.0), the channel responded to acidification and alkalinization of the lumenal side of the membrane. When the lumenal pH dropped to 5.5, the Cl^- current amplitude increased from 6.4 pA (at pH=7.0) to 9.6 pA. Conversely, the amplitude decreased to 2.8 pA when the pH was raised from 7.0 to 9.0 (Townsend and Rosenberg, 1995). SR Cl^- channels may also interact with other SR proteins, such as the ryanodine receptor (Sukarheva et al., 1996) or phospholamban (Decrouy et al., 1995).

Purified Cl^- channels

Recently purified Cl^- channels from intracellular membranes include a 64 kDa protein common to human fibroblasts, T84 intestinal cells, Sf9 insect cell line and Chinese Hamster Ovary (CHO) cells in culture. Using immunolabelling, this channel did not appear to be localized on the plasma membrane in these cells, suggesting that it is present on an intracellular organelle (Landry et al., 1993). A 100 kDa anion-selective channel purified from rabbit skeletal muscle SR vesicles by Ide et al. (1991) could be blocked by 10-100 mM SO_4^{2-} (cytoplasmic) and the stilbene derivative DIDS. A purified, 35 kDa Cl^- channel with characteristics similar to those of the voltage-dependent anion channel (VDAC) was recently purified from rabbit skeletal muscle SR (Shoshan-Barmatz et al., 1996). Three peptides were sequenced from the skeletal muscle SR Cl^- channel protein and were found to be identical to sequences from the mitochondrial VDAC protein. Skeletal muscle VDAC also cross-reacted with four monoclonal antibodies raised against mitochondrial VDAC. The SR VDAC activity was completely inhibited by 100 μM DIDS, and was inhibited 80% by 300 μM DCCD. [^{14}C]DCCD also labelled both the SR and mitochondrial VDAC specifically (Shoshan-Barmatz et al., 1996). A 38 kDa protein was recently purified from tracheal smooth muscle intracellular and plasmalemmal membranes. When the protein was incorporated into a lipid bilayer, it generated a 25-30 pS Cl^- channel (Ran et al., 1992). An isolated SR Cl^- channel (Lewis et al., 1994) from amphibian skeletal muscle displayed a bell-shaped voltage dependence similar to a VDAC found in mitochondrial membranes. An antibody to VDAC labelled both mitochondria and other intracellular membranes which were presumed to be SR in

skinned skeletal muscle fibres (Lewis et al., 1994).

To date, information on the molecular architecture of Cl^- channels has been limited to plasmalemmal Cl^- channels. Jentsch and Gunter (1997) reported that there are presently three structurally distinct Cl^- channel classes. The first includes both glycine and GABA receptors, which are activated by ligand binding and exist as pentamers of monomers which are characterized by four transmembrane domains. The second class contains only one known Cl^- channel, the cystic fibrosis transmembrane regulator (CFTR). It belongs to the gene superfamily known as ATP-binding cassette transporters, which include sulfonyluria receptors. This channel is of interest since it has been identified as a small conductance Cl^- channel (5-8 pS) in the plasma membrane of cardiac muscle and can be activated by cAMP. The CFTR has a permeability sequence of $Br^- \approx Cl^- > I^-$ (Jentsch and Gunter, 1997). Lastly, the CLC family of Cl^- channels is the biggest class of Cl^- channels and contains nine different gene products. CLC channels contain 12 transmembrane domains, and are generally voltage-gated. The one exception is the CLC-2 channel, which is of ubiquitous distribution and is activated by cell swelling and hyperpolarization. The CLC-1 channel is expressed in skeletal muscle and demonstrates a permeability sequence of $Cl^- > Br^- > I^-$. It was recently discovered that CLC-1 is mutated in dominant myotonia congenita, and results in altered voltage-dependence of the channel (Pusch et al., 1995).

Conclusion

Although the evidence discussed above is consistent with the involvement of Cl^-

in counter-ion movement in striated muscle, the precise role that the above channels play in this movement remains to be determined. Even less is known about Cl^- channels and counter charge movement in smooth muscle cells. One way to study the involvement of Cl^- in charge compensation and to determine the properties of the channel that are most important during SR Ca^{2+} uptake is to measure uptake in the presence of agents that are likely to alter Cl^- movement. This approach provides functional information that can be used to assess the contribution of Cl^- channels in the context of an intact, operational organelle.

To determine the role of Cl^- movement during Ca^{2+} uptake in smooth muscle cells, the experiments described in this study have utilized a saponin-skinned isolated cell preparation from rabbit stomach muscle. The effects on Ca^{2+} uptake of Cl^- channel blockers and anion substitution (Br^-, I^- and methanesulfonate) for Cl^- were determined. Similar experiments were also carried out with canine cardiac SR vesicles for comparison with the data obtained from isolated smooth muscle cells.

METHODS AND MATERIALS

The following four sections detail the different protocols used for the isolated skinned cell and cardiac SR vesicle experiments. These include: 1) cell isolation, which describes the preparation of isolated and skinned smooth muscle cells taken from rabbit stomach, 2) the preparation of canine cardiac SR vesicles, 3) Ca^{2+} uptake experiments with isolated cells, and 4) Ca^{2+} uptake experiments using cardiac SR vesicles.

SMOOTH MUSCLE CELL ISOLATION

Stomachs were excised from rabbits which were sacrificed with an overdose of phenobarbital, according to established protocols approved by the Canadian Council on Animal Care. The stomach was immediately emptied of its contents and flushed with Hank's Balanced Salt Solution (HBSS). A small, healthy piece of tissue was then chosen by visual inspection and cut to a size of approximately 5 cm in diameter: healthy tissue was identified by a mucosa of uniform pink colour which loosely covered the underlying muscle. The mucosa was cut away from the muscle with scissors and discarded while the gastric smooth muscle was secured on an O-ring with dissecting pins to ensure uniform exposure to the enzymatic solution during the digestion process. The tissue was incubated in a solution of 0.2% collagenase and 0.2% DNase in HBSS for 1h at 37°C. The tissue was then triturated in HBSS and transferred to a second solution comprised of 0.2% protease and 0.2% DNase dissolved in HBSS and was incubated for 30 min at 37°C. The tissue was then cut into approximately $1mm^2$ - sized pieces and triturated to

release individual cells. Next, the resulting cell suspension was filtered through cheesecloth to separate the isolated cells from the undigested tissue. The undigested tissue was discarded, and EGTA (final concentration, 2.5 mM) was added to the cell-HBSS suspension. The suspension was then centrifuged at 500 x *g* in a bench top centrifuge for 5 minutes and the supernatant was aspirated away. The cells were then resuspended in rigor buffer (see below) and skinned with saponin (50 μg/ml) during a 5 minute centrifugation at 500 x *g*. To wash away saponin, the resulting pellet was resuspended in rigor buffer, incubated for five minutes, then centrifuged (500 x *g*) for five minutes. By skinning the isolated cells with saponin, the plasma membrane can be selectively permeabilized based on the uniform distribution of cholesterol throughout the membrane. Since the SR membrane is not comprised of cholesterol, saponin allows the SR membrane to remain intact and the smooth muscle cells to retain their contractile capacity. This closely approximates a physiological condition while allowing buffers and dye to enter individual cells (see for example, Seeman et al., 1973). After the wash in rigor buffer, the cells were washed four times in an appropriate uptake buffer. For each wash, buffer was added to the pellet from the previous centrifugation and the resulting cell suspension was allowed to equilibrate on ice for seven minutes before centrifugation (500 x *g*), aspiration and addition of fresh buffer for the next wash. After the final wash and centrifugation, the cells were resuspended in 500-1000 μl uptake buffer.

Buffers for cell isolation: Hanks' Balanced Salt Solution (HBSS) contained (in mM): 5 KCl, 0.3 KH_2PO_4, 138 NaCl, 5.6 D-glucose, 12.5 taurine, and 4 $NaHCO_3$; pH 7.0.

Rigor buffer contained (in mM): 1.03 Mg-methanesulfonate, 150 K-methanesulfonate, 5 EGTA, 20 PIPES; pH 7.0. The uptake buffer used to wash and finally resuspend the isolated cells contained (in mM): 10 $MgCl_2$, 20 HEPES-K, and 100 KCl in most cases. For some experiments (see below) variations of this buffer were made with I^-, Br^- or methanesulfonate substituted for Cl^-. Other details of the ways in which these buffers were used are given below (in the section entitled "Solutions and compounds for isolated cell experiments").

Chemical sources for cell isolation: D-glucose, taurine, collagenase IV, protease, EGTA, methanesulfonic acid, piperazine-N,N'-bis(2-ethanesulfonic acid) (PIPES dipotassium salt) and saponin were obtained from Sigma Chemical Co. (St. Louis, MO). DNase was obtained from Boehringer-Mannheim (Laval, Quebec). To minimize contamination, Ca^{2+} uptake buffers were made from microselect (>99.5%) $MgCl_2 \cdot 6H_2O$, purum grade Mg-gluconate, microselect (>99%) $MgBr_2 \cdot 6H_2O$, and 4-(2-hydroxyethyl)-piperazine-1-ethane-sulfonic acid (HEPES-K^+ salt; >99%), all obtained from Fluka (Ronkonkoma, NY); analytical reagent grade KH_2PO_4, $NaHCO_3$,NaCl, and $Mg(OH)_2$ and suprapur grade KI, AnalaR grade KBr and KCl, and aristar grade KOH were all obtained from BDH (Toronto, ON).

CARDIAC SR VESICLE PREPARATION

SR vesicles were prepared by Mr. E. Wirch, as previously described in Chamberlain et al. (1983) and were not separated into light and heavy fractions. For

each preparation, the heart of a dog euthanized with fentanylcitrate was immediately removed, immersed in 150 mM NaCl, and trimmed of fat and connective tissue. The remaining steps were performed at 0-4°C. Three samples (30-40 g) were taken from ventricular and atrial muscle. Each sample was carried through the following steps.

The sample was first homogenized in 160 ml of solution A (see below). The homogenate was centrifuged for 15 minutes at 3 800 x *g* in a Beckman JA-14 rotor. The supernatant was then filtered through four layers of cheesecloth, adjusted to 150 ml with solution A and centrifuged again for 15 minutes at 28 000 x *g* (JA-14 rotor). The supernatants from each of the three samples were combined at this point. This supernatant was filtered through cheesecloth, adjusted to 360 ml with solution A and aliquoted into 6 (60 ml each) Beckman tubes. These were then centrifuged for 2h at 120 000 x *g* in a Beckman Type 35 rotor. After centrifugation, the supernatant was aspirated and the pellet was set on ice for ten minutes, which allowed easy separation of hard and soft pellets. The upper, soft pellet was then pipetted off and suspended in 66 ml solution A (with salt concentration increased to 0.65 M KCl) for salt washing by hand homogenization (15 strokes with teflon hand homogenizer). This step selectively extracts actin and myosin. The suspension was separated into three 22ml tubes which were incubated for 30 minutes on ice. The tubes were centrifuged at 4 300 x *g* for 10 minutes in a Beckman JA-20 rotor. The upper pellet was once again resuspended in solution A and centrifuged for 100 minutes at 182 500 x *g* in a Beckman 50.2 rotor. The loose top pellet was homogenized in a small volume of ultrapure storage buffer (for composition see below). 200 μl aliquots of crude SR in storage buffer were then rapidly frozen in

liquid N_2 and stored at -80 ^{0}C for future use.

Buffers for SR vesicle preparation: Solution A contained (in mM): 290 sucrose, 0.5 dithiothreitol (DTT), 3 NaN_3, and 10 imidazole-HCl; pH 6.9. The high-salt version of the above (for protein extraction) also contained 650 mM KCl. Storage buffer was made using ultrapure sucrose and KCl and contained (in mM): 300 sucrose, 100 KCl, 5 histidine, 0.5 DTT; pH 7.1.

Chemical sources: NaN_3, DTT, imidazole-HCl, and histidine were obtained from Sigma Chemical Co. (St. Louis, MO). Aristar grade KCl and sucrose were obtained from BDH (Toronto, ON).

Ca^{2+} UPTAKE EXPERIMENTS USING ISOLATED CELLS

Fifty μl of saponin-permeabilized, isolated cells in uptake buffer were added to a small chamber on the stage of an inverted microscope and background light scatter and fluorescence were measured. 2 μl of fura-2 was then added to the chamber (final fura-2 concentration = 4 μM). Fura-2 is a Ca^{2+}-selective dye (Kd_{Ca2+} 200 nm) which demonstrates strong selectivity against Mg^{2+} (Kd_{Mg2+} of 5.0 mM, Grynkiewicz et al., 1985). Uptake was initiated by the addition of (in final concentrations): 8 μM ATP, 8 μM creatine phosphate (CP) and 14.3 U/ml creatine phosphokinase (CPK) while the contents of the chamber were continually stirred. The addition of exogenous Ca^{2+} was not required as an initial $[Ca^{2+}] > 1$ μM was typical of a good cell preparation. A

SPEX fluorometer provided an excitation source, alternating between 340 and 380 nm excitation wavelengths. Emission was measured at 510 nm with a photomultiplier tube. Ca^{2+} uptake results in a decrease in 340/380 ratio over the duration of the experiment (as described below).

Solutions and compounds: Uptake buffers were made using ultrapure chemicals and double-distilled water and the pH was consistently adjusted to 7.0. The standard KCl buffer contained (in mM): 100 KCl, 10 $MgCl_2$ and 20 HEPES-K. KBr buffer contained: 100 KBr, 10 $MgBr_2$ (or Mg-gluconate), 20 HEPES-K; KI buffer contained 100 KI, 10 Mg-gluconate and 20 HEPES-K; K-methanesulfonate buffer contained 100 K-methanesulfonate, 10 Mg-gluconate and 20 HEPES-K.

ATP and CP were dissolved in H_2O and the solution was brought to a pH of 7.0 with KOH. CPK was then added at 1 mg/ml (163 U/mg). Final stock concentration was 0.0917 M for ATP and 0.0981 M for CP.

Fura-2 was dissolved in double distilled water to a concentration of 1.2 mM. For daily use, the stock solution was diluted 1:10 in uptake buffer and used at a final concentration of 4.2 μM.

Indanyloxyacetic acid ((R)-IAA-94), a Cl^- channel blocker, was dissolved in 100% ethanol to make a stock solution of 5 mM. This was frozen at -4°C, and daily aliquots were made in 95% ethanol / 5% H_2O to allow addition of 1 μl of the drug to the microscope chamber for each trial. The final concentration of ethanol in the experiments

Figure 1. Fura-2 fluorescence excitation spectra in the presence and absence of ethanol: The effect of ethanol on fura-2 fluorescence, measured at 510 nm, was tested since ethanol was used as a solvent for NPPB and (R)-IAA-94. The concentration of ethanol (0.3%) used was the maximium final concentration used in the experiments. Two trials are displayed in this figure: the control trace was obtained in KCl buffer and 4.2 μM fura-2. The second trace was obtained with 0.3% ethanol added to the buffer and fura-2. Both traces are overlapped, indicating that the addition of 0.3% ethanol to the chamber does not change the fluorescence of fura-2 over a range from 300-400 nm when compared to the control.

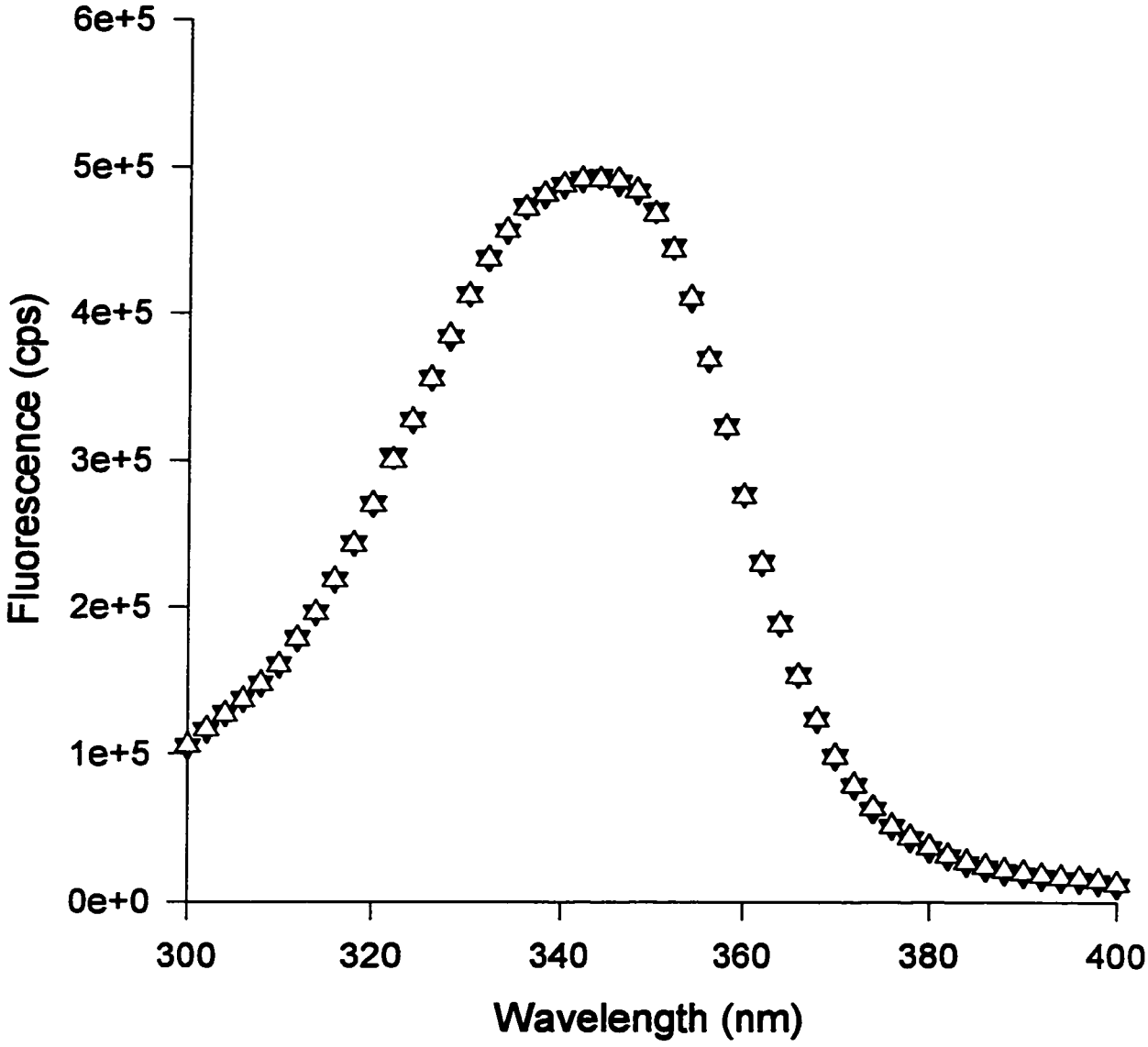
6e+5
5e+5
4e+5
3e+5
2e+5
1e+5
0e+0
Fluorescence (cps)
300
320
340
360
380
400
Wavelength (nm)

with NPPB (see below) or (R)-IAA-94 did not exceed 0.3%. This concentration of ethanol had no effect on the excitation spectra of fura-2 (Figure 1) or on uptake rate in control experiments (see results).

A second Cl^- channel blocker, 5-nitro-2-(3-phenylpropylamino) benzoic acid (NPPB), was dissolved in 95% ethanol / 5% H_2O to make a stock solution of 33 mM. Lower concentrations were made from the stock solution in 95% ethanol / 5% H_2O.

Experimental setup for experiments with isolated cells: The experimental apparatus used to monitor Ca^{2+} uptake for isolated skinned experiments is shown in Figure 2. Light emitted from a xenon lamp passed through a beam splitter and two monochromators set at 340 nm and 380 nm, respectively, before passing through a chopper which allowed alternation of the two wavelengths at 300 ms intervals. The fluorimeter was interfaced with an Olympus inverted microscope via a fibre optic cable. A dichroic mirror within the microscope directed the 340 nm and 380 nm wavelength light towards a 100 μl chamber, which contained the cell suspension, ATP and fura-2. Fura-2 fluorescence was measured at a wavelength of 510 nm. The fluorescence emission first passed through the dichroic mirror and then through a 10 nm band pass filter centred at 510 nm. This prevented scattered 340 nm and 380 nm light from entering the photomultiplier. The photomultiplier, discriminator and amplifier served to detect and amplify the fluorescence emission at 510 nm, with excitation at 340 nm and 380 nm. The ratio of 510 nm emission during excitation at 340 nm over that at 380 nm excitation was calculated over one second time intervals.

Figure 2. Experimental setup for experiments with isolated cells: Light emitted from a xenon lamp was passed through a beam splitter and two monochromaters set at 340 nm and 380 nm, respectively. A chopper was used to alternate the two wavelength light beams which passed through the fibre optic interfaced to an inverted microscope. The cell suspension was placed in a chamber with fura-2 and ATP and was illuminated by the 340 nm and 380 nm wavelength light. The excitation light was directed toward the chamber with a dichroic mirror. The fura-2 fluorescence was passed through a 10 nm band pass filter centred at 510 nm and a shutter, and was then detected with a photomultiplier tube (PMT).

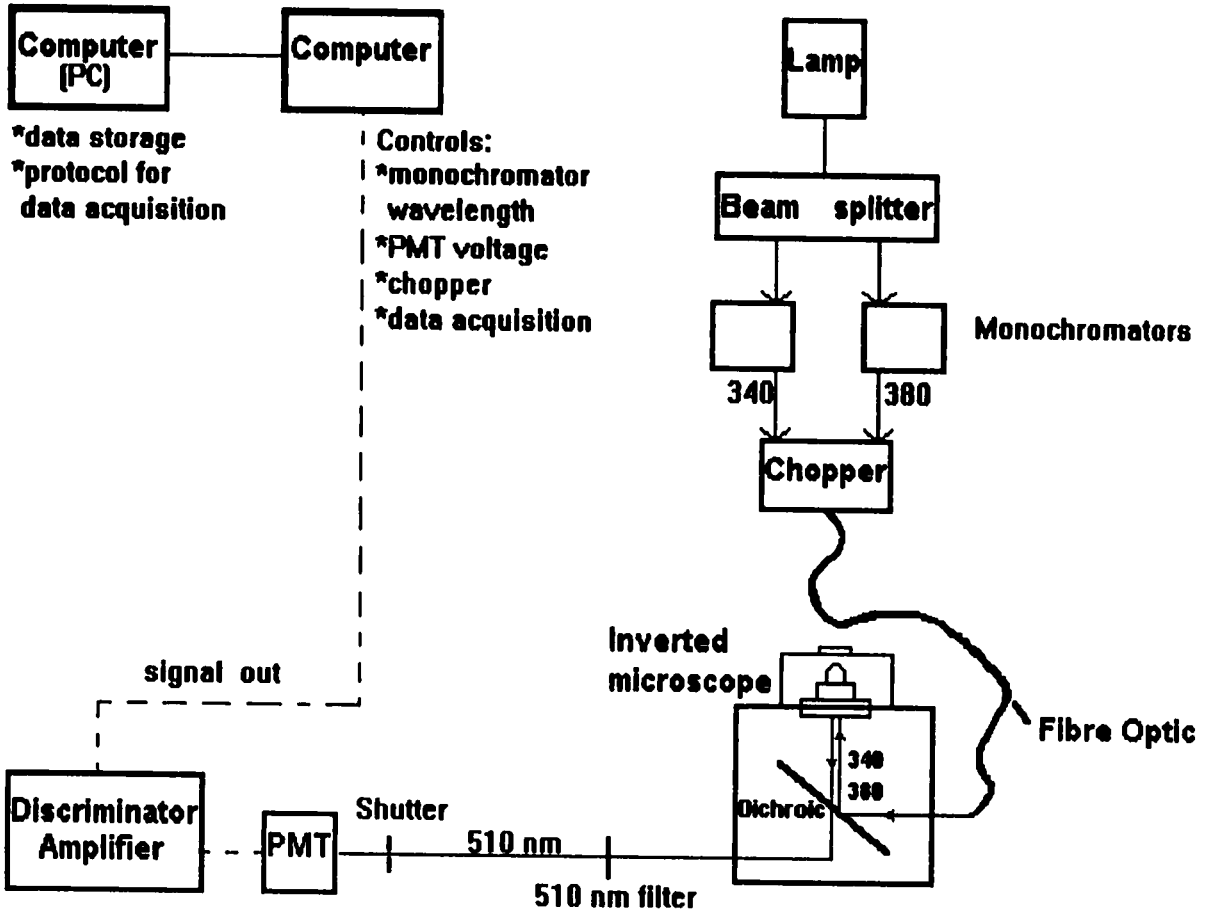
Computer (PC)
Computer
*data storage
*protocol for data acquisition
Controls:
*monochromator wavelength
*PMT voltage
*chopper
*data acquisition
Lamp
Beam splitter
Monochromators
340
380
Chopper
Inverted microscope
Fibre Optic
signal out
Discriminator Amplifier
PMT
Shutter
510 nm
510 nm filter
Dichroic
340
380

Excitation spectra measurements with NPPB and (R)-IAA-94: The excitation spectra of the uptake buffers containing either high Ca^{2+}, zero Ca^{2+}, or intermediate Ca^{2+} were measured with and without the blockers to determine whether they were fluorescent altered the fluorescence of fura-2 . For example, Ca^{2+} uptake in the presence of the blockers would appear to be altered if these compounds modified fura-2 fluorescence, selectively absorbed either the 340 nm or 380 nm excitation light, fluoresced themselves, or bound Ca^{2+}.

Excitation spectra were measured by scanning the excitation wavelength from 300-400 nm while measuring emission at 510 nm. Excitation spectra were measured for uptake buffer alone with no fura-2 added and compared to those in uptake buffer with NPPB or (R)-IAA-94 in order to determine if these compounds were fluorescent. (R)-IAA-94 did not alter the background signal significantly. Figure 3 shows that NPPB fluoresces minimally in the absence of fura-2.

The fura-2 excitation spectra at intermediate Ca^{2+} were also measured in the presence and absence of NPPB and (R)-IAA-94 to determine the effect of these compounds on fura-2 fluorescence. NPPB (90 μM) did change the fura-2 excitation spectrum in the presence of Ca^{2+} (Figure 4). Because of this, an absorbance spectrum for 90 μM NPPB was also obtained and showed that NPPB selectively absorbed more at 380 nm wavelengths (compared to buffer alone, percent transmittance was decreased by approximately 60%) than at 340 nm wavelengths (percent transmittance was decreased approximately 35% compared to buffer alone (Figure 5)). Increased absorbance by NPPB of 380 nm wavelength light compared to 340 nm was corrected for by measuring

Figure 3. Effect of 90 μM NPPB on the background fluorescence over excitation wavelengths ranging from 300-400 nm. Two measurements were taken to determine the autofluorescence of NPPB, which would affect the background fluorescence that is substracted from fura-2 fluorescence. The solid line shows the background fluorescence and light scatter measured with excitation wavelengths (300-400 nm) when only KCl buffer was present in the sample chamber. When 90 μM NPPB was added to the buffer, the background fluorescence increased from 613 cps to 883 cps with excitation wavelength at 340 nm and from 569 cps to 608 cps with 380 nm excitation. These spectra were measured with buffer (+/- NPPB in cuvets (see setup in Figure 9)). When fura-2 was added to a concentration of 2.9 μM, the signal intensities were approximately 500 000 cps and approximately 42 000 cps with excitation at 340 nm and 380 nm respectively. Thus, although NPPB had a small but detectable effect on background fluorescence, NPPB only minimally altered fura-2 fluorescence in the experiments reported here.

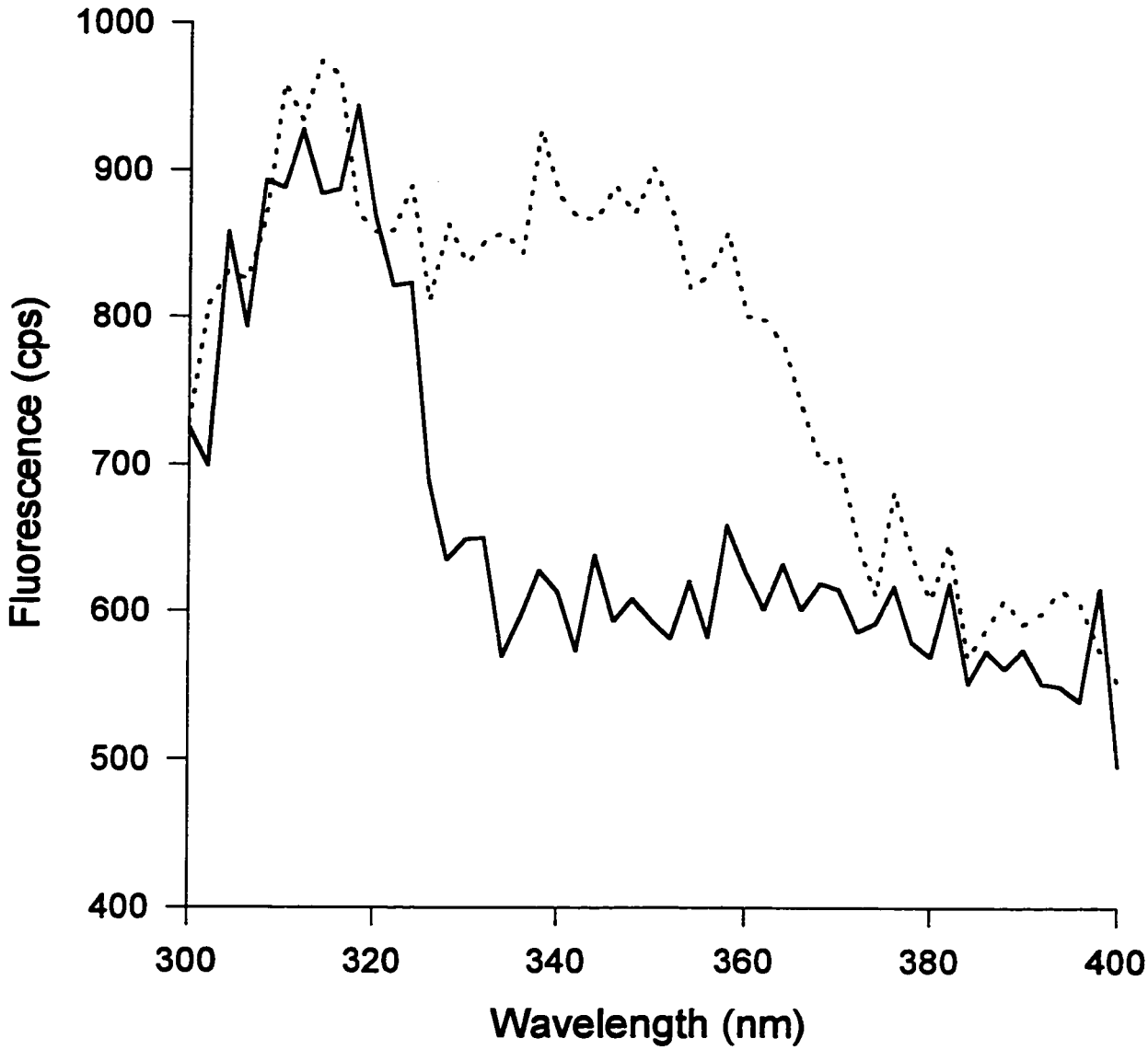
1000
900
800
700
600
500
400
Fluorescence (cps)
300
320
340
360
380
400
Wavelength (nm)

Figure 4. Excitation scan of 2.9 μM fura-2 with and without 90 μM NPPB. A scan was obtained for excitation wavelengths between 300-400 nm. In the control scan (open triangles), the cuvet contained KCl buffer and 2.9 μM fura-2. The closed triangles show a decrease in fura-2 fluorescence when 90 μM NPPB was added to a cuvet with KCl buffer and 2.9 μM fura-2.

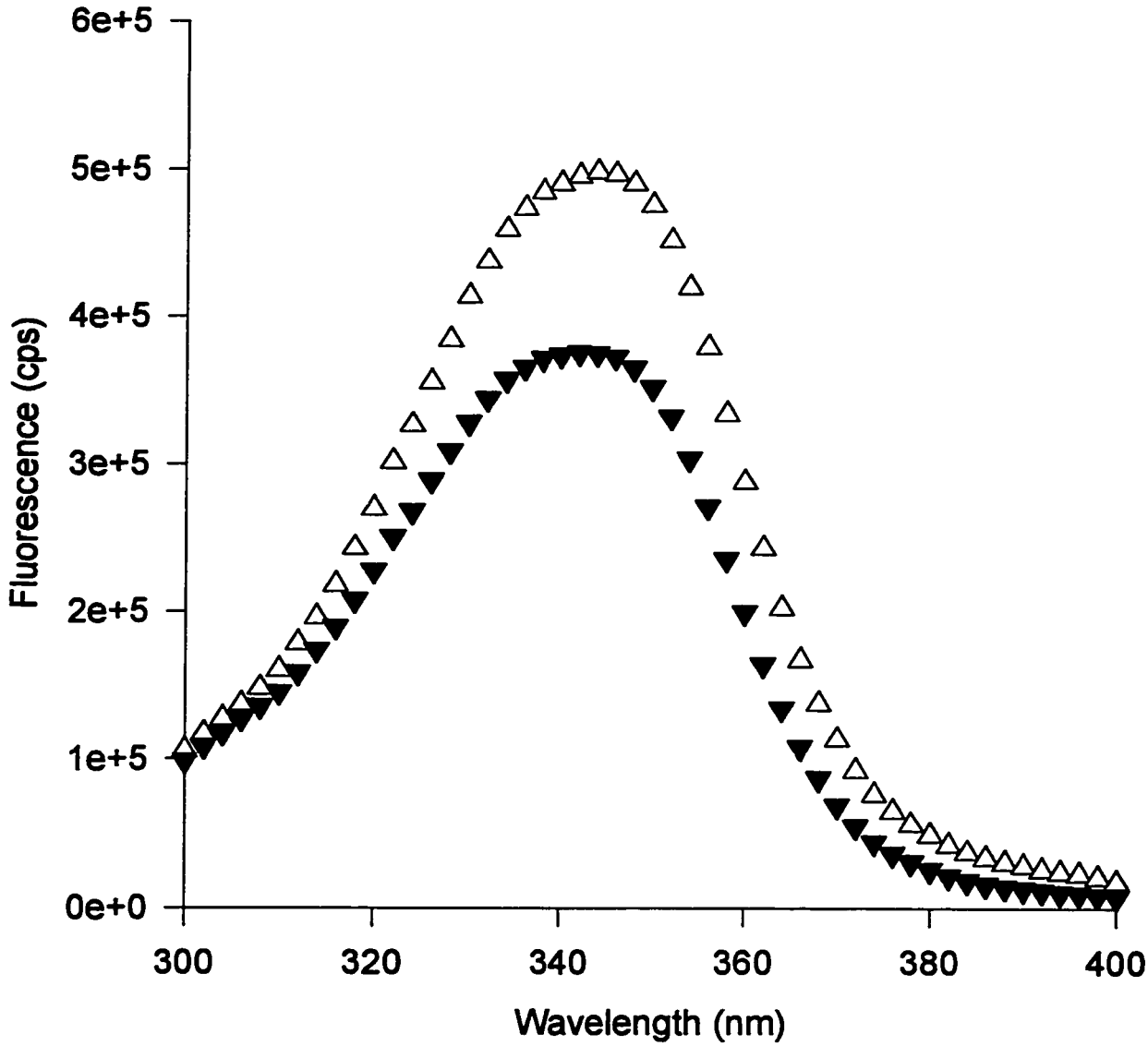
6e+5
5e+5
4e+5
3e+5
2e+5
1e+5
0e+0
Fluorescence (cps)
300
320
340
360
380
400
Wavelength (nm)

Figure 5. Absorbance spectra for 90 μM NPPB. *A:* Percent transmittance decreases with increasing excitation wavelength (300-400 nm) indicating that NPPB absorbs more light at 380 nm than at 340 nm. The percent transmittance at 340 nm is decreased by approximately 35% whereas percent transmittance at 380 nm is decreased by approximately 60%. *B:* Above 480 nm, absorbance decreases and transmittance approaches 100%.

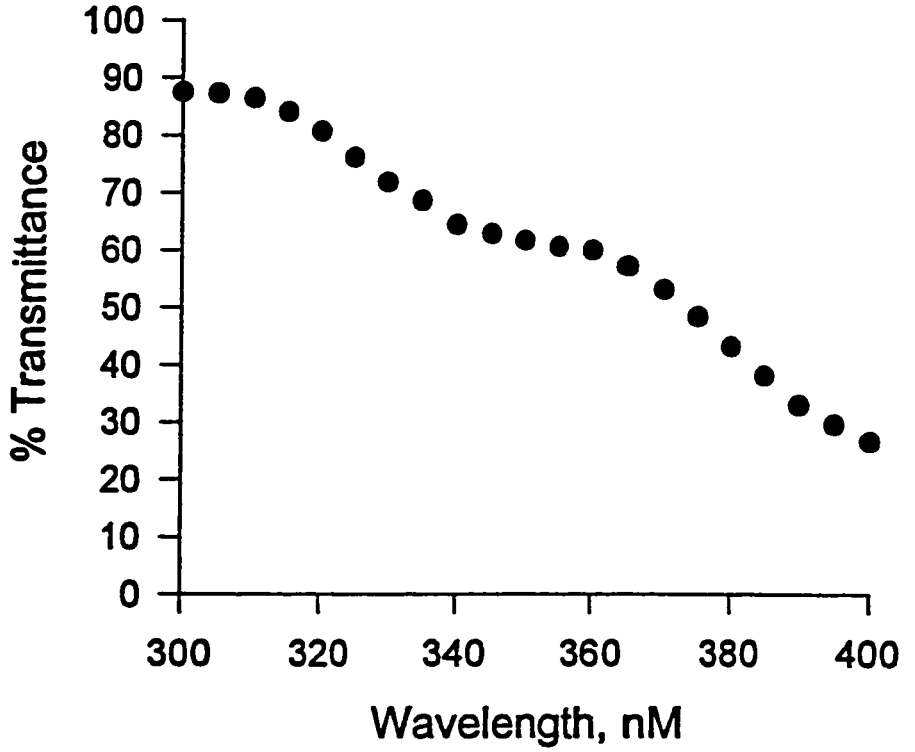
100
90
80
70
60
50
40
30
20
10
0
% Transmittance
300
320
340
360
380
400
Wavelength, nM

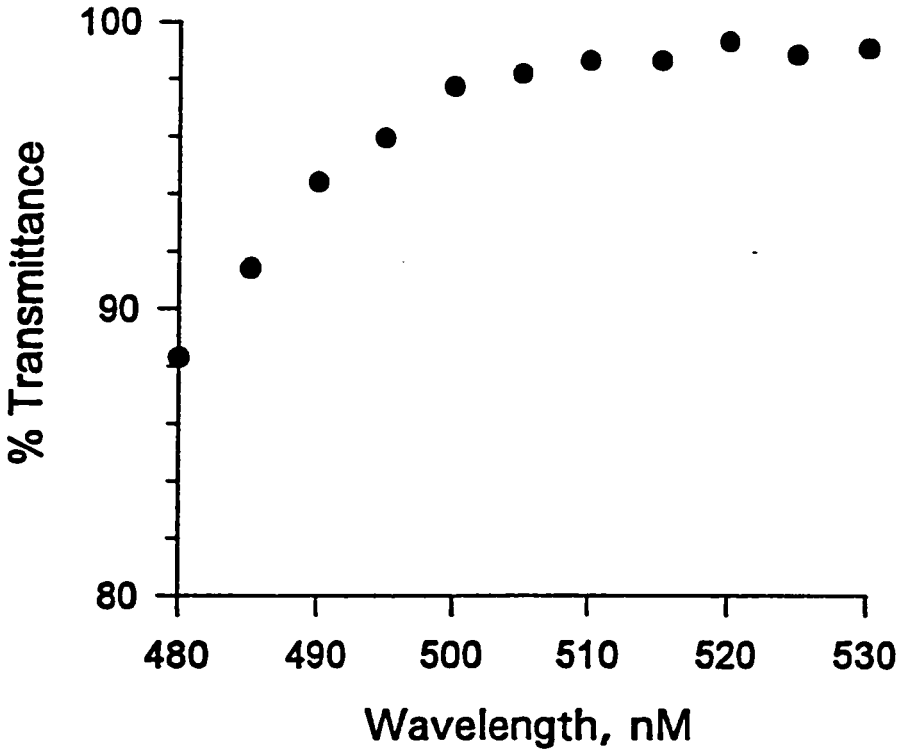
100
90
80
% Transmittance
480
490
500
510
520
530
Wavelength, nM

R_{min} and R_{max} (see below) in the presence of NPPB for each NPPB concentration used, and using these values in the calculation of $[Ca^{2+}]_{free}$ and $[Ca^{2+}]_{total}$ (see Table 2). (R)-IAA-94 at 75 μM had no effect on fura-2 fluorescence at 340 or 380 nm excitation wavelengths (see Figure 6).

Chemical sources: $MgCl_2 \cdot 6H_2O$, Mg-gluconate, $MgBr_2 \cdot 6H_2O$, HEPES, KI, KBr, KCl and KOH were obtained from sources listed above. ATP, creatine phosphokinase and creatine phosphate were obtained from Sigma Chemical Co. (St. Louis, MO). Fura-2 free acid was obtained from Molecular Probes (Eugene, OR). 5-Nitro-2-(3-phenylpropylamino) benzoic acid (NPPB) was obtained from ICN (Montreal, Quebec) and indanyloxyacetic acid ((R)-IAA-94)) was obtained from RBI (Natick, MA).

Fura-2 calibration and determination of $[Ca^{2+}]_{free}$ and $[Ca^{2+}]_{total}$ for isolated cell experiments: When fura-2 is bound to Ca^{2+}, its excitation spectrum is shifted to a shorter wavelength. As Ca^{2+} is taken up by the SR, the Ca^{2+} concentration in the uptake buffer decreases, resulting in a decrease in the ratio (R) of fura-2 emission excited at 340 and 380 nm wavelengths. $[Ca^{2+}]_{free}$ was calculated from the 340/380 ratio (R) using the parameters listed in Table 2, and the following equation (Grynkiewicz et al, 1985):

$$Ca_f = K_{d(Ca2+)} \times \beta \times (R-R_{min})/(R_{max}-R) \quad (1)$$

R_{max} is determined from the 510 nm emission of fura-2 with excitation at 340 nm divided

Figure 6. Fura-2 excitation spectra from 300-400 nm with and without 75 μM (R)-IAA-94. Open triangles show the excitation spectra in KCl buffer (control); closed triangles indicate measurements taken after the addition of 75 μM (R)-IAA-94 to the buffer. Experiments were done at excitation wavelengths of 340 and 380 nm; therefore, the deviation from the control at 300-330 nm did not affect our experimental results.

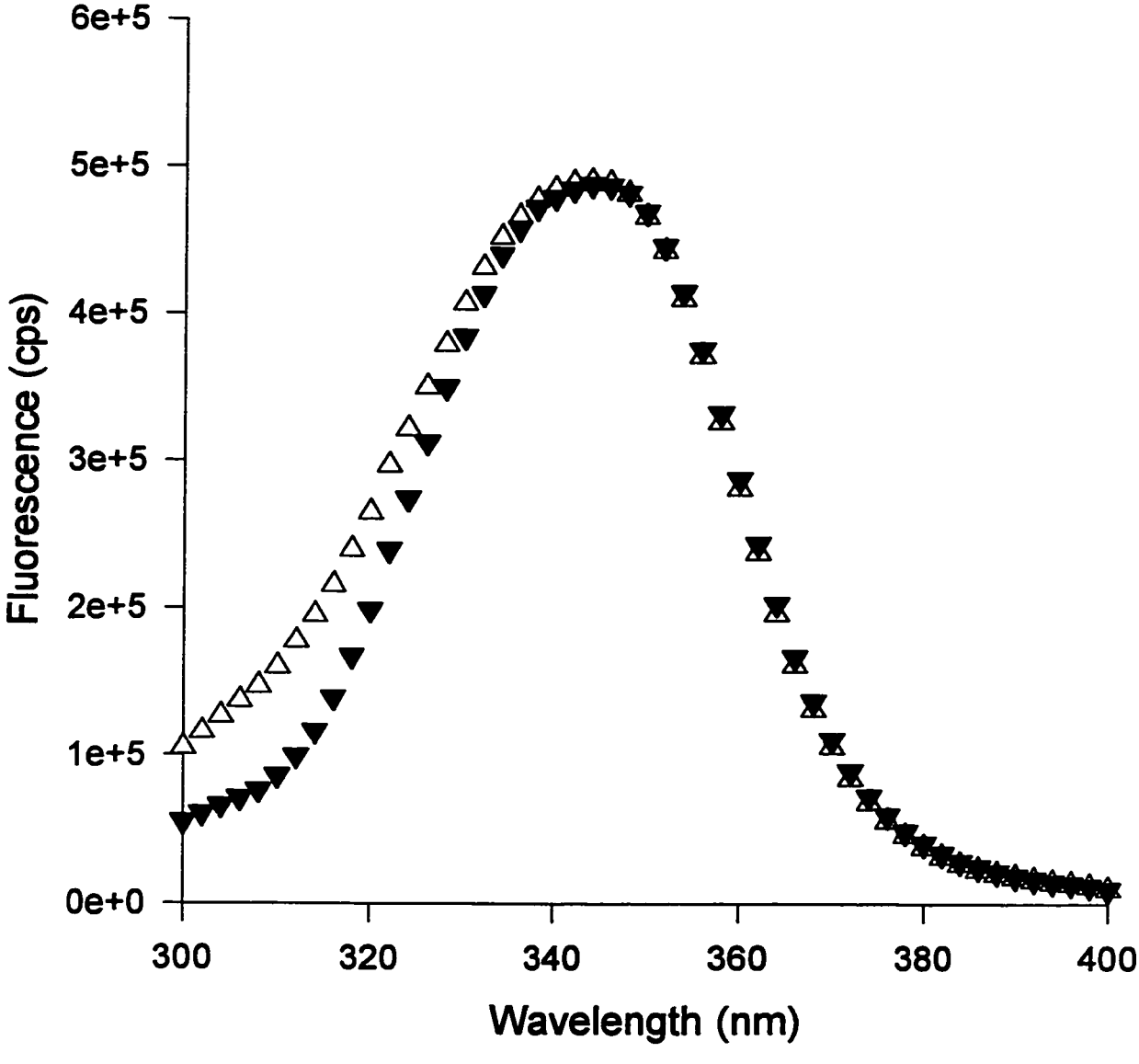
6e+5
5e+5
4e+5
3e+5
2e+5
1e+5
0e+0
Fluorescence (cps)
300
320
340
360
380
400
Wavelength (nm)

Table 2. List of parameters for calculation of $[Ca^{2+}]_{free}$ and $[Ca^{2+}]_{total}$ calculation for smooth muscle cells.

R_{max}	- determined for each day of experiments	pH	- 7.0
R_{min}	- determined for each day of experiments	[buffer]	- 20 mM
β	- determined for each new fura-2 batch	charge	- +1
$K_{dCa2+\text{-}fura\text{-}2}$	- 0.2 μM	pK_a	- 7.55
[fura-2]	- varied, approximately 4.2 μM	total $[Mg^{2+}]$	- 10 mM
[ATP]	- varied, approximately 8 mM	% error	- 0.13
$K_{d(Mg2+)}$	- 5000 μM		
[CP]	- varied, approximately 8.5 mM		
volume	- total volume of cell suspension varied from 57 - 63 μl		
ionic strength	- 0.14 - 0.16		
$[K^+]$	- varied, approximately 135 mM		
Δ time	- 1 second		

by the 510 nm emission with 380 nm excitation when the dye is fully saturated with Ca^{2+} (2.5 mM). R_{min} is the 340 / 380 ratio of fura-2 when it is measured in a zero Ca^{2+} solution made using a high EGTA concentration of 25 mM (final concentration). The experimental R values fall between these R_{max} and R_{min} values. β is the ratio of 510 emission (with excitation at 380 nm) measured in the zero Ca^{2+} solution over that measured for a saturating Ca^{2+} solution (see Grynkiewicz et al., 1985), and was determined for each lot of fura-2 used in this study. β, as well as R_{min} and R_{max} values, were also determined for the ion-substituted buffers (see Table 3): these results show that the β, R_{min}, and R_{max} were not dependent on the anion composition of the buffer. The values obtained in these determinations were used in the calculation of $[Ca^{2+}]_{free}$ and $[Ca^{2+}]_{total}$. R_{min} and R_{max} calibrations were made each day of experimentation to correct for any changes in the relative output of 340 nm and 380 nm light from the xenon lamp. $[Ca^{2+}]_{total}$ was calculated from $[Ca^{2+}]_{free}$, taking into account binding of Ca^{2+}, Mg^{2+} and H^{+} by fura-2, ATP and CP (Kargacin and Kargacin, 1995).

Maximal uptake rates for each sample were calculated from the change in $[Ca^{2+}]_{total}$ over time, and were normalized to protein concentration in that sample aliquot. Protein assays were performed on each sample to obtain a comparative value for each trial on a given day of experimentation. Figure 7 shows the range of values for the rate of Ca^{2+} uptake in controls from four different days. Each set of symbols shows the data from a single set of experiments (and therefore from one cell preparation). Ca^{2+} uptake remained relatively constant for a single preparation if conditions (such as room temperature, pipetting accuracy) were kept constant.

Table 3. Comparison of β, R_{min} and R_{max} values for different buffers. These values were measured for buffers in cuvettes and show that β, R_{min}, R_{max} are not dependent on the anion composition of the uptake buffer.

Buffer	β value	R_{min}	R_{max}
KBr	9.06	0.876	21.77
KI	8.92	0.876	21.70
K-MeS	9.01	0.877	21.53
KCl	8.97	0.886	21.77

Figure 7. Variation in Ca^{2+} uptake rates from four different days of experimentation. Ca^{2+} uptake rates normalized to sample [protein] and expressed as nmol / g/ sec are shown on the y-axis. Samples from different days are shown with separate symbols. Comparision of uptake rates with one symbol type shows the variation in Ca^{2+} uptake rates obtained from a single cell preparation. Experiment numbers indicate the order in which the sample uptake rates were measured and show that the uptake rate remains relatively constant throughout the day. Comparison of uptake rates between symbols shows the variation in Ca^{2+} uptake rates from different cell preparations. The average uptake rate from the cell preparation indicated by closed triangles was 37.6 $\pm$ 14.3 nmol / g / sec, and the open triangles had an average uptake rate of 32.0 $\pm$ 7.2 nmol / g / sec. Ca^{2+} uptake in the experimental condition indicated with open squares is 27.0 $\pm$5.6 nmol / g / sec and with closed circles is 22.2 $\pm$ 9.4 nmol / g / sec.

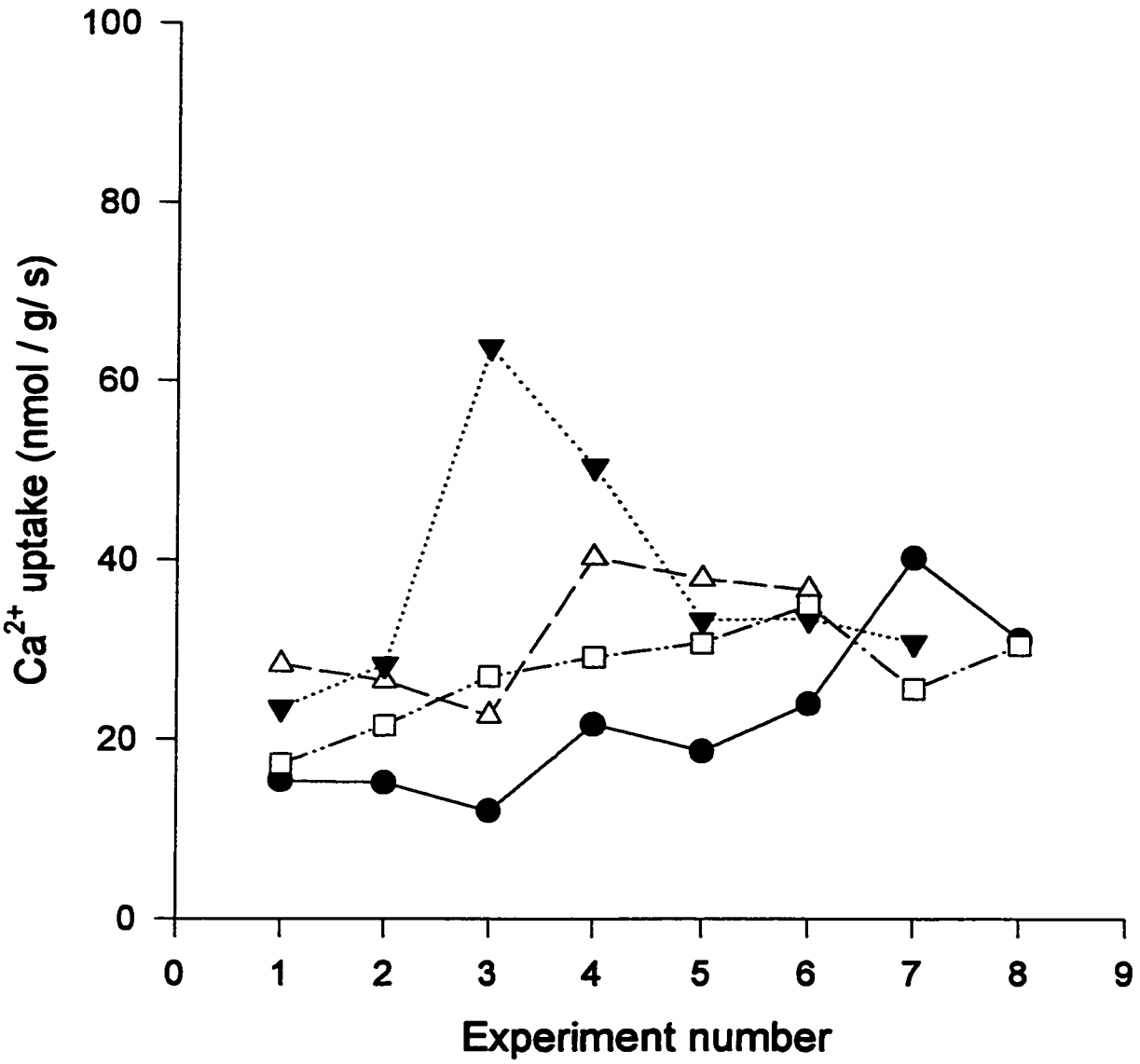
100
80
60
40
20
0
Ca2+ uptake (nmol / g/ s)
0
1
2
3
4
5
6
7
8
9
Experiment number

Calibration buffers and protein assay: R_{max} calibration stock solution contained (in mM): 95 KCl, 20 HEPES-K, 2.5 $CaCl_2$, and 10 $MgCl_2$; pH 7.0. 50 μl of R_{max} stock solution was combined with fura-2 (4 μM final concentration) and a value for R_{max} was obtained as described above. R_{min} calibrations were done using a 100 mM EGTA stock solution (pH 7.0) diluted 1:4 in uptake buffer. After addition of 5 μl fura-2 (4 μM final concentration), R_{min} measurements were performed.

After the completion of an experiment with a single aliquot of cells, the cells suspension in the chamber was pipetted into an Eppendorf tube for later protein assay. The protein samples were commonly diluted 1:100 in uptake buffer. Bradford protein assay dye reagent was diluted 1:4 in double-distilled deionized H_2O and was combined with 100 μl of the diluted protein sample. Absorbance was measured at 595 nm with a spectrophotometer, and protein concentrations were determined from a standard curve obtained with known concentrations of bovine serum albumin (BSA).

Additional quantitative analysis was performed to determine the relative amount of the SR Ca^{2+}-ATPase proteins present in smooth muscle cells washed in KI buffer. This was motivated by the finding that cell preparations washed and resuspended in KI buffers had consistently lower protein concentrations (in 5 of 6 experiments, determined by Bradford protein assay). This led us to suspect that the concentration of the SR pump protein could have been changed relative to the total protein content of the cells. This would produce falsely high or low rates of Ca^{2+} uptake, since our uptake experiments were normalized to the total protein content of the cell samples. To test this possibility, sodium dodecylsulfate polyacrylamide gel electophoresis (SDS-PAGE) and Western blot

analysis were performed to directly measure the amounts of Ca^{2+}-ATPase present in the KI versus KCl cell suspensions relative to the total protein content of the suspension. SDS-PAGE and Western blotting were done in our laboratory by Mr. Erwin Wirch.

SDS-PAGE was done using a 10% polyacrylamide discontinuous buffer system, as described in Laemmli et al. (1970). New England Biolabs (NEB) prestained broad-range molecular weight markers were used to determine the approximate molecular weight of the pump protein. Using the Western blotting technique, proteins were blotted onto nitrocellulose membrane (see Higashihara et al., 1989). After blocking overnight in 1% Boeringer-Mannheim blocking reagent/Tris-HCl buffered saline (TBS), the membrane was incubated in 1:100 dilution of purified antibody to the SERCA2b Ca^{2+} pump (0.16 mg/ml) for two hours in 0.5% blocker/TBS with shaking. The membrane was then washed four times (10 minutes each) with TBS/ 0.5% Tween-20 and incubated for one hour with peroxidase-conjugated (POD) anti-mouse IgG. The membrane was then washed four times and SERCA2b was visualized using a chemiluminescent substrate from Boehringer-Mannheim and X-OMAT-AR film. The Ca^{2+}-ATPase migrated as a band at approximately 110 kDa. The Ca^{2+}-ATPase bands were then quantified using scanning densitometry with a Pharmacia LKB Image Master.

Chemical sources for dye calibration, protein assay, SDS-PAGE and Western blotting: R_{max} and R_{min} buffers were made with components previously specified for the uptake buffers. Monoclonal anti-SERCA2b was developed in our laboratory by Dr. Zenobia Ali and Ms. Gail McMartin. The dye reagent for the protein assay, the Coomassie Brilliant

Blue R-250 and the anti-mouse IgG were all obtained from BioRad Laboratories (Hercules, CA). SDS, nitrocellulose and polyacrylamide were all purchased from Sigma (St. Louis, MO). The broad molecular weight standards were purchased from New England Biolabs (Beverly, MA). X-OMAT-AR film was purchased from Kodak. All other chemicals and reagents were of Analar grade or better and purchased from BDH. The POD, blocking reagent and chemiluminescent substrate were also from Boehringer-Mannheim (Laval, Quebec).

Data analysis for isolated cell experiments: For each experiment, data points were chosen so that the maximal Ca^{2+} uptake rate (nmol Ca^{2+}/ g protein/ sec) could be calculated. The mean $[Ca^{2+}]_{free}$ during the time that the uptake rate was measured was subsequently determined. The maximum uptake rates occurred at roughly the same time point after initiation of Ca^{2+} uptake by addition of ATP to the chamber. We also wanted to determine uptake rates before the SR accumulated a substantial amount of Ca^{2+}, which would limit the rate of uptake into the SR. Ca^{2+} uptake was first recorded as a decline in 340/380 fluorescence ratio (Figure 8A), after correction for background fluorescence and light scatter. Background fluorescence and light scatter was determined before the addition of ATP and fura-2 to the cell suspension and buffer in the chamber. This was determined for each sample at the beginning of each experiment, to correct for chamber imperfections. The decline in the 340/380 fluorescence ratio with time is a reflection of a decrease in $[Ca^{2+}]_{free}$ in the buffer. $[Ca^{2+}]_{free}$ and $[Ca^{2+}]_{total}$ calculations were then completed and the resulting concentration versus time curves were each graphed

separately (see Figure 8B & 8C). The negative slope of the $[Ca^{2+}]_{total}$ versus time curve, $(-\Delta[Ca^{2+}]_{total} / \Delta(t))$, was used to calculate the Ca^{2+} uptake rate according to the following equation:

$$\text{velocity} = (\text{volume/weight}) \times (-\Delta[Ca^{2+}{}_{total}]/\Delta(t)) \qquad (2)$$

where volume is the volume of solution in the chamber and weight is the total amount of protein in the chamber. Data points used to obtain the negative slope on the $[Ca^{2+}]_{total}$ versus time graph were chosen so that the maximal Ca^{2+} uptake rate was obtained for each experiment. This generally took approximately 26 data points, however, additional points were used when the initial rate of Ca^{2+} uptake was not at a maximum for that experiment. On the $Ca^{2+}{}_{free}$ graph, the points which correspond to those on the $Ca^{2+}{}_{total}$ versus time plot that were used to find the slope were then averaged to determine the mean $[Ca^{2+}]_{free}$ for that data segment. The data were then plotted as uptake rate vs. mean $[Ca^{2+}]_{free}$ for the data segment used in the calculation (see Figure 8D).

Ca^{2+} UPTAKE EXPERIMENTS USING CARDIAC SR VESICLES

SR vesicles in uptake buffer: Measurements of Ca^{2+} uptake by cardiac SR vesicles were made in a manner similar to those made for the isolated cell experiments described above. They were, however, performed in cuvettes in a sample compartment, rather

Figure 8. Determination of Ca^{2+} uptake rates for isolated cell experiments. *A.* 340/380 fluorescence ratio versus time, after correction for background fluorescence and light scatter. *B.* Ca^{2+}_{free} (μM) versus time (s) graph (determined from equation 1), showing the data segment (open circles) which corresponds to the Ca^{2+}_{total} versus time data points (C) from which the slope was obtained. The average $[Ca^{2+}]_{free}$ for the highlighted area was 0.986 μM. *C.* Ca^{2+}_{total} (μM) versus time (s) graph. The negative value of the slope (0.043 μM/sec), along with a sample volume of 57 μM and sample protein concentration of 5.0 μg/ml was used to calculate the Ca^{2+} uptake rate. *D.* Data point indicating the rate of Ca^{2+} uptake (μmol/g/s) at a mean Ca^{2+}_{free} (μM). The Ca^{2+} uptake rate in this case was 8.62 nmol/g/s.

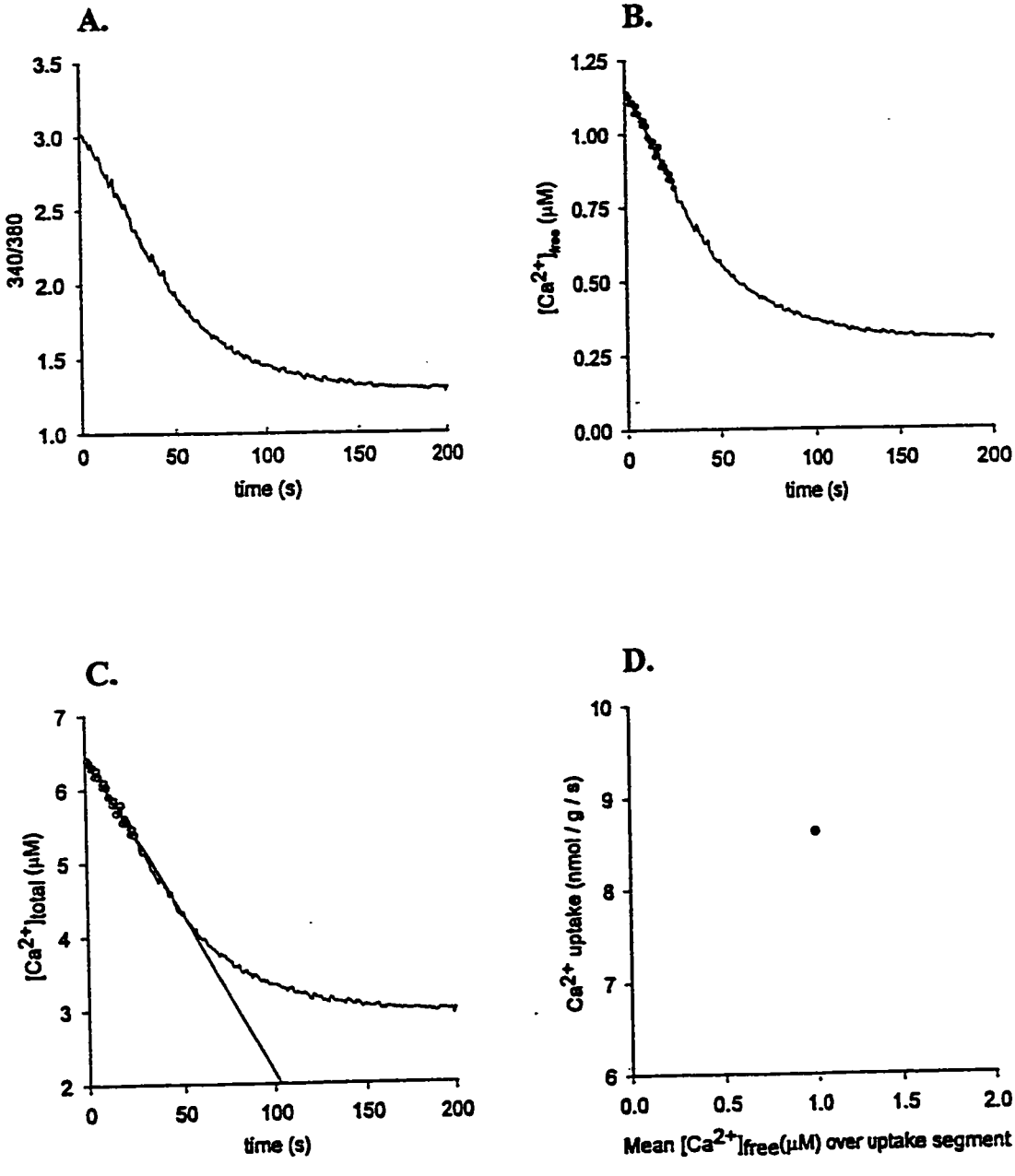
A.
3.5
3.0
2.5
2.0
1.5
1.0
340/380
0
50
100
150
200
time (s)
B.
1.25
1.00
0.75
0.50
0.25
0.00
[Ca2+]free (μM)
0
50
100
150
200
time (s)
C.
7
6
5
4
3
2
[Ca2+]total (μM)
0
50
100
150
200
time (s)
D.
10
9
8
7
6
Ca2+ uptake (nmol / g / s)
0.0
0.5
1.0
1.5
2.0
Mean [Ca2+]free(μM) over uptake segment

Figure 9. Experimental setup for experiments with cardiac SR vesicles. The experimental apparatus used for SR vesicles closely resembles that of the isolated cell setup as described in the legend for Figure 1. However, the fibre optic cable was attached to a sample compartment which contained a cuvette (with the SR, buffer, fura-2 and ATP). The contents of the cuvette were continuously mixed with a stir bar. Emitted light is passed through a 10 nm band pass filter centred at 510 nm and a shutter, and was detected by a photomultiplier tube (PMT).

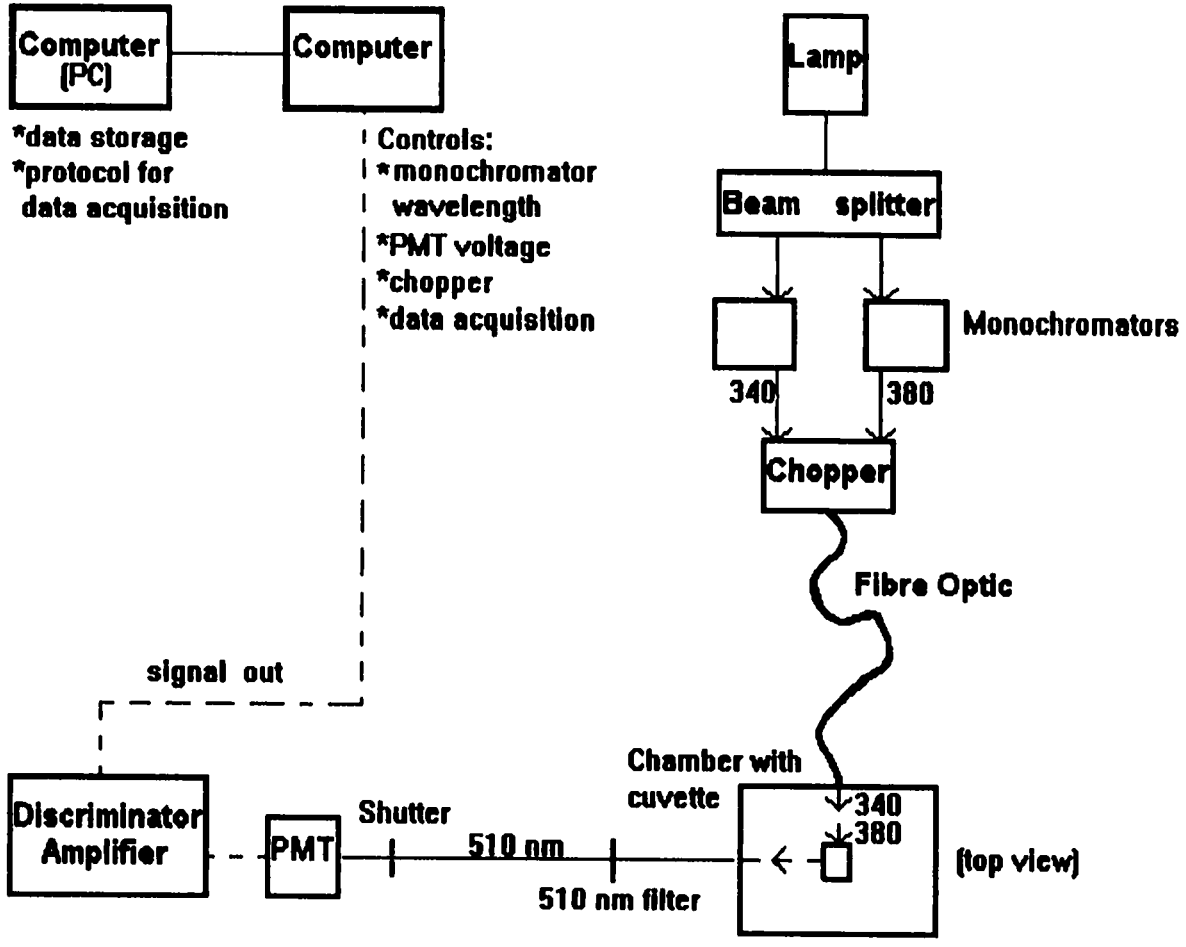
Computer (PC)
Computer
*data storage
*protocol for data acquisition
Controls:
*monochromator wavelength
*PMT voltage
*chopper
*data acquisition
Lamp
Beam splitter
Monochromators
340
380
Chopper
Fibre Optic
signal out
Chamber with cuvette
340
380
(top view)
Discriminator Amplifier
PMT
Shutter
510 nm
510 nm filter

than in a chamber on a microscope stage (see Figure 9). Samples of 125-250 μg SR protein from canine cardiac tissue were added to 2 ml of uptake buffer in a cuvette. In addition to the SR and buffer, ATP (final concentration 1.8 mM), CP (final concentration 1.9 mM), CPK (final concentration 3.1 U/ml) and fura-2 (final concentration 2.9 μM) were added to the cuvette. Addition of Ca^{2+} to the cuvette was required to initiate uptake in the cardiac SR experiments since $[Ca^{2+}]_{free}$ was below usually 1 μM without Ca^{2+} added. Experiments were carried out at room temperature (20-22 °C) and cuvette contents were continuously stirred during the course of the experiment.

Solutions and compounds for canine cardiac SR vesicles: Uptake buffers for SR vesicles were made in double-distilled, deionized H_2O and had a pH of 7.0. The KCl buffer contained (in mM): 100 KCl, 4 $MgCl_2$ and 20 HEPES-K. KBr buffer contained 100 KBr, 4 Mg-gluconate and 20 HEPES-K; KI buffer contained 100 KI, 4 Mg-gluconate and 20 HEPES-K; K-methanesulfonate buffer contained 100 K-methanesulfonate, 4 Mg-gluconate and 20 HEPES-K. ATP and fura-2 stock solutions were the same as those used for uptake experiments using isolated cells. Stock solutions of the Cl^- channel blockers, NPPB and (R)-IAA-94 were the same as described above. Reagents were obtained from the sources listed above.

Experimental setup for vesicle experiments: The experimental apparatus used to monitor Ca^{2+} uptake for canine cardiac SR vesicle experiments is shown in Figure 9. The setup is the same as that used for the isolated cell experiments, with the exception that the fibre

optic cable illuminated a cuvette in a separate sample compartment. The solution in the cuvette was constantly stirred. Emitted light passed through a 510 nm filter (10 nm band pass) and a shutter, and was then detected with a photomultiplier tube.

Determination of Ca^{2+} uptake rates and data analysis for vesicle experiments: Ca^{2+} uptake rates were determined in a manner similar to that described above for the isolated cell experiments. R_{max} calibration was performed using 2 ml of the R_{max} calibration buffer and 2.9 μM fura-2. R_{min} calibrations were obtained using a 100 mM EGTA solution, diluted 1:4 in uptake buffer to a total volume of 2 ml (final EGTA concentration 25 mM). 2.9 μM fura-2 was added for the measurements. Graphs obtained from the cardiac SR vesicles were similar to those obtained using skinned smooth muscle cells.

CARDIAC SR VESICLE EXPERIMENTS WITH OXALATE

Experiments were also performed using uptake buffers which contained 10 mM oxalate. Oxalate is capable of crossing the SR membrane, and acts as a Ca^{2+} precipitating anion within vesicles. This results in an acceleration of the rate and amount of Ca^{2+} uptake because efflux of Ca^{2+} from the SR is minimized and Ca^{2+} accumulation within the SR does not inhibit further uptake when SR Ca^{2+} is bound to oxalate (Inesi and de Meis, 1989). Because oxalate permits greater unidirectional Ca^{2+} movement, quantification of V_{max}, Hill coefficient and $Ca^{2+}{}_{50\%}$ were possible.

In these experiments, SR vesicles were initially diluted in uptake buffers without oxalate to a concentration of 1 mg/ml. From this dilution, 20 μg of cardiac SR vesicles were added to a 3 ml cuvette along with 2 ml uptake buffer containing 10 mM oxalate. This allowed oxalate to equilibrate across the SR membrane. In addition to the SR and buffer, ATP (final concentration 1.8 mM), CP (final concentration 1.9 mM), 3.1 U/ml CPK, and fura-2 (final concentration 2.9 μM) were added to the cuvette. Measurements were made as described above (see Ca^{2+} uptake experiments for cardiac SR vesicles).

Determination of uptake velocity and data analysis for cardiac SR experiments with oxalate: After correction for background fluorescence and light scatter, the 340/380 fluorescence data were smoothed using a moving window averaging technique (Kargacin and Kargacin, 1995). The Ca^{2+}_{free} versus time curves were calculated from the 340/380 ratio vs time data using equation (1) as described above. The Ca^{2+}_{total} versus time data were calculated as described above also taking into account the binding of Ca^{2+} to oxalate. In the calculations, a K_d for Ca^{2+}-oxalate of 4 mM (Hove-Madsen and Bers, 1993) was used. The Ca^{2+}_{total} versus time graph was used to determine instantaneous velocity (μmoles Ca^{2+} / mg / minute) using the following equation:

$$\text{velocity} = (\text{volume/mg protein}) \times (-\Delta[Ca^{2+}]_{total}/\Delta(t)) \qquad (3)$$

The maximal velocity of Ca^{2+} uptake (V_{max}), the Hill coefficient (nH), and the Ca^{2+}_{free}

concentration at half-maximal pump velocity ($Ca^{2+}_{50\%}$) were calculated from a plot of uptake velocity versus Ca^{2+}_{free}. A commercially available curve-fitting program (Sigma Plot, Jandel Scientific) was used to fit the velocity versus $[Ca^{2+}]_{free}$ curve to the following equation and to determine the values for V_{max}, nH, and $Ca^{2+}_{50\%}$:

$$V/V_{max} = ([Ca^{2+}]_{free}{}^{nH})/([Ca^{2+}]_{50\%}{}^{nH} + [Ca^{2+}]_{free}{}^{nH}) \qquad (4)$$

Sample calculations for the determination of uptake velocity and the kinetic parameters described are illustrated in Figure 10.

Figure 10. Determination of Ca^{2+} uptake rates for cardiac SR vesicle experiments with oxalate. The calculations used are similar to those described in the legend for Figure 3. However, with the inclusion of oxalate in the buffer, the binding of Ca^{2+} to oxalate was accounted for in the calculation of $[Ca^{2+}]_{total}$. The 340/380 fluorescence data was smoothed using a moving window averaging technique. *A.* 340/380 ratio versus time (s). *B.* Ca^{2+}_{free} (μM) versus time (s). *C.* Ca^{2+}_{total} (μM) versus time (s). *D.* Instantaneous velocity (μmoles/mg/min) versus Ca^{2+}_{free} (μM). This was calculated from the Ca^{2+}_{total} vs. time graph and from the data in *B.* A maximal velocity of 0.449 μmol/min/mg, a Hill coefficient of 2.00 and a $Ca^{2+}_{50\%}$ of 0.386 μmol were determined from this graph.

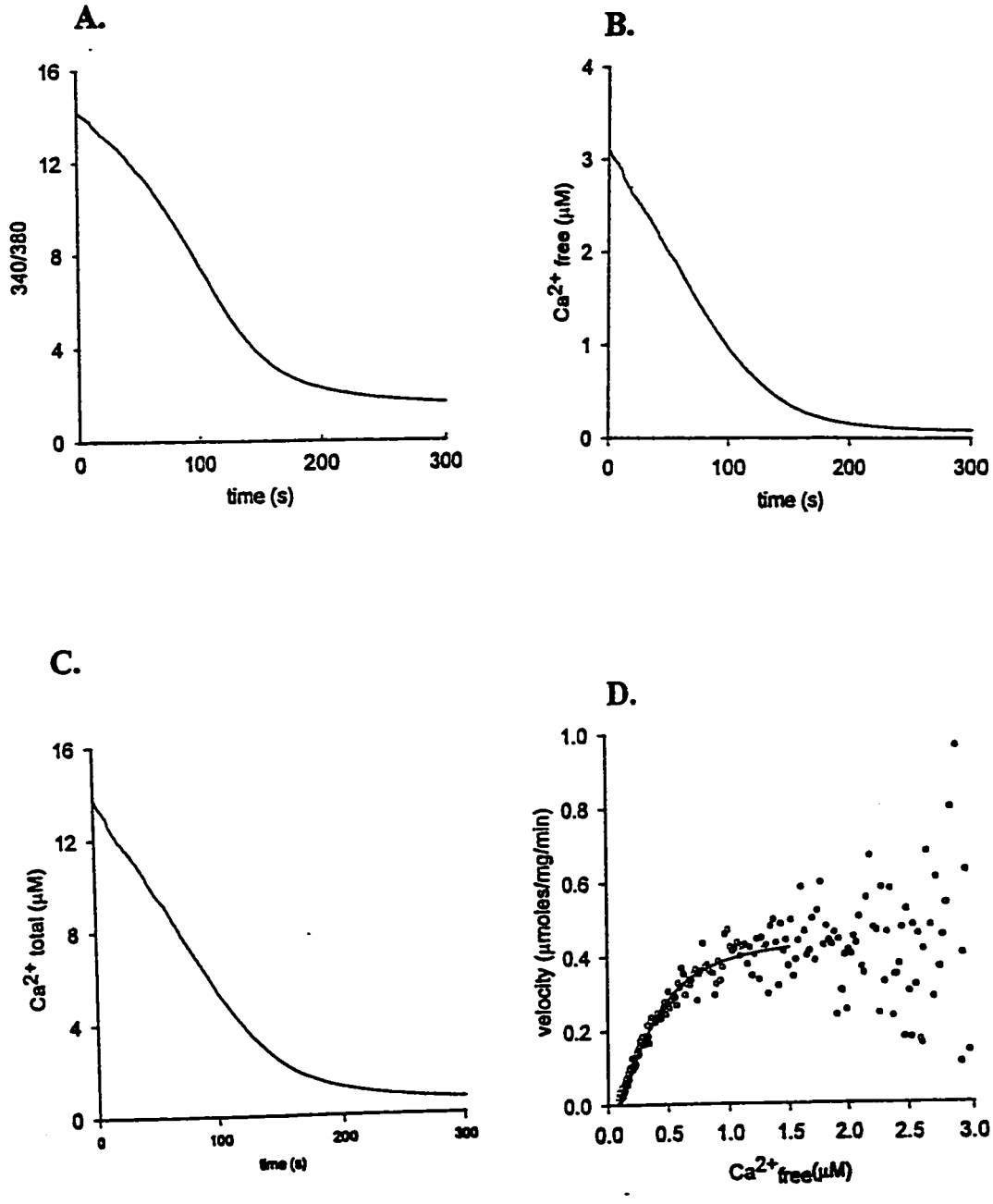
A.
340/380
time (s)
B.
Ca2+ free (µM)
time (s)
C.
Ca2+ total (µM)
time (s)
D.
velocity (µmoles/mg/min)
Ca2+free(µM)

RESULT

SMOOTH MUSCLE CELLS

Effect of NPPB on SR Ca^{2+} uptake

To examine the effects of NPPB on SR Ca^{2+} uptake, NPPB concentrations of 6 μM and 17 μM were used. These concentrations were chosen to minimize the non-specific effects of the blocker which have been reported in the literature (100 μM NPPB was found to demonstrate protonophoric activity and a related activation of K_{ATP} channels in neutrophils and macrophages; Lukacs et al., 1991). Lower concentrations have been shown to be effective in inhibiting plasma membrane Cl^- channels. The K_i values for the inhibition of sarcolemmal Cl^- channels by NPPB were found to range from 0.1-100 μM in phagocytic cells (Lukacs et al., 1991). Sorota et al. (1994) found NPPB to be effective in concentrations between 10-40 μM, which produced an immediate, reversible blockage of the swelling-induced plasmalemmal Cl^- channel in canine cardiac myocytes.

Ca^{2+} uptake was measured in saponin-permeabilized, isolated smooth muscle cells from rabbit stomach as described in the *Methods* section. For the experiments, total volume was kept constant and serial dilutions of the NPPB stock solution were used to lower [NPPB]. NPPB was added and mixed with the cell suspension immediately before ATP was added to initiate Ca^{2+} uptake. To ensure that pipetting errors did not create inconsistencies in uptake rates, the results of the experiments were normalized to the

protein content of the chamber (measured using the micro-assay method described in *Methods*). Ca^{2+} uptake rates are reported in nmol Ca^{2+}/g protein/sec.

Ca^{2+} uptake was inhibited significantly with 17 μM NPPB. Figure 11 shows typical traces of $[Ca^{2+}]_{free}$ versus time for a control experiment and an experiment done in the presence of 17 μM NPPB. Maximum uptake rate in the control experiment was 16.7 nmol/g/sec. As [NPPB] increased, uptake rate decreased; the Ca^{2+} uptake rate in the presence of 17 μM NPPB was 11.4 nmol/g/sec. Figure 12 summarizes the results of 27 samples from 2 cell preparations in which the initial rate of Ca^{2+} uptake was determined in the presence of 0, 6 μM and 17 μM NPPB. The addition of 6 μM NPPB did not affect the initial rate of Ca^{2+} uptake ($p = 0.24$). The addition of 17 μM NPPB decreased the initial rate of Ca^{2+} uptake by 54.7 $\pm$ 18.9%, with a p value of 1.2×10^{-4}. In this and ensuing experiments, p values were determined using the unpaired t-test. The initial uptake rates in KCl buffer from one data set were grouped and compared to a second group of uptake rates in the buffer of interest, from the same day of experimentation. Statistical significance was defined as $p \leq 0.01$.

Effect of (R)-IAA-94 on SR Ca^{2+} uptake

(R)-IAA-94 has been used as an inhibitor of Cl^- channels in experiments on a variety of tissue sources. Sorota et al. (1994) found that 100 μM (R)-IAA-94 fully blocked swelling-induced Cl^- channels of the plasma membrane of dog atrial cells

Figure 11. Effect of NPPB on Ca^{2+} uptake in smooth muscle cells. Traces show the decrease in $[Ca^{2+}]_{free}$ (μM) vs. time (s) for two experiments. Ca^{2+} uptake rate in the control trace (labelled as 0) was 16.7 nmol/g/sec (determined at the steepest part of the curve). In the second experiment (labelled as 17), 17 μM NPPB was added at t = 0, and slowed the rate of uptake to 11.4 nmol/g/sec.

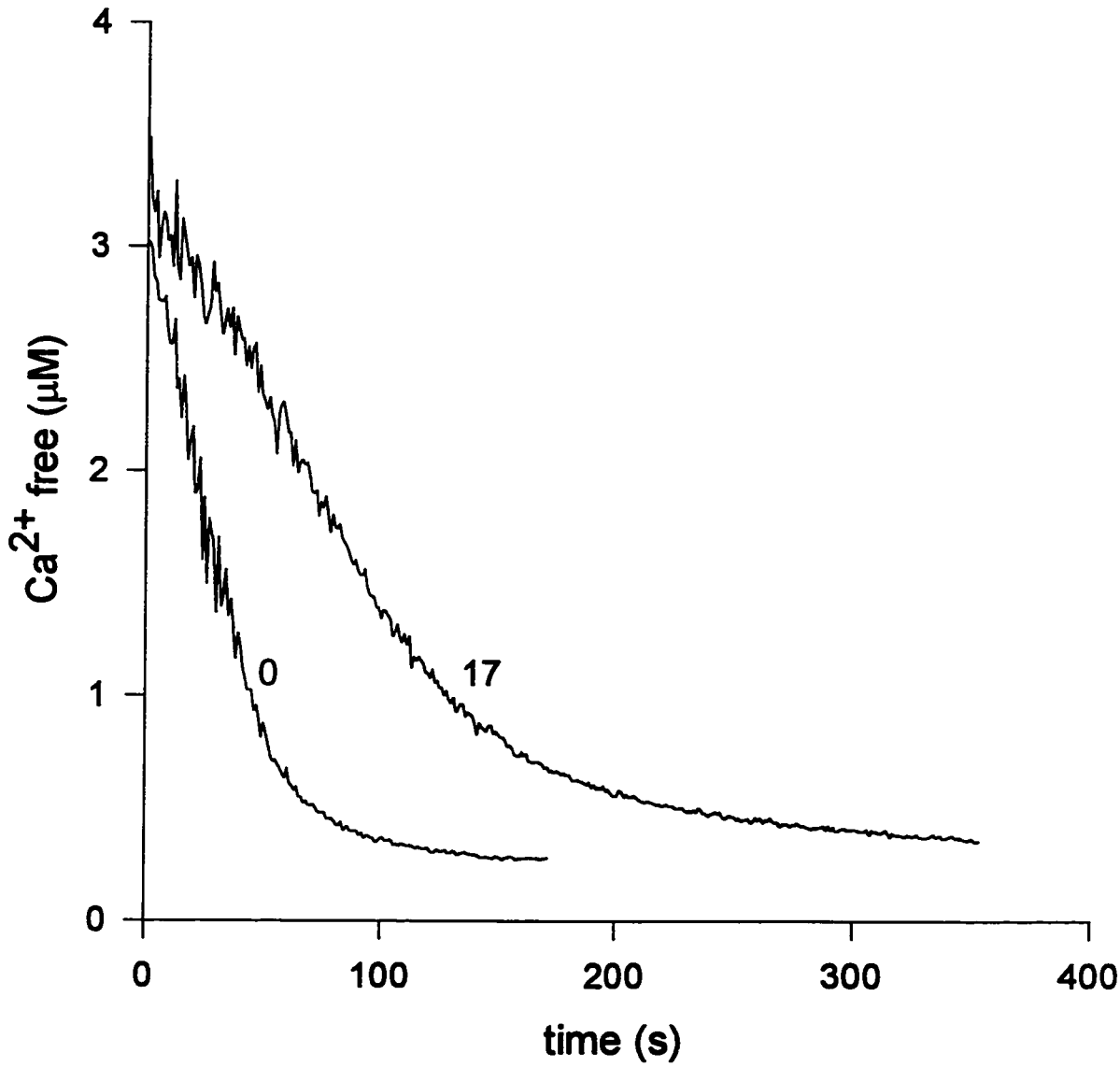
4
3
2
1
0
Ca^{2+} free (μM)
0
17
0
100
200
300
400
time (s)

Figure 12. Summary of the effect of NPPB on the maximum rate of Ca^{2+} uptake in smooth muscle cells. The uptake rates were normalized to the mean value for control, which was defined as 100% (n = 15). The error bar for the control trace shows the standard deviation (SD) of the individual control rates relative to the mean uptake rate. 6 μM did not reduce Ca^{2+} uptake to a significant degree ($p = 0.24$). 17 μM NPPB (n = 8) decreased the uptake rate to 45.3% ($\pm$ 18.9) of the control. This was significant at $p = 1.2 \times 10^{-4}$. * indicates statistical significance at $p \leq 0.01$.

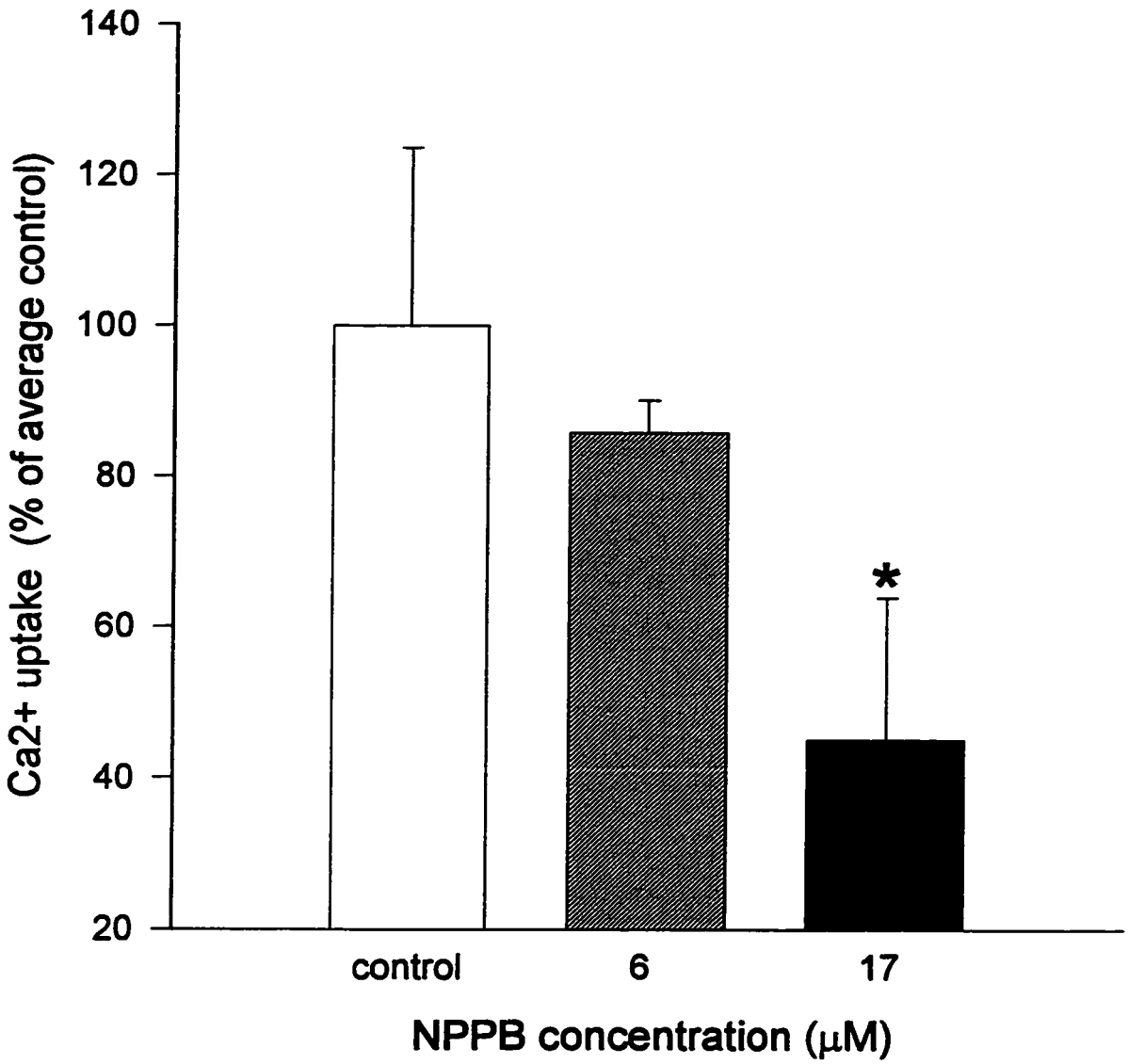
140
120
100
80
60
40
20
Ca2+ uptake (% of average control)
*
control
6
17
NPPB concentration (μM)

after a 20-minute incubation. The effect was slowly reversible and required another 20 minutes to wash out completely. Redhead et al. (1992) used (R)-IAA-94 to screen for a Cl^- channel in bovine kidney cortex microsomes. The purified 64 kDa channel was presumed to be from intracellular membranes, based on the presence of Golgi markers (Redhead et al., 1992). Weber-Schurholz et al. (1993) observed an (R)-IAA-94-sensitive Cl^- channel which was localized in the sarcolemma but not the SR membrane. This drug has not been tested on smooth muscle SR Cl^- channels to date, nor has it been tested on cardiac SR vesicles.

Experiments in saponin permeabilized smooth muscle cells demonstrated a dose-dependent decrease in Ca^{2+} uptake with increasing [(R)-IAA-94]. We found (R)-IAA-94 had an inhibitory effect on Ca^{2+} uptake as soon as it was added to the cell suspension. Figure 13 shows the results of three experiments in which the rate of Ca^{2+} uptake was measured in the presence of 1μM and 17 μM (R)-IAA-94. The control experiment demonstrated maximal uptake, with a Ca^{2+} uptake rate of 58.7 nmol/g/sec. In this set of experiments, the initial rate of Ca^{2+} uptake was reduced to 21.9 nmol/g/sec with 1 μM (R)-IAA-94, and in 17 μM (R)-IAA-94 uptake was further reduced to 2.8 nmol/g/sec.

Figure 14 combines data from three cell preparations. The addition of 1 μM (R)-IAA-94 to the cell suspension decreased the initial rate of Ca^{2+} uptake to 49.5 $\pm$ 21.1% of the mean control rate, set at 100% ($\pm$ 44.7%). 17 μM (R)-IAA-94 decreased Ca^{2+} uptake to 13.5 $\pm$ 10.7%. The number of individual experiments were 25, 7, and 9 for the control, 1 μM, and 17 μM, respectively. The concentrations over which (R)-IAA-94 inhibited Ca^{2+} uptake in our experiments are consistent with its action on Cl^- channels.

Figure 13. Effect of (R)-IAA-94 on Ca^{2+} uptake in smooth muscle cells. Traces show the decrease in $[Ca^{2+}]_{free}$ (μM) vs. time (s) for three different experiments: The control experiment (labelled trace 0) had an uptake rate of 58.7 nmol/g/sec. In the presence of 1 μM (R)-IAA-94 (labelled trace 1), Ca^{2+} uptake was 21.9 nmol/g/sec. In the presence of 17 μM (R)-IAA-94 (labelled trace 17) Ca^{2+} uptake was 2.78 nmol/g/sec. All uptake rates were determined from the steepest part of the curve.

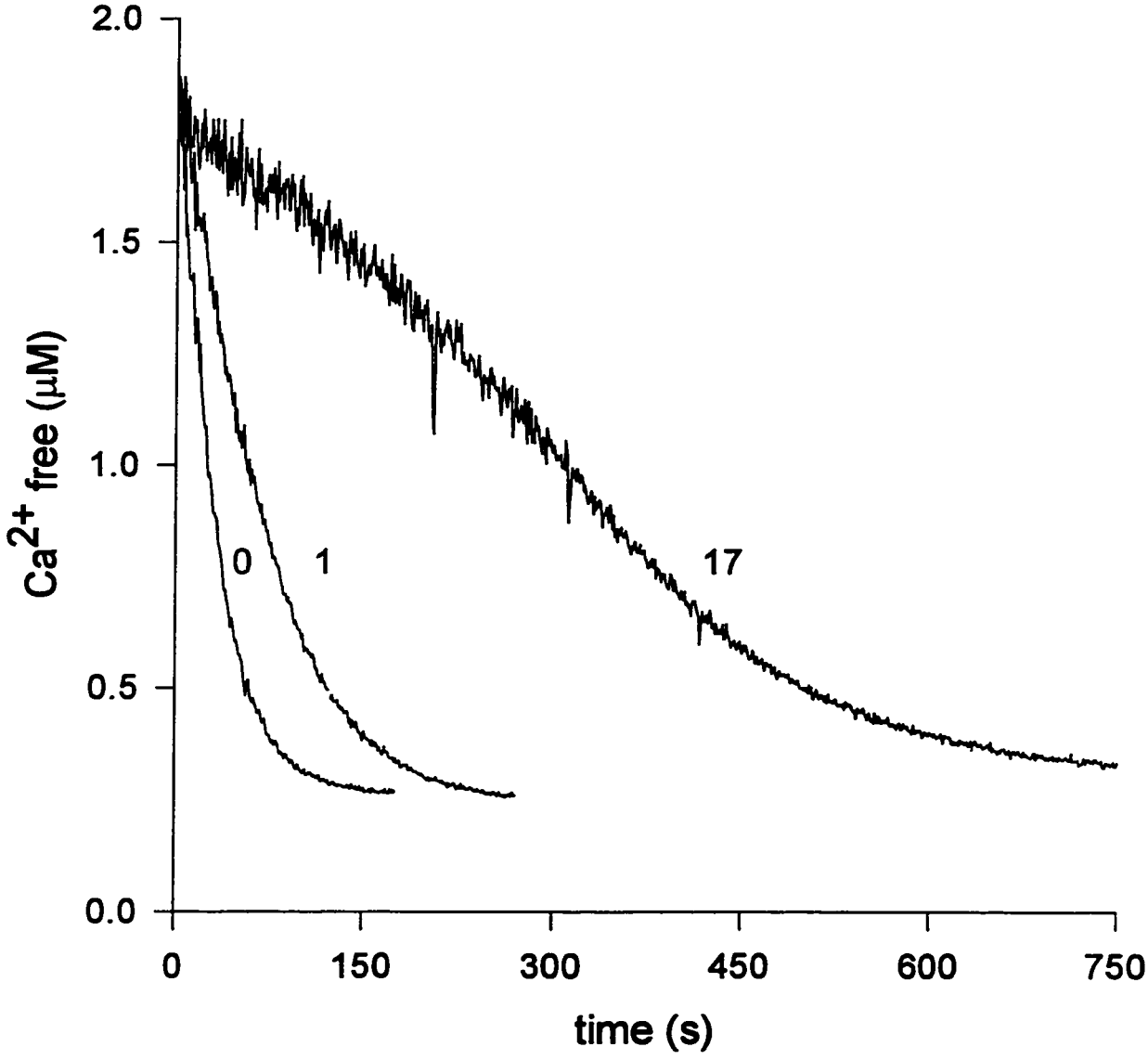
2.0
1.5
1.0
0.5
0.0
Ca^{2+} free (μM)
0
1
17
0
150
300
450
600
750
time (s)

Figure 14. Summary of the effect of (R)-IAA-94 on the rate of initial Ca^{2+} uptake in smooth muscle cells. This figure combined the data from three different cell preparations. The uptake rates were normalized to the mean value for control, which was defined as 100% (n = 25). The error bar for the control trace shows the standard deviation (SD) of the individual control rates for an experiment relative to the mean uptake rate for the same experiment. 1 μM (R)-IAA-94 decreased the initial rate of Ca^{2+} uptake to 49.5 $\pm$ 21.1% of the control (n = 7). 17 μM (R)-IAA-94 decreased initial uptake rate to 13.5 $\pm$ 10.7% of the control (n = 9). Both 1 μM ($p = 0.007$) and 17 μM ($p = 3 \times 10^{-6}$) (R)-IAA-94 inhibited Ca^{2+} uptake significantly. Error bars are +1 standard deviation. * indicates significant difference at $p \leq 0.01$

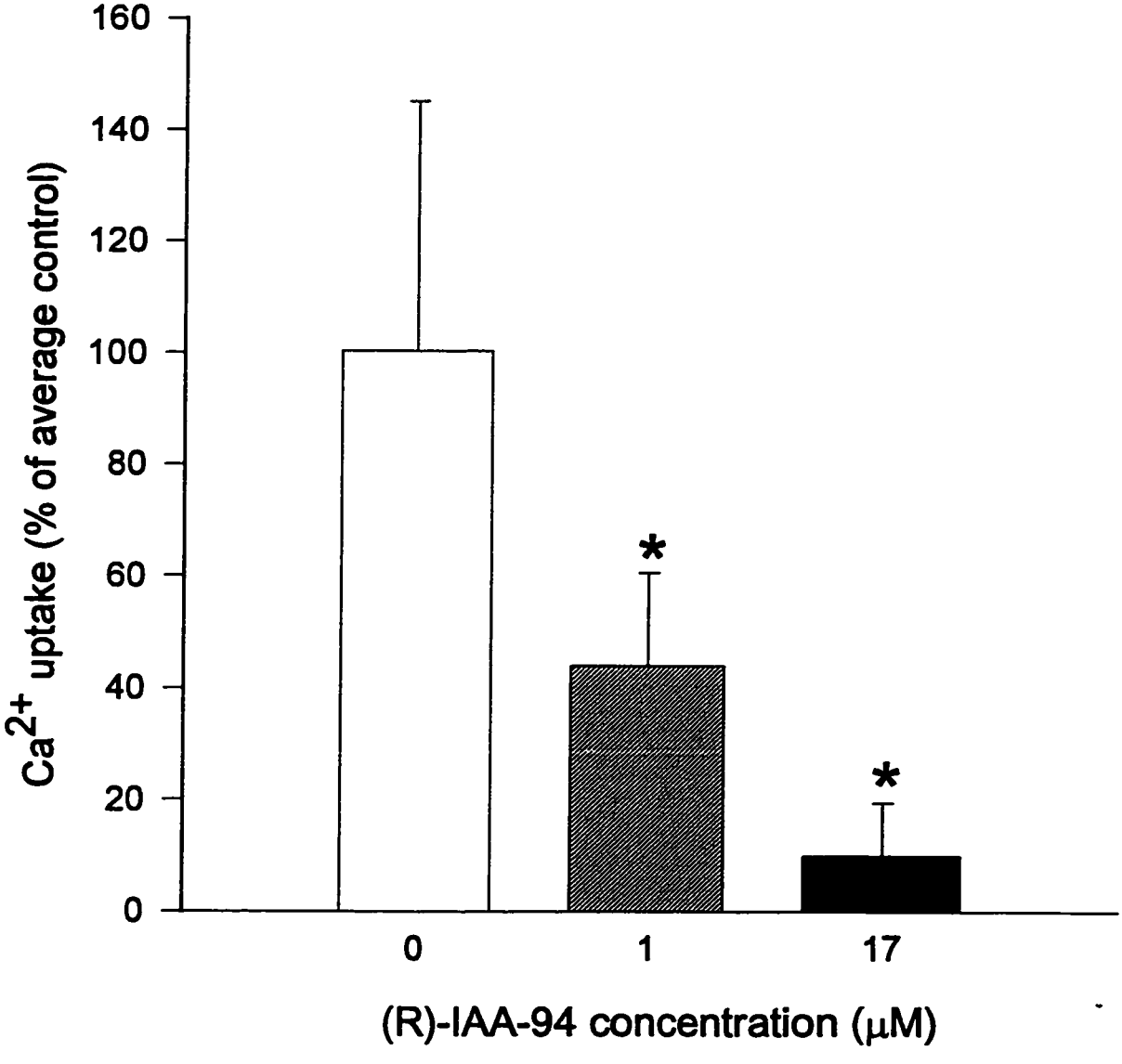
160
140
120
100
80
60
40
20
0
Ca^{2+} uptake (% of average control)
*
*
0
1
17
(R)-IAA-94 concentration (μM)

Landry et al. (1989) observed that (R)-IAA-94 was a potent Cl^- channel inhibitor in bovine tracheal and kidney microsomes with a K_i of 1 μM. Reeves et al. (1992) showed that (R)-IAA-94 reduced the open probability of an endosomal Cl^- channel from rabbit kidney cortex with a K_i of 15 μM.

Effect of ion substitution on SR Ca^{2+} uptake

Plasma membrane Cl^- channels and, more recently, SR Cl^- channels have been shown to have differing permeability to anions. These differences have been used to begin to partially classify Cl^- channels. To determine the effects of anion substitution on smooth muscle SR, Ca^{2+} uptake rates were compared between permeabilized smooth muscle cells which were washed and resuspended in equal amounts of physiological buffer differing in anionic composition. For the experiments, Cl^- was replaced with buffers containing methanesulfonate (MeS), Br^- or I^-.

As was the case for the experiments with NPPB and (R)-IAA-94 described above, results of the anion substitution experiments were normalized to the amount of protein present in the chamber in each experiment. Figure 15 demonstrates a scatter plot of uptake rates obtained in KBr and KCl buffers. In this summary plot the Ca^{2+} uptake rates (nmol/g/s) are normalized to the mean uptake rate in KCl (which is assigned a value of 1). The normalized data values are calculated separately for each day's data set, and are relative to the mean KCl value for that day. The uptake values are plotted against the mean $[Ca^{2+}]_{free}$ from which the initial uptake rates were calculated. Closed symbols represent initial Ca^{2+} uptake rates in KCl (n=18) and the open symbols indicate initial

Figure 15. Summary of the effect of Br^- substitution on initial rate of Ca^{2+} uptake in smooth muscle cells. Each data point represents the initial rate of Ca^{2+} uptake in KCl (n = 15) or KBr (n = 18) buffers. Different cell preparations are denoted as different symbol types, and are paired as controls (closed symbols) and KBr trials (open symbols) from the same day. Data points were normalized to protein quantity in the experimental chamber (nmol/g/sec). The mean $[Ca^{2+}]_{free}$ value at which the data segment was obtained is indicated on the x-axis (μM). The horizonal line indicates the average rate of Ca^{2+} uptake in KCl buffer (assigned a value of 1). The scatter above and below indicates the variability in uptake rates in both KCl and KBr buffer. An increase in $[Ca^{2+}]_{free}$ did not seem to affect uptake rates in this range. The scatter of data points did not reveal a discernible difference between initial uptake rates in KCl compared with KBr buffer ($p = 0.32$).

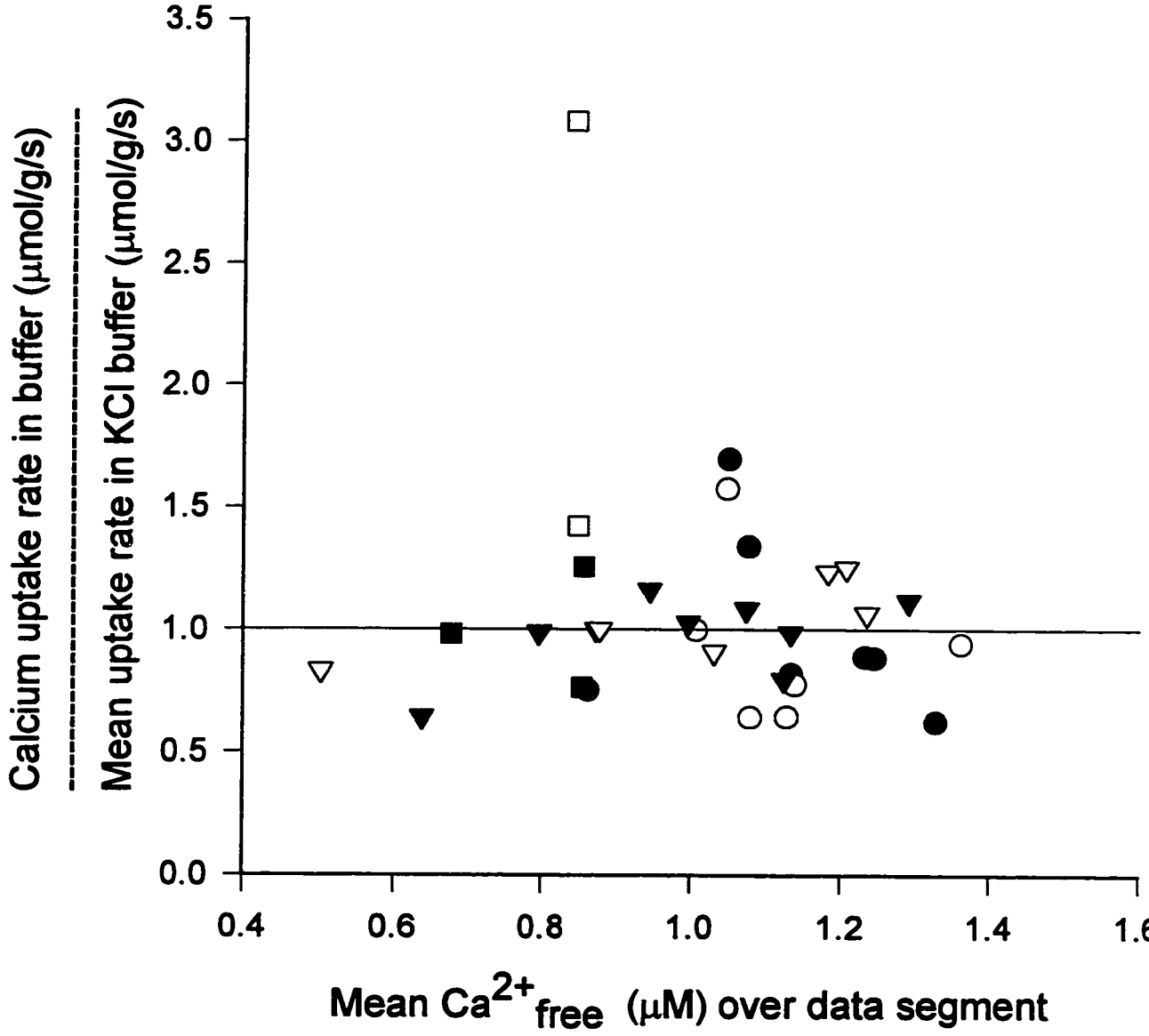
Calcium uptake rate in buffer (µmol/g/s)
Mean uptake rate in KCl buffer (µmol/g/s)
3.5
3.0
2.5
2.0
1.5
1.0
0.5
0.0
0.4
0.6
0.8
1.0
1.2
1.4
1.6
Mean Ca2+free (µM) over data segment

uptake rates in KBr buffer (n=15). Different symbol types indicate different days of experimentation. The data points from KBr buffer are not distributed consistently above or below the reference line, and therefore have similar rates of uptake compared with KCl controls ($p = 0.32$) over $[Ca^{2+}]_{free}$ ranging from 0.50-1.40 μM.

Figure 16 compares initial uptake rates (as in Figure 15) in either K-MeS (n=22) or KCl (n=23) buffer. There was significant difference between Ca^{2+} uptake rates in the two buffers ($p = 0.04$).

Initial Ca^{2+} uptake rates in KI and KCl buffer are shown in two figures. Figure 17 summarizes uptake rates in KI buffer normalized to protein concentration compared to the average Ca^{2+} uptake rate in KCl buffer. Six different cell preparations are shown, each with a different symbol. Once again, control rates in KCl buffer are indicated with the closed symbols, and Ca^{2+} uptake rates in KI buffer are shown with open symbols. In this figure, almost all of the KI data points are above the control points. However, as indicated above (see *Methods*), washing the permeabilized smooth muscle cells in KI buffer might have selectively extracted protein since the protein assays revealed a lower protein concentration in the KI suspensions in five of the six preparations. If the protein extracted was not Ca^{2+}-ATPase, then the quantity of pump protein/ mg of protein would be higher in the KI-washed cells. Therefore, determination of the protein concentration may not have been a reliable method of comparing relative amounts of Ca^{2+} pump between experimental buffers. To examine this possibility, SDS-PAGE and Western blots (Figure 18) were done to determine whether the Ca^{2+}-ATPase was being extracted along with other cellular proteins, or if the pump was becoming concentrated in the KI

Figure 16. Summary of the effect of MeS substitution on initial rate of Ca^{2+} uptake in smooth muscle cells. Each data point represents the initial rate of Ca^{2+} uptake in KCl (n = 23) or K-MeS (n = 22) buffers. This is normalized to protein quantity in the experimental chamber (nmol/g/sec). As described in Figure 15, the average initial uptake rate in KCl buffer was assigned a value of 1; individual control experiments are shown with dark symbols. The three sets of symbols indicate data obtained from three different cell preparations. The mean $[Ca^{2+}]_{free}$ value at which the data segment was obtained is indicated on the x-axis (μM). KCl values are scattered above and below the average control, and although the K-MeS data points were generally in the lower half of the plot, there is no significant difference between uptake rates in the two buffers ($p = 0.04$).

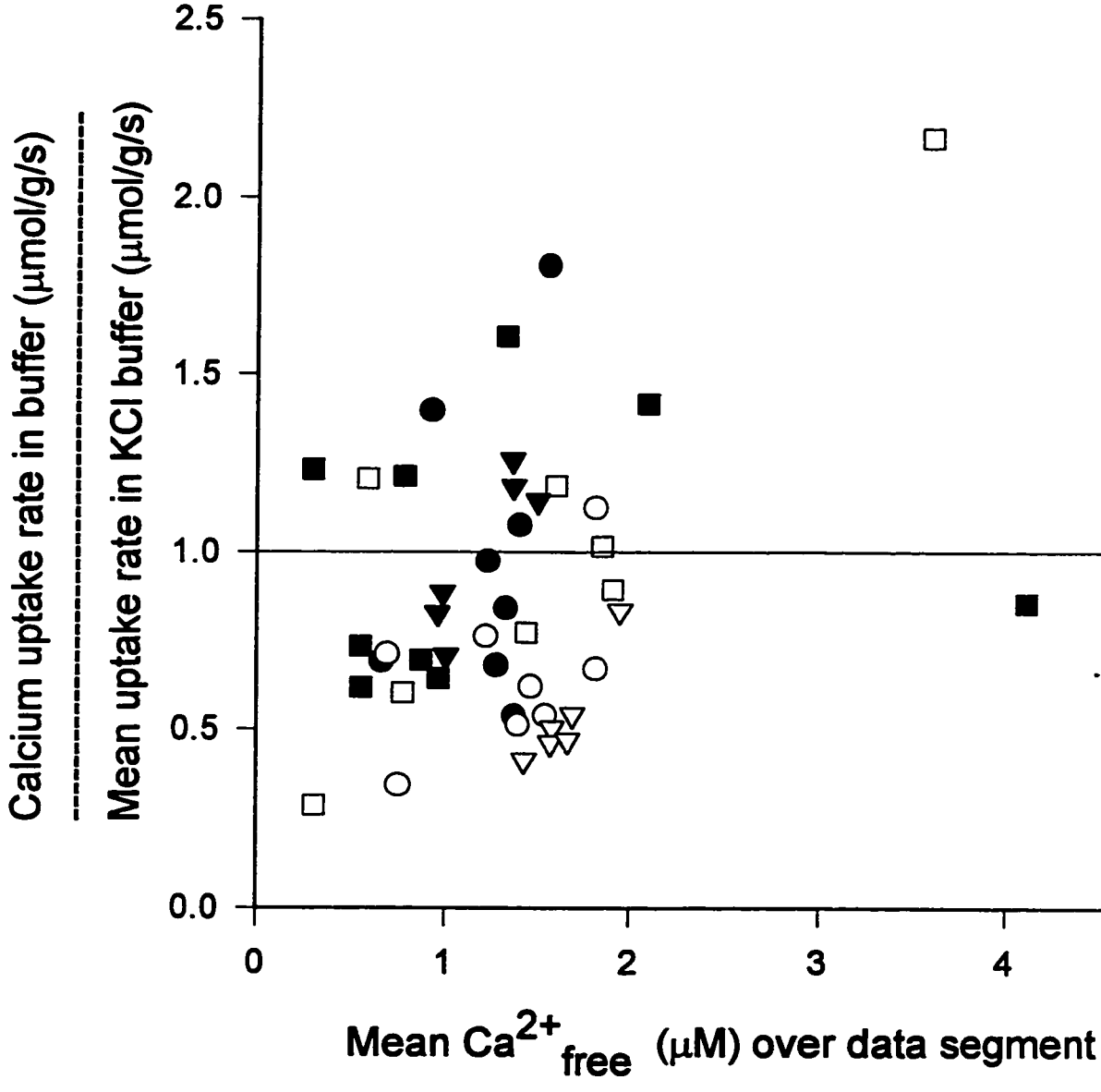
Calcium uptake rate in buffer (µmol/g/s)
Mean uptake rate in KCl buffer (µmol/g/s)
2.5
2.0
1.5
1.0
0.5
0.0
0
1
2
3
4
Mean Ca2+free (µM) over data segment

Figure 17. Summary of the effect of I^- substitution on initial rate of Ca^{2+} uptake in smooth muscle cells. Each data point represents the initial rate of Ca^{2+} uptake in KCl (closed symbols) or KI (open symbols) buffers. Uptake rates were normalized to relative [protein] using a Bradford protein assay on samples taken from each uptake experiment. Protein concentrations of the cell suspension in KI buffer were less than those of the cell suspension in KCl buffer. The figure includes initial uptake rates from six different cell preparations. Different symbol types denote results from different days. Ca^{2+} uptake rates in KI are significantly higher than the controls ($p = 6.9 \times 10^{-9}$); however, Western analysis showed that the SR Ca^{2+}-ATPase was concentrated due to selective protein extraction during the washing process in KI buffer (see Figure 18).

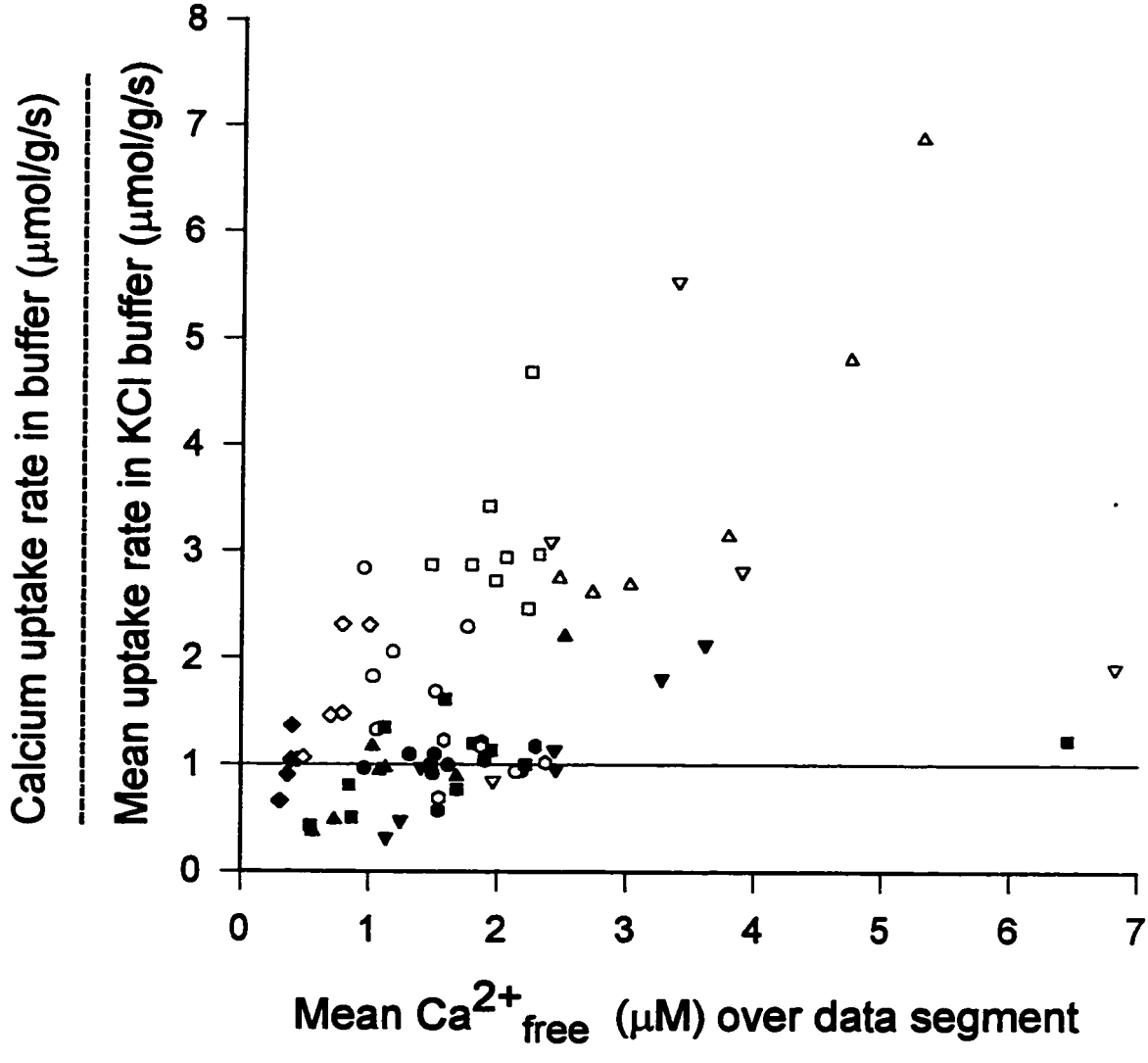
Calcium uptake rate in buffer (μmol/g/s)
Mean uptake rate in KCl buffer (μmol/g/s)
0
1
2
3
4
5
6
7
8
0
1
2
3
4
5
6
7
Mean Ca^{2+}_{free} (μM) over data segment

Figure 18. Western blot of SERCA2 protein bands from cells washed in KI vs. KCl buffers. This image shows Ca^{2+}-ATPase bands which were labelled with a monoclonal antibody to the SERCA2b pump. 20 μg of protein (determined by Bradford protein assay) obtained from cells which were washed and suspended in KI buffer was loaded into lane 1 (left). The O.D x mm^2 for this band was 2.318. 20 μg of protein was loaded into lane 2 (middle) from cells which were washed and suspended in KCl buffer, and had an O.D. x mm^2 of 1.432. The right lane was loaded with half the amount of protein loaded onto the second lane (10 μg), and was included to assess the accuracy of the densitometry in determining relative Ca^{2+}-ATPase quantities. The O.D. x mm^2 obtained was 0.803.

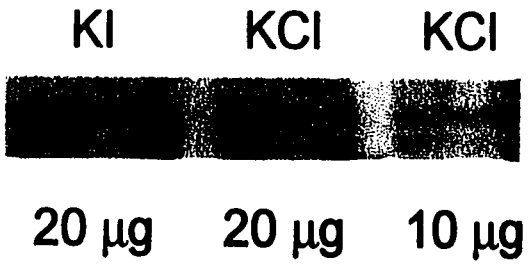
KI
KCl
KCl
20 µg
20 µg
10 µg

cell samples due to the extraction of other cellular proteins (e.g. myosin). Densitometry was used to quantify the amount of pump protein directly from the Western blots, so Ca^{2+} uptake rates relative to the amount of ATPase present in the cell suspension could be compared. Equal amounts of protein were added to SDS-PAGE gels. After electrophoretic transfer and Western blotting, the density of the Ca^{2+}-ATPase band (identified with an antibody to SERCA2b; see *Methods*) was determined. The Ca^{2+}-ATPase bands obtained from smooth muscle cells washed in KI buffer were 1.6 fold greater (O.D. x mm^2) than the bands from the cells washed in KCl buffer (Figure 18). The corrected uptake values from this day are indicated as squares in Figure 19. The second Western blot showed a 3.23 fold concentration of the Ca^{2+}-ATPase band obtained from cells washed in KI compared to KCl buffer. After accounting for the relative amount of pump protein present in the different preparations, the Ca^{2+} uptake rates per pump protein in KI and KCl buffers were again compared and found to be similar ($p = 0.389$). Figure 19 illustrates the range of initial uptake rates per Ca^{2+}-ATPase band density (O.D. x mm^2). The anion substitution data shows similar rates of Ca^{2+} uptake rates in anion-substituted buffers. This suggests that the different anions have similar permeabilities, and can serve equally as co-ions to maintain electroneutrality during Ca^{2+} uptake. Since we are indirectly assessing anion conductance based on Ca^{2+} uptake rate, it is impossible to rule out the role of other ions (ie. K^+) which may compensate for changes in anion permeability. This consideration seems unlikely, however, due to the inhibition of Ca^{2+} uptake in the presence of Cl^- channel blockers.

When comparing the percent inhibition of Ca^{2+} uptake with NPPB, we found that

Figure 19. Ca^{2+} uptake rates for smooth muscle cells in KI vs. KCl buffers, after correction for relative Ca^{2+}-ATPase band density. Correction for the differences in [Ca^{2+} pump protein] between buffers was made by dividing Ca^{2+} uptake rates by the Ca^{2+}-ATPase density. Western blots were done with two different cell preparations. The two different symbol types denote different days, and controls are indicated with closed symbols, KI rates are indicated with open symbols. No significant difference between the uptake rates in KCl ($n = 11$) and KI ($n = 11$) buffers emerged after correction for pump concentration ($p = 0.389$).

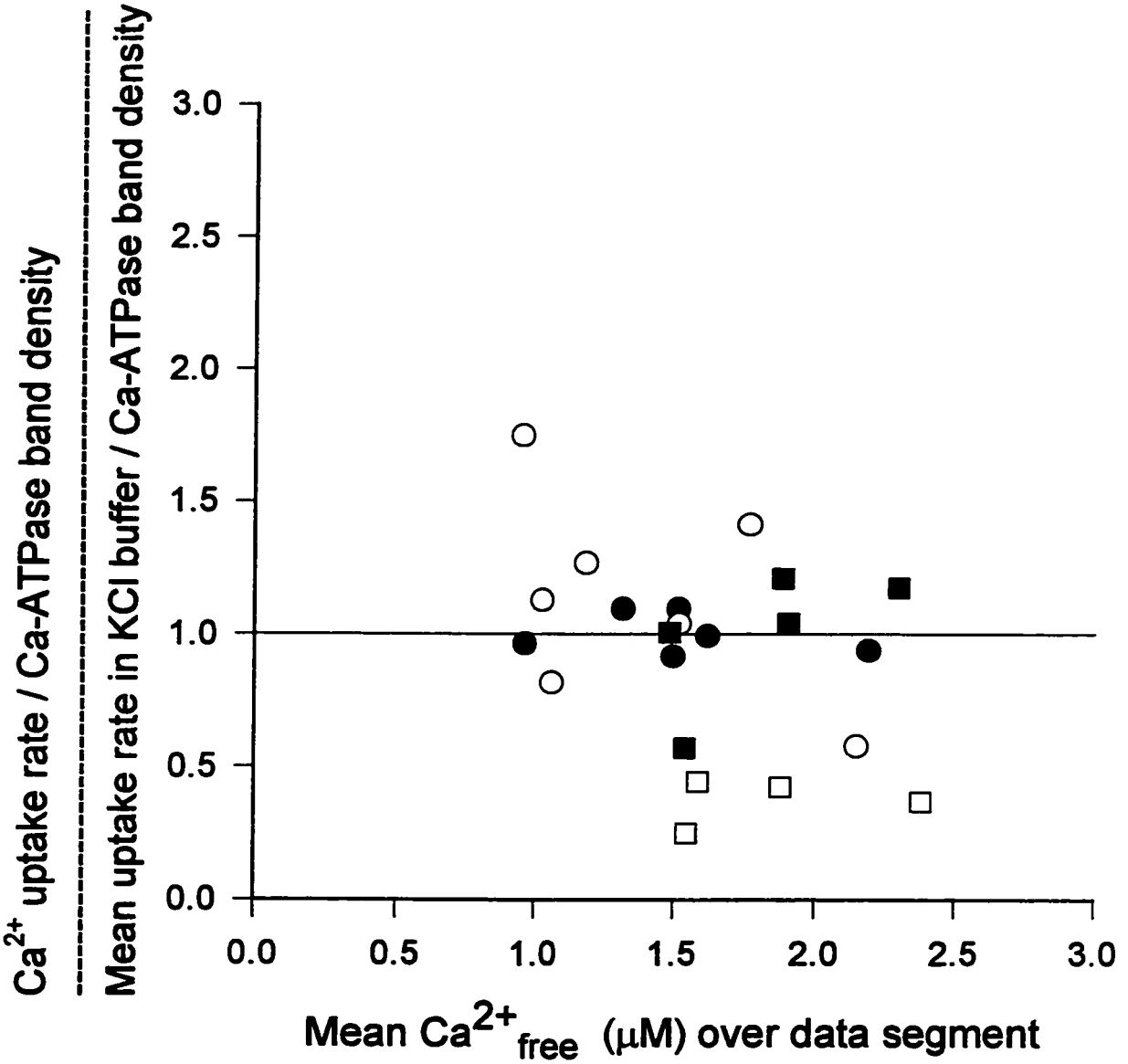
Ca2+ uptake rate / Ca-ATPase band density
Mean uptake rate in KCl buffer / Ca-ATPase band density
3.0
2.5
2.0
1.5
1.0
0.5
0.0
0.0
0.5
1.0
1.5
2.0
2.5
3.0
Mean Ca2+free (μM) over data segment

Figure 20. The effect of 17 μM NPPB in KI and KCl buffers in smooth muscle cells. These results are from one cell preparation and show that NPPB inhibits Ca^{2+} uptake rate in either KCl or KI buffers. In KCl buffer, 17 NPPB reduced Ca^{2+} uptake to 8.58% of the control (n = 5). In KI buffer, 17 μM NPPB reduced Ca^{2+} uptake to 4.93% of the control (n = 3). Since uptake was inhibited to approximately the same extent by NPPB in both buffers, this suggests that KI did not enter the SR through a different pathway than KCl.

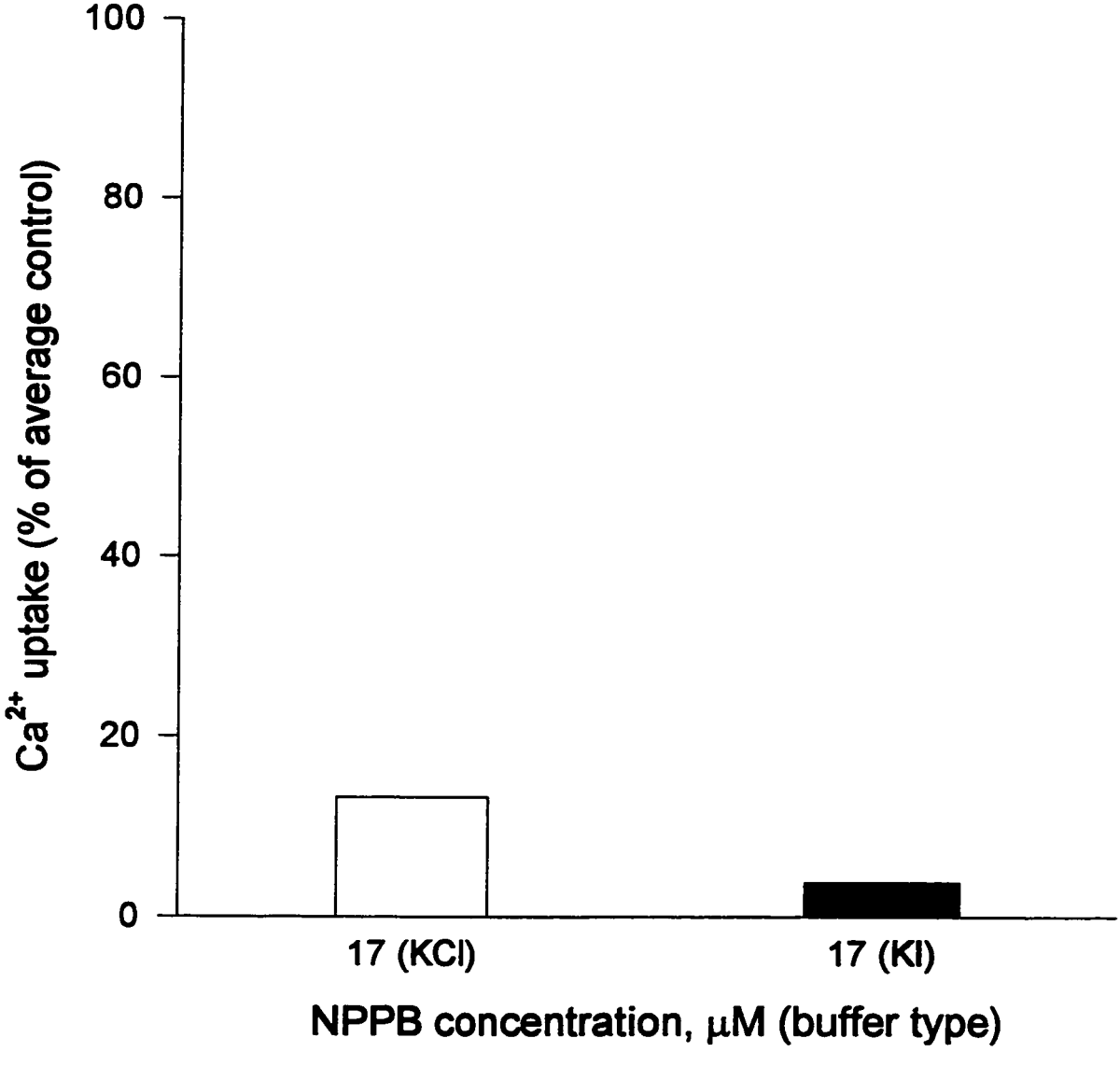
100
80
60
40
20
0
Ca^{2+} uptake (% of average control)
17 (KCl)
17 (KI)
NPPB concentration, μM (buffer type)

NPPB had a similar effect in either KCl or KI buffer: the addition of 17 μM NPPB to smooth muscle cells in KCl buffer decreased Ca^{2+} uptake to 8.58% of the original rate ($n = 5$; $p = 0.019$) and in KI buffer ($n = 3$; $p = 0.329$), 17 μM NPPB reduced Ca^{2+} uptake to 4.9% of the control rate. Figure 20 suggests, however, that only one anionic pathway was present in these experiments and that KI likely enters through the same (or a similar) NPPB-sensitive channel as Cl^-.

CANINE CARDIAC VESICLES

Effect of NPPB and (R)-IAA-94 on Ca^{2+} uptake in cardiac SR vesicles

Since NPPB and (R)-IAA-94 were shown to inhibit Ca^{2+} uptake by the SR in smooth muscle cells, the effects of these agents were also examined in cardiac vesicles. Cardiac SR vesicles were insensitive to the Cl^- channel blockers NPPB and (R)-IAA-94 at concentrations $\approx$6-fold higher than those which were efficacious in smooth muscle cells. Representative traces were included to compare uptake curves with and without NPPB. In Figure 21, Ca^{2+} uptake in the control condition had an initial Ca^{2+} uptake rate of 176 nmol/g/sec, and in the presence of 96 μM NPPB the initial uptake rate was 236 nmol/g/sec. The initial uptake slopes of these two experiments show the rapid rate at which the Ca^{2+}-ATPase can reduce $[Ca^{2+}]_{free}$. These uptake curves fall within the expected rate of Ca^{2+} uptake for a cardiac vesicle preparation, in which the SR (and therefore the Ca^{2+}-ATPase) is highly concentrated. Figure 22 shows that 96 μM NPPB had no effect on the rate of Ca^{2+} uptake in SR vesicles compared to controls (p =

Figure 21. Effect of NPPB on Ca^{2+} uptake in cardiac SR vesicles. Traces show the decrease in $[Ca^{2+}]_{free}$ (μM) vs. time (s) for two different experiments. The control trace (labelled as 0) had a maximum Ca^{2+} uptake rate of 177 nmol/g/sec. In the sample labelled 96, Ca^{2+} uptake rate was higher in the presence of 96 μM NPPB (236 nmol/g/sec). All uptake rates were determined from the steepest part of the curve.

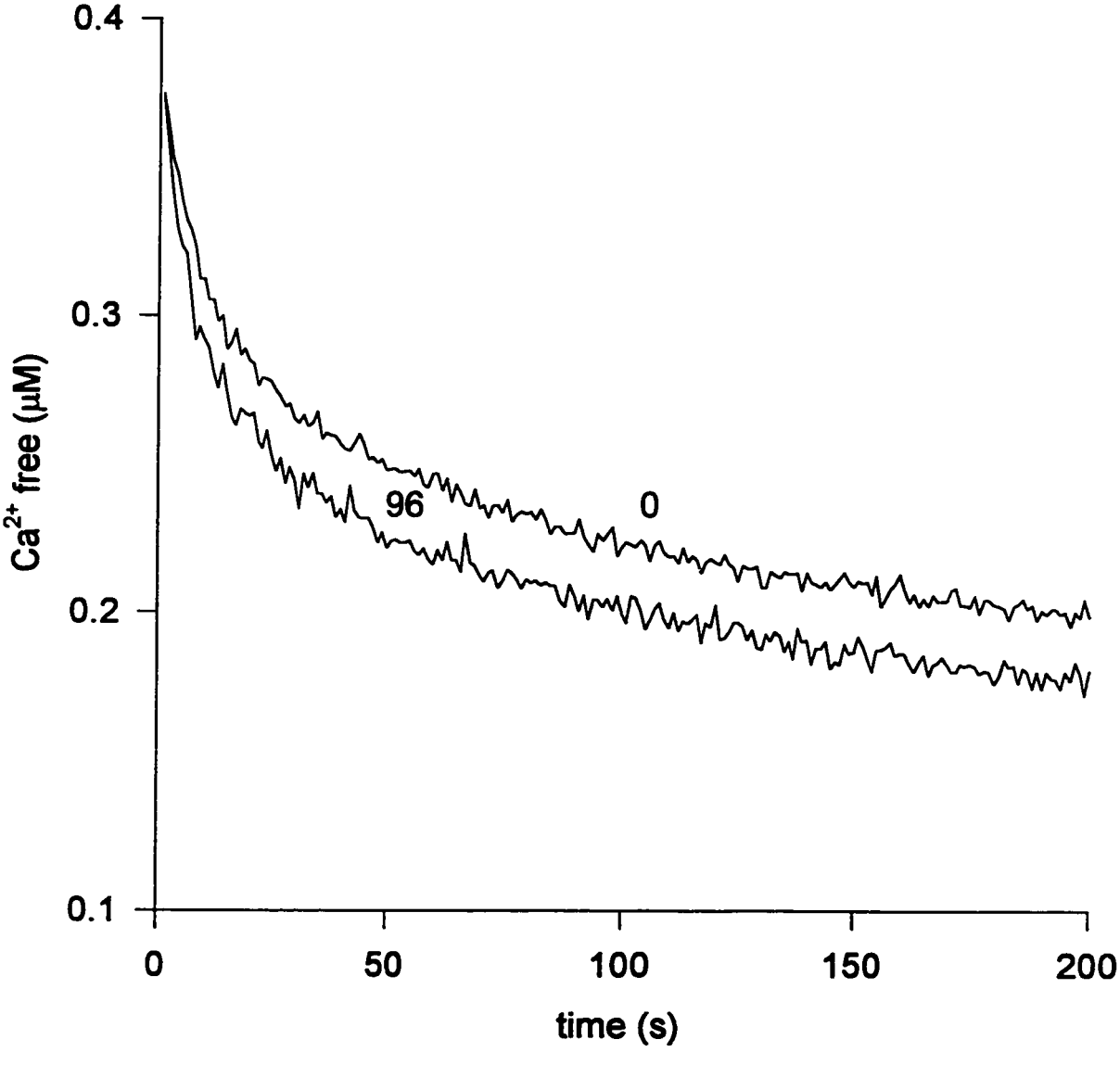
0.4
0.3
0.2
0.1
Ca2+ free (µM)
96
0
0
50
100
150
200
time (s)

Figure 22. Summary of the effect of NPPB on the rate of initial Ca^{2+} uptake in cardiac SR vesicles. Initial Ca^{2+} uptake rates are expressed as percentages of the mean control so that two different days of data could be combined. The mean control rate was assigned a value of 100% and had a S.D. of 26.5% ($n = 11$). In the presence of 96 μM NPPB the Ca^{2+} uptake rate was 78.9 $\pm$ 15.2% of the control ($n = 6$), which was not statistically significantly different ($p = 0.094$).

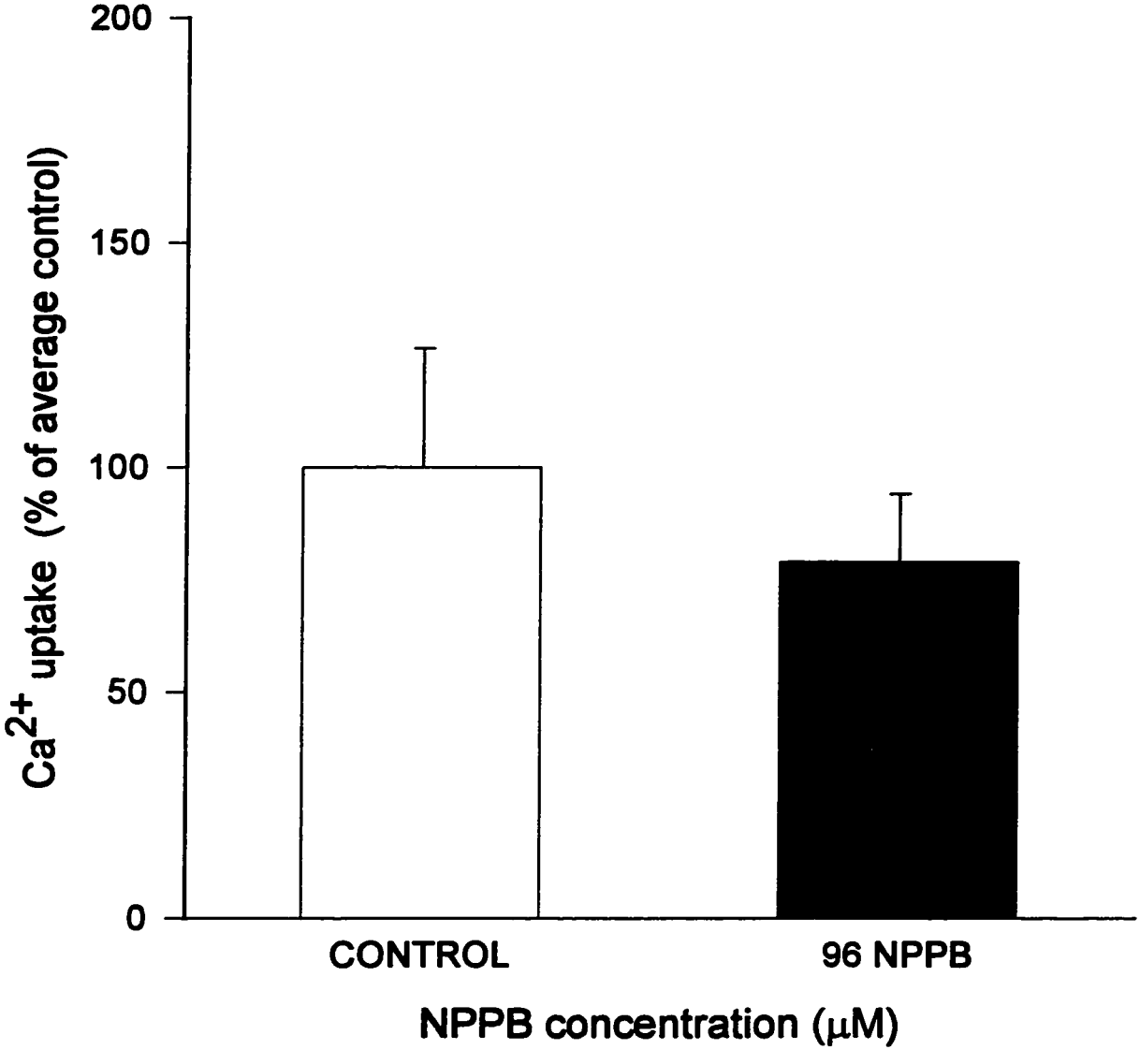
200
150
100
50
0
Ca^{2+} uptake (% of average control)
CONTROL
96 NPPB
NPPB concentration (μM)

Figure 23. Effect of (R)-IAA-94 on Ca^{2+} uptake in cardiac SR vesicles. Traces show the decline in $[Ca^{2+}]_{free}$ (μM) vs. time (s) for two different experiments. The control trace (labelled as 0) had a Ca^{2+} uptake rate of 162 nmol/g/sec. In the presence of 96 μM (R)-IAA-94 the Ca^{2+} uptake rate was 181 nmol/g/sec (trace labelled 96). Both uptake rates were determined from the steepest part of the curve.

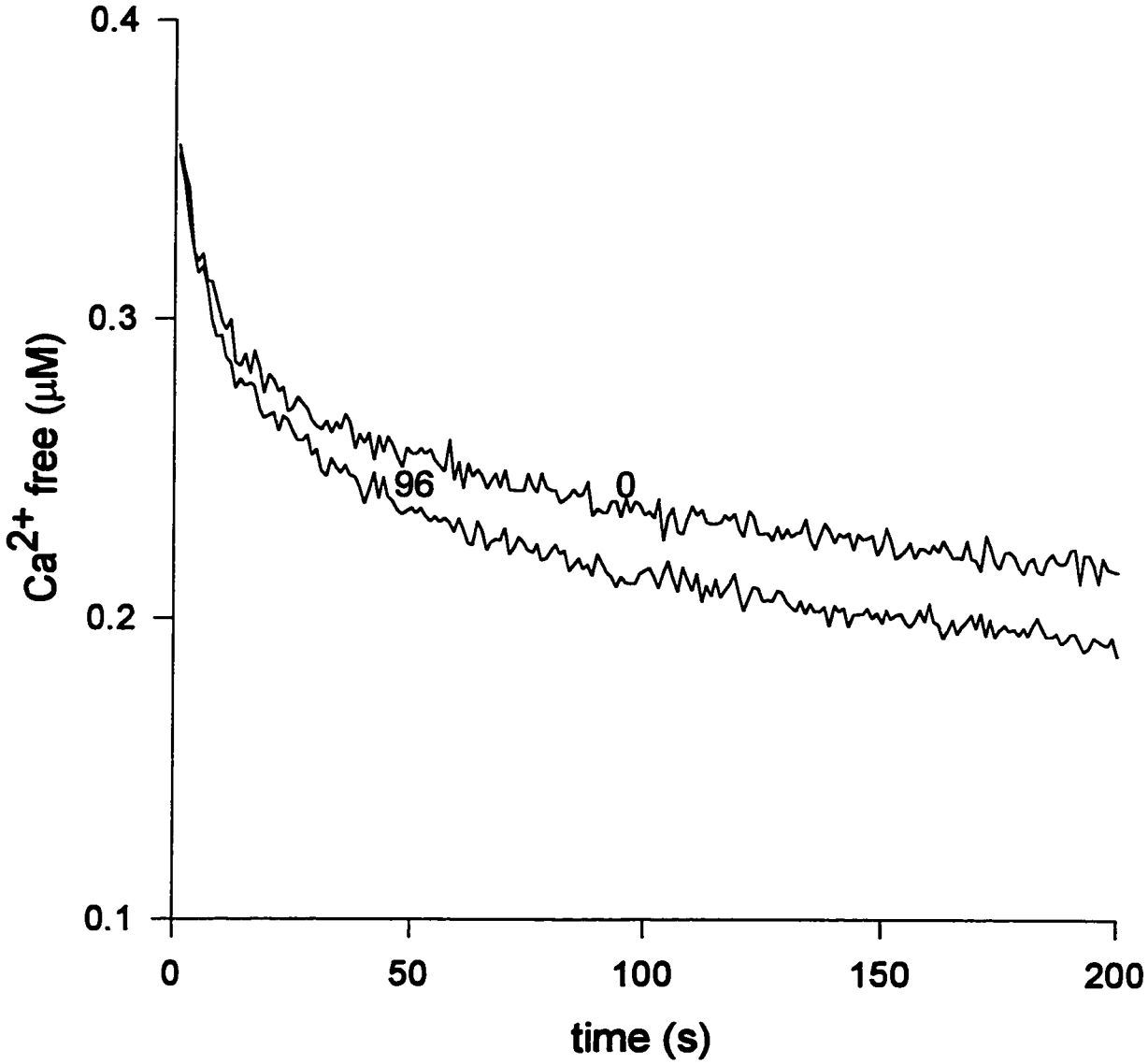
0.4
0.3
0.2
0.1
Ca^{2+} free (μM)
96
0
0
50
100
150
200
time (s)

0.094). These data show mean Ca^{2+} uptake rates as percentages of the average control with (n = 11) and without (n = 6) 96 μM NPPB. (R)-IAA-94 was also found to be ineffective at reducing Ca^{2+} uptake rate in cardiac SR. Figure 23 compares traces in which the initial control Ca^{2+} uptake rate of 162 nmol/g/sec was marginally increased to 181 nmol/g/sec in the presence of 96 μM (R)-IAA-94. These increases in Ca^{2+} uptake rate in the presence of NPPB or (R)-IAA-94 were within the standard deviations of the control values and do not represent a significant effect of the Cl^- channel blockers in cardiac vesicles. The data in Figure 24 are also expressed as a percent of the average control from that day's data set so that two different days of data could be combined. The mean uptake rate in the control condition (n = 11) was 100 $\pm$ 26.5% and the mean uptake rate with 96 μM (R)-IAA-94 (n = 7) was 93.5 $\pm$ 37.2%, and therefore not significantly different (p = 0.46).

Effect of ion substitutions experiments on Ca^{2+} uptake in SR vesicles

Since there was such a dramatic difference between the response of Ca^{2+} uptake by smooth muscle cells and cardiac SR vesicles to treatment with NPPB and (R)-IAA-94, we next performed anion substitution experiments on the cardiac vesicles. The cardiac vesicles were added to cuvets containing uptake buffers with Br^-, I^-, MeS or Cl^- as the predominant anion at the beginning of each experiment. The pH and ionic strength were held constant and only the primary anion was varied (see *Methods* for details).

In Figure 25, we found no significant difference in uptake rate between KCl and KMeS buffers (p = 0.151). This figure shows the results of two different days of

Figure 24. Summary of the effect of (R)-IAA-94 on the rate of initial Ca^{2+} uptake in cardiac SR vesicles. Initial Ca^{2+} uptake rates are expressed as percentages of the mean control so that two different days of data could be combined. The mean control rate was assigned a value of 100% and had a S.D. of 26.5% (n = 11). In the presence of 96 μM (R)-IAA-94 the Ca^{2+} uptake rate was 93.5 $\pm$ 37.2% of the control (n = 7), which was not statistically significantly different (p = 0.460).

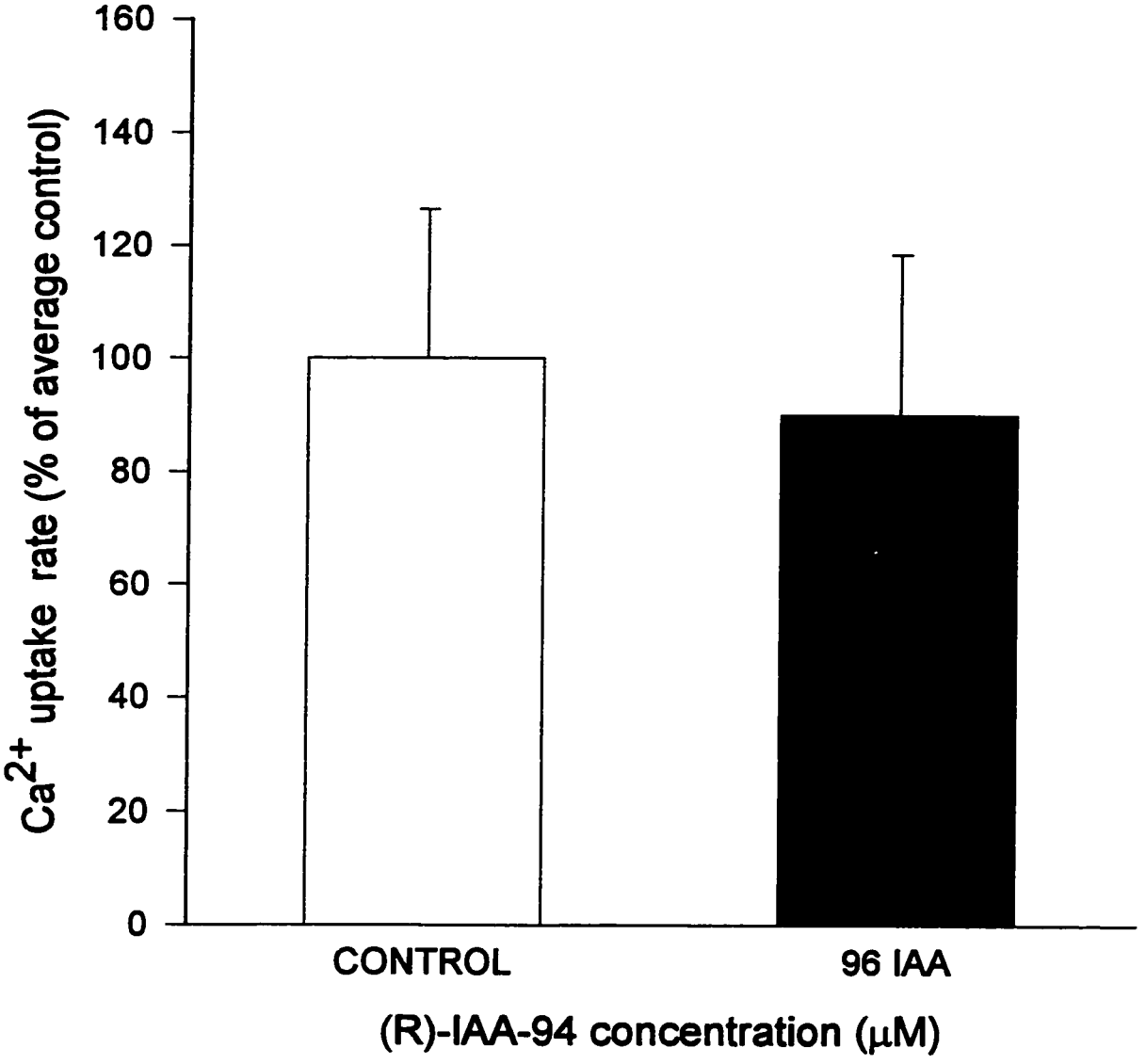
160
140
120
100
80
60
40
20
0
Ca^{2+} uptake rate (% of average control)
CONTROL
96 IAA
(R)-IAA-94 concentration (μM)

Figure 25. Effect of MeS substitution on initial rate of Ca^{2+} uptake in cardiac SR vesicles. Each data point represents the initial rate of Ca^{2+} uptake in KCl (n = 9) or KMeS (n = 9) buffers. Different days of experimentation are denoted as different symbol types, and are paired as controls (closed symbols) and KMeS trials (open symbols). Uptake rates were normalized to protein quantity in the experimental chamber (nmol/g/sec). The mean $[Ca^{2+}]_{free}$ value at which the data segment was obtained is indicated on the x-axis (μM). The horizontal line indicates the average rate of Ca^{2+} uptake in KCl buffer (assigned a value of 1). The scatter above and below indicate the variability in individual uptake rates in both KCl and KMeS buffers. The scatter of data points did not reveal a consistent difference between initial uptake rates in KCl compared with KMeS buffer ($p = 0.151$).

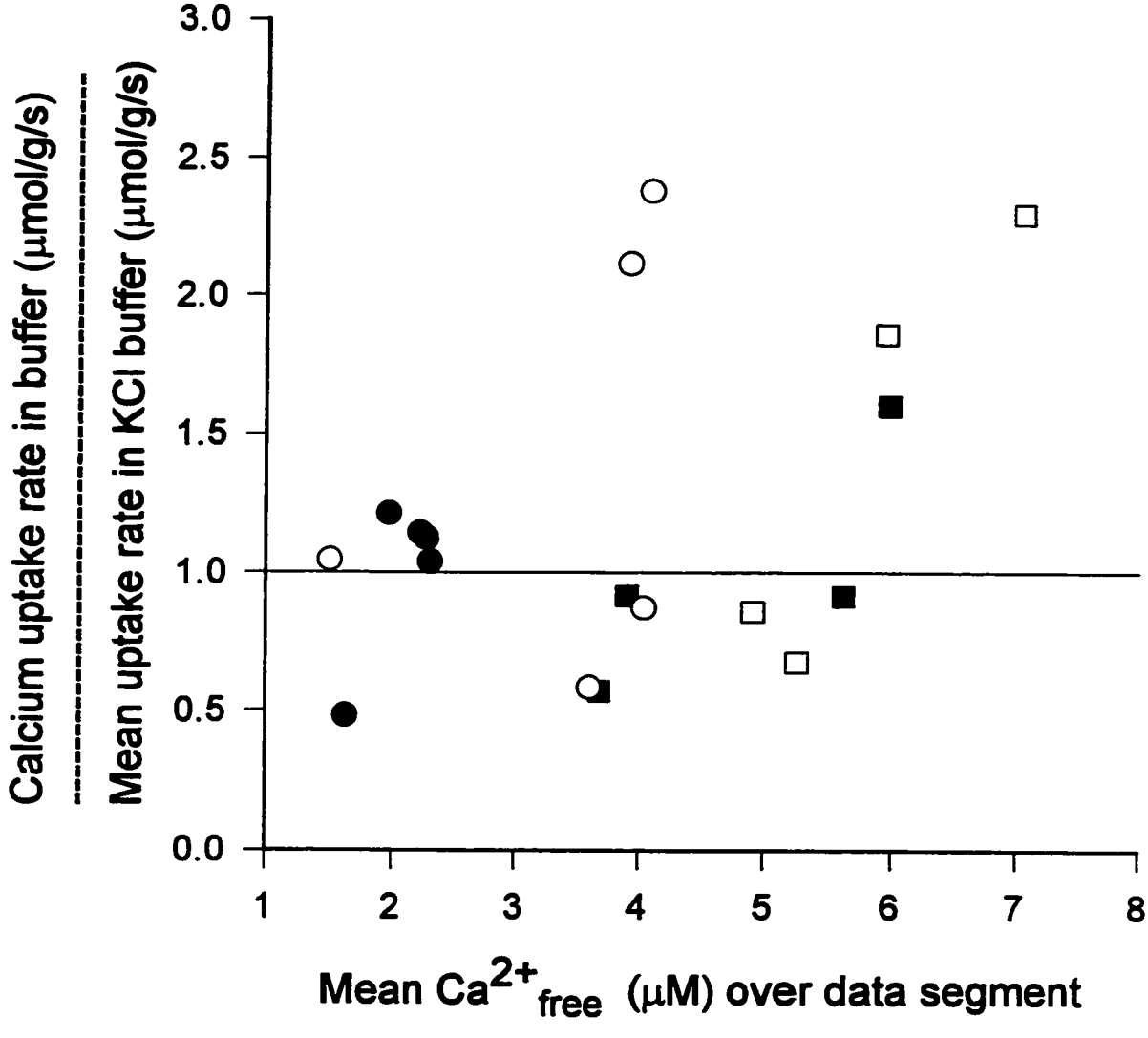
Calcium uptake rate in buffer (µmol/g/s)
Mean uptake rate in KCl buffer (µmol/g/s)
3.0
2.5
2.0
1.5
1.0
0.5
0.0
1
2
3
4
5
6
7
8
Mean Ca2+free (µM) over data segment

Figure 26. Effect of Br^- substitution on initial rate of Ca^{2+} uptake in cardiac SR vesicles. Each data point represents the initial rate of Ca^{2+} uptake in KCl (n = 13) or KBr (n = 13) buffers. Different days of experimentation were denoted as different symbol types, and are paired as controls (closed symbols) and KBr trials (open symbols). Data points were normalized to protein quantity in the experimental chamber (nmol/g/sec). The scatter above and below the mean uptake rate in KCl buffer indicated the variability in individual uptake rates in both KCl and KMeS buffers. When all data points were used, the scatter of KBr data points did not reveal a significant difference in initial uptake rates compared with KCl buffer (P = 0.30). However, at $[Ca^{2+}]_{free}$ less than 5 μM, KBr is significantly lower in initial uptake rate compared to KCl with a p-value of 4.0×10^{-6}.

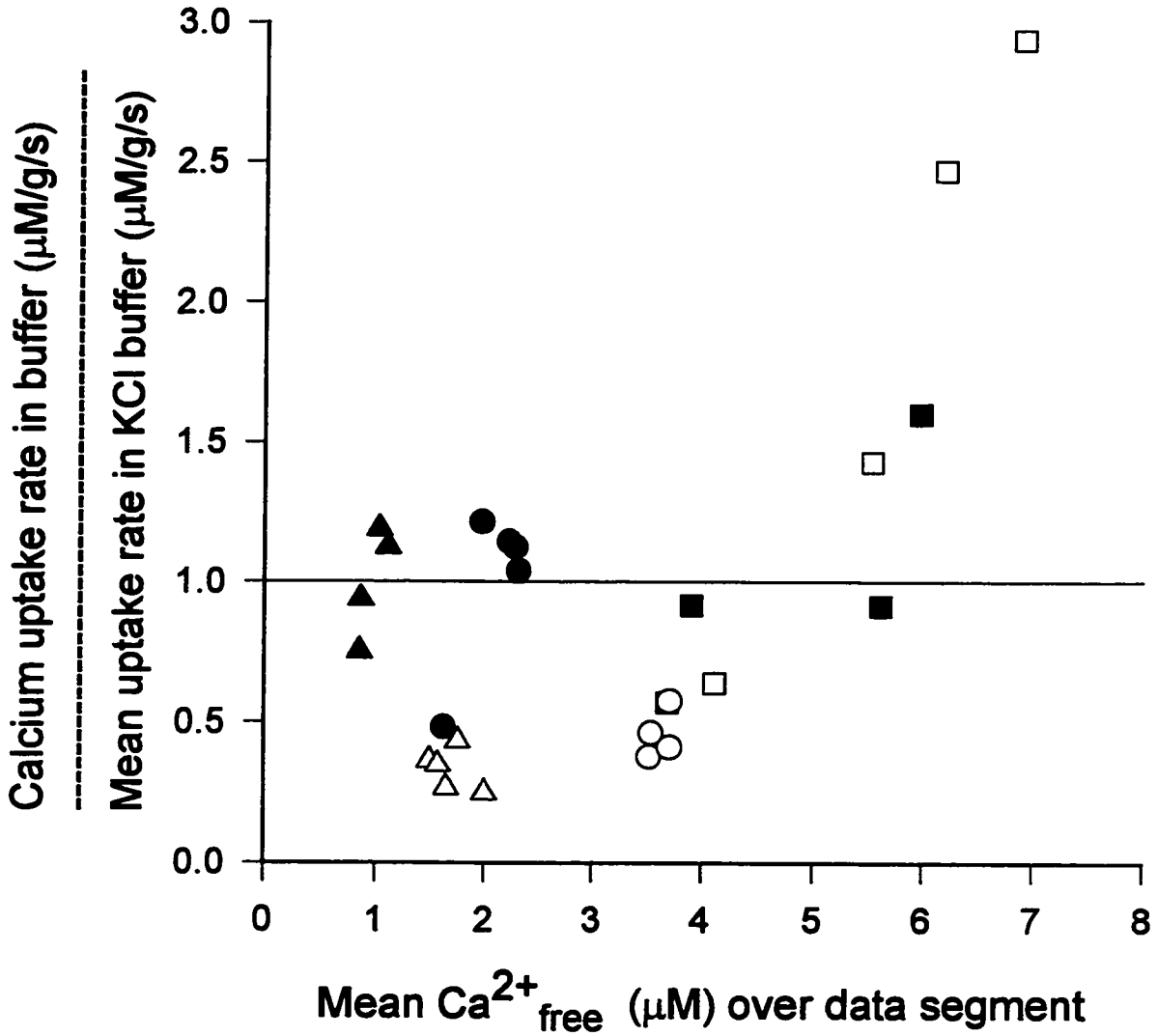
Calcium uptake rate in buffer (μM/g/s)
Mean uptake rate in KCl buffer (μM/g/s)
3.0
2.5
2.0
1.5
1.0
0.5
0.0
0
1
2
3
4
5
6
7
8
Mean Ca2+free (μM) over data segment

experimentation. Normalized uptake rates in KCl buffer are depicted with closed symbols (n=9) and Ca^{2+} uptake rates in MeS buffer are shown as open symbols (n=9). Figure 26 shows diminished rates of uptake in KBr buffer at low Ca^{2+} between concentrations of $\leq 5\ \mu M$ ($p = 6.70 \times 10^{-6}$). When compared to the average rate in KCl buffer; at higher $[Ca^{2+}]$, this did not appear to be the case. A combined p-value of 0.30 suggests that when comparing data at all $[Ca^{2+}]_{free}$ values, the effect of Br^- substitution was not significant. Conversely, SR vesicles suspended in KI buffer consistently sequestered Ca^{2+} at a slower rate than vesicles in KCl buffer (Figure 27; $p = 3.0 \times 10^{-5}$). Protein extraction was not a concern in these experiments on SR vesicles as they were not washed in the KI buffer, and were added to uptake buffer just before initiation of the experiment. Ca^{2+} uptake rates of cardiac SR were also measured in SO_4^{2-} buffer. Figure 28 shows two days of experiments comparing Ca^{2+} uptake in KCl (n=9) versus SO_4^{2-} (n=13). Uptake rates in SO_4^{2-} buffer (open symbols) were generally below the control rates (closed symbols), however, this was not significant with a p value of 0.025. From these SR experiments, the anion permeability sequence of the cardiac SR was determined to be: MeS $\approx Cl^- \approx SO_4^{2-} \approx Br^- > I^-$.

CANINE CARDIAC VESICLES WITH OXALATE

Experiments using NPPB, (R)-IAA-94 and anion substitution were repeated on canine cardiac vesicles with oxalate in the buffers. This was done for three reasons: 1)

Figure 27. Effect of I^- substitution on initial rate of Ca^{2+} uptake in cardiac SR vesicles. Uptake rates are shown as ratios of the average control in KCl buffer, so that two days of data collection could be combined. Different days of experimentation are denoted as different symbol types, and are paired as controls (closed symbols) and KI trials (open symbols). Data points were normalized to protein quantity in the experimental chamber (nmol/g/sec) and the mean $[Ca^{2+}]_{free}$ value at which the data segment was obtained is indicated on the x-axis (μM). The horizontal line indicates the average rate of Ca^{2+} uptake in KCl buffer (assigned a value of 1). The scatter above and below indicated the variability in individual uptake rates in both KCl (n = 13) and KI (n = 11) buffers. The Ca^{2+} uptake data points from vesicles in KI buffer were all below the average control rate. This decrease in Ca^{2+} uptake was statistically significant ($p = 3.0 \times 10^{-5}$).

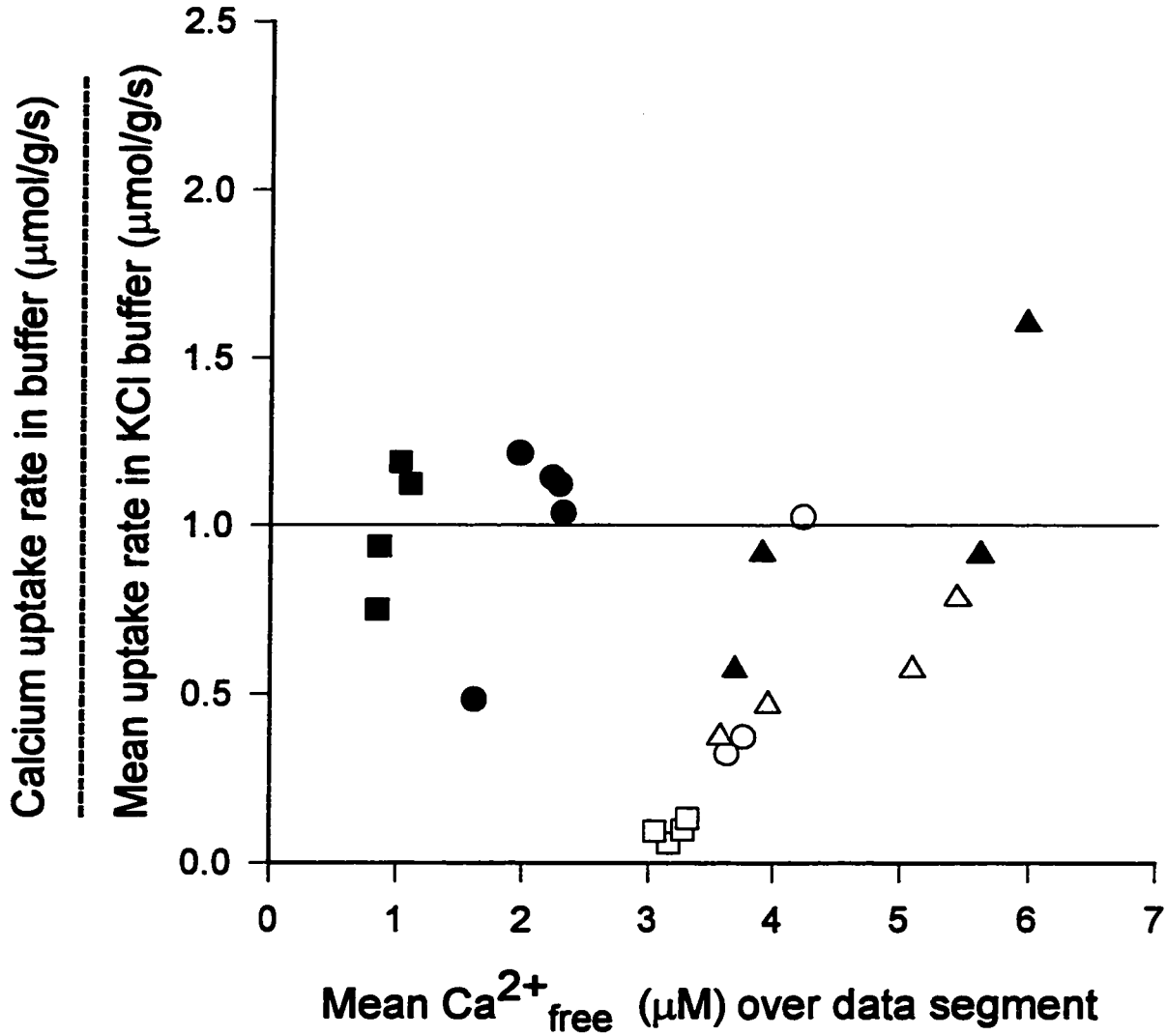
Calcium uptake rate in buffer (µmol/g/s)
Mean uptake rate in KCl buffer (µmol/g/s)
2.5
2.0
1.5
1.0
0.5
0.0
0
1
2
3
4
5
6
7
Mean Ca2+free (µM) over data segment

Figure 28. Effect of SO_4^{2-} substitution on initial rate of Ca^{2+} uptake in cardiac SR vesicles. Each data point represents the initial rate of Ca^{2+} uptake in KCl (n = 9) or K_2SO_4 (n = 13) buffers from two different days of data. Different days of experimentation are denoted as different symbol types, and are paired as controls (closed symbols) and K_2SO_4 trials (open symbols). Data points were normalized to protein quantity in the experimental chamber (nmol/g/sec) and the mean $[Ca^{2+}]_{free}$ value at which the data segment was obtained is indicated on the x-axis (μM). The Ca^{2+} uptake data points from vesicles in SO_4^{2-} buffer were all below the average control rate in KCl buffer, but were not statistically significantly different ($p = 0.0253$).

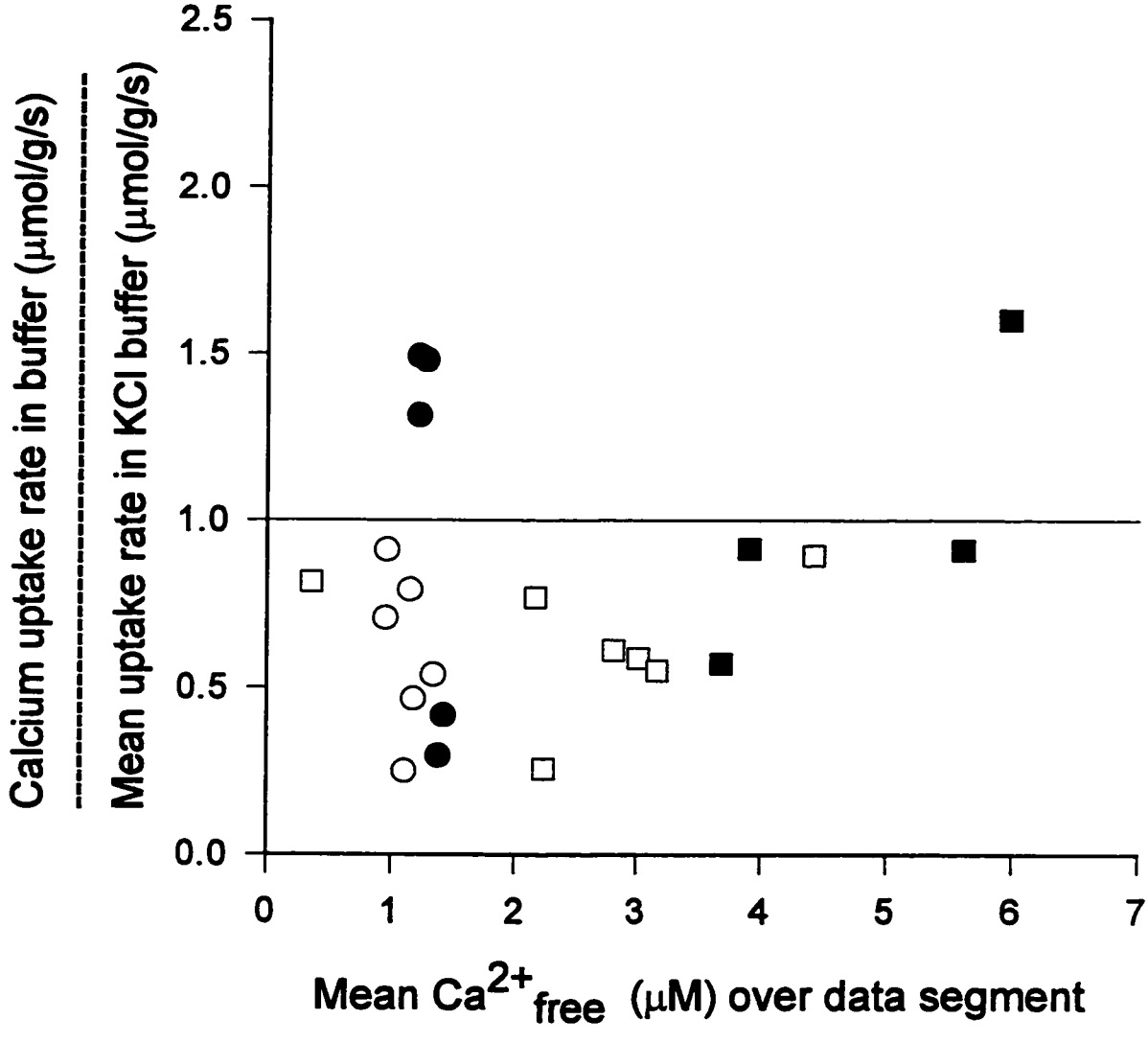
Calcium uptake rate in buffer (μmol/g/s)
Mean uptake rate in KCl buffer (μmol/g/s)
2.5
2.0
1.5
1.0
0.5
0.0
0
1
2
3
4
5
6
7
Mean Ca2+free (μM) over data segment

oxalate has been used in past uptake experiments with SR vesicles due to its formation of a Ca^{2+}-oxalate complex inside the SR. This prevents high intravesicular $[Ca^{2+}]_{free}$ from inhibiting Ca^{2+} uptake into the SR. 2) By keeping $[Ca^{2+}]_{free}$ low within the SR, uptake rates to be significantly higher in the presence of oxalate which facilitates the assessment of Ca^{2+} uptake . 3) The addition of oxalate to the uptake buffers allows calculation of Ca^{2+} uptake kinetics and further characterization of the Ca^{2+} pump in the various anion-substituted buffers. V_{max}, $Ca_{50\%}$ and Hill coefficient were calculated for these experiments.

In the presence of oxalate, neither 98 μM NPPB nor 96 μM (R)-IAA-94 decreased the rate of Ca^{2+} uptake significantly in cardiac vesicles. These results were similar to those obtained without oxalate, and are therefore not shown.

The results from ion substitution experiments were similar to those using cardiac SR vesicles without oxalate. However, the trials were highly reproducible and clearly display the effects of anion substitution in Figures 29-31 as changes in 340/380 fluorescence ratio versus time (s). Traces from the Cl^--substituted buffers are shown with dotted lines, and are displayed on the same figure as the control curves obtained in the presence of KCl for comparison (solid lines). Figure 29 shows traces from cardiac vesicles in KBr and KCl buffers. The rates of Ca^{2+} uptake in the KBr buffer (dotted lines) appear to be slower than the control rates. Ca^{2+} uptake rates in KCl and K-MeS buffers were similar (Figure 30). Ca^{2+} uptake in KI buffer was considerably slower than uptake by vesicles in the control buffer (Figure 31). The experiments with oxalate generally replicate the results obtained with SR vesicles in the absence of oxalate. Ca^{2+}

Figure 29. 340/380 ratio vs. time (s) traces of cardiac SR vesicles in KCl and KBr buffer with oxalate. The differences between the traces indicate that the KBr uptake curves (dotted lines) may be slower than the uptake curves in KCl buffer (solid lines).

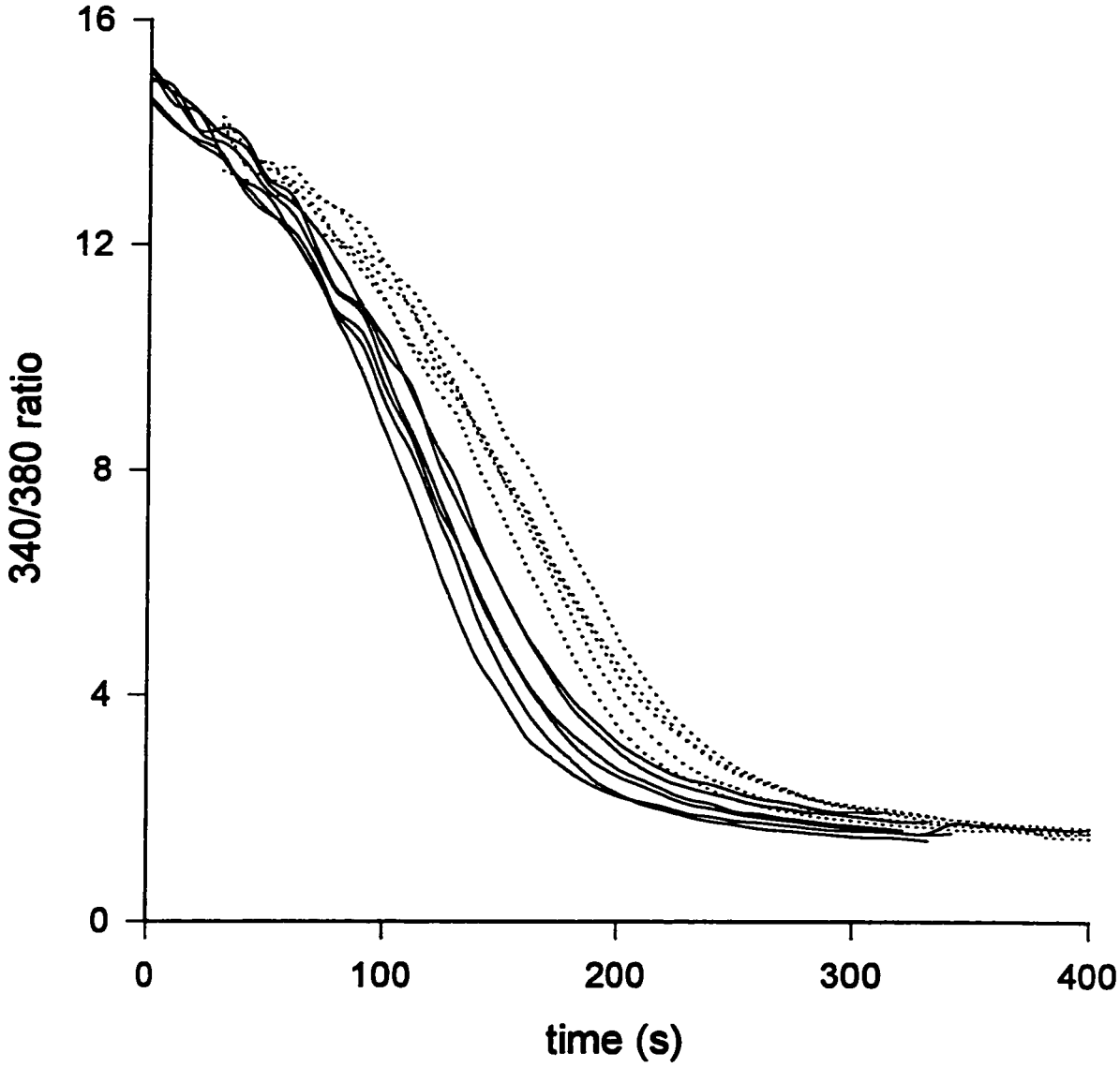
16
12
8
4
0
340/380 ratio
0
100
200
300
400
time (s)

Figure 30. 340/380 ratio vs. time (s) traces of cardiac SR vesicles in KCl and K-MeS buffer with oxalate. The traces from vesicles in KCl buffer are shown as solid lines the traces from vesicles in K-MeS buffer are shown as dotted lines for clarity.

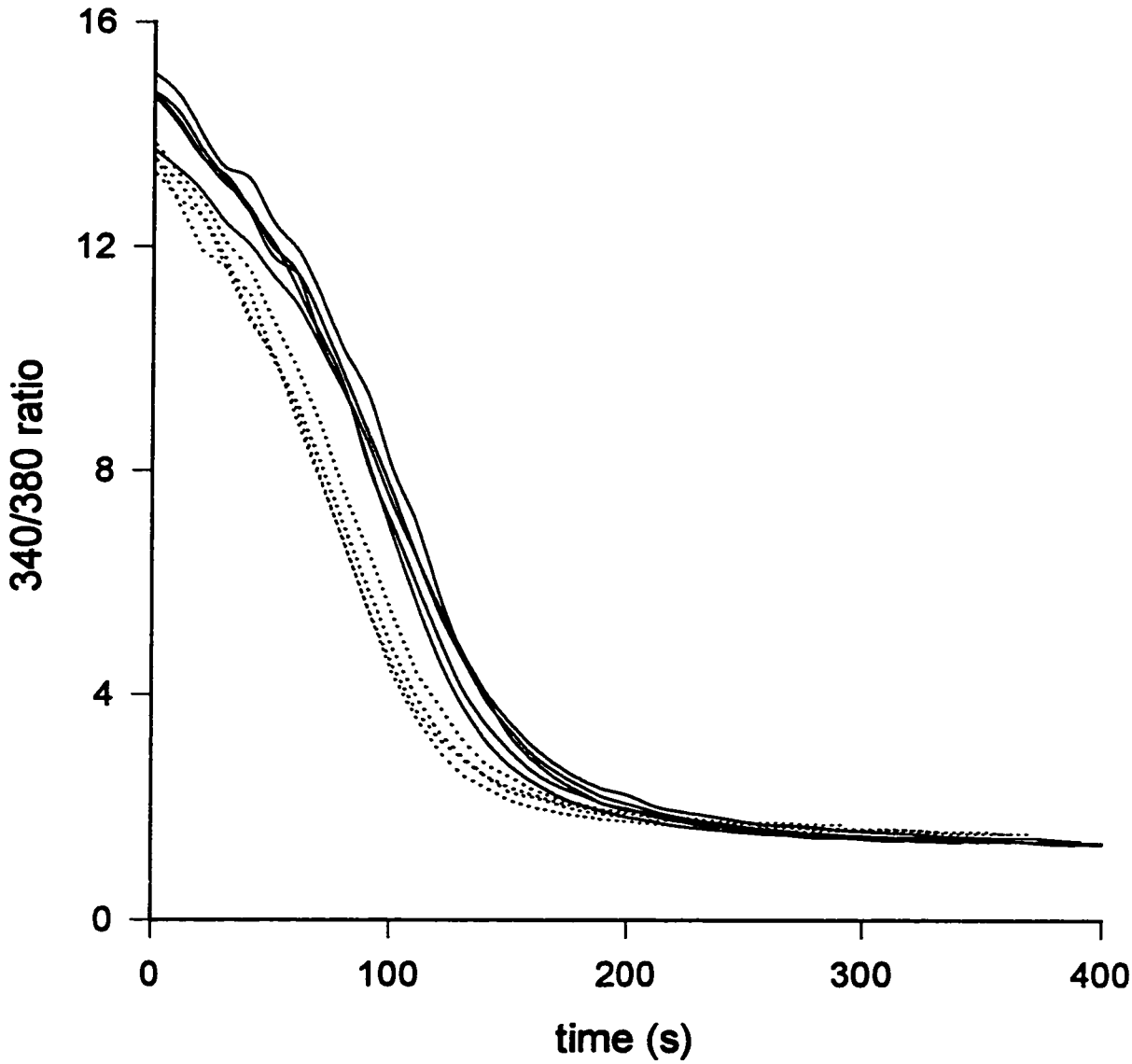
16
12
8
4
0
340/380 ratio
0
100
200
300
400
time (s)

Figure 31. 340/380 ratio vs. time (s) of cardiac vesicles in KCl and KI buffer with oxalate. The uptake curves from the vesicles in KI buffer (dotted line) were slower than the control curves from vesicles in KCl buffer (solid line). Figure shows 5 control traces and 5 traces in KI buffer.

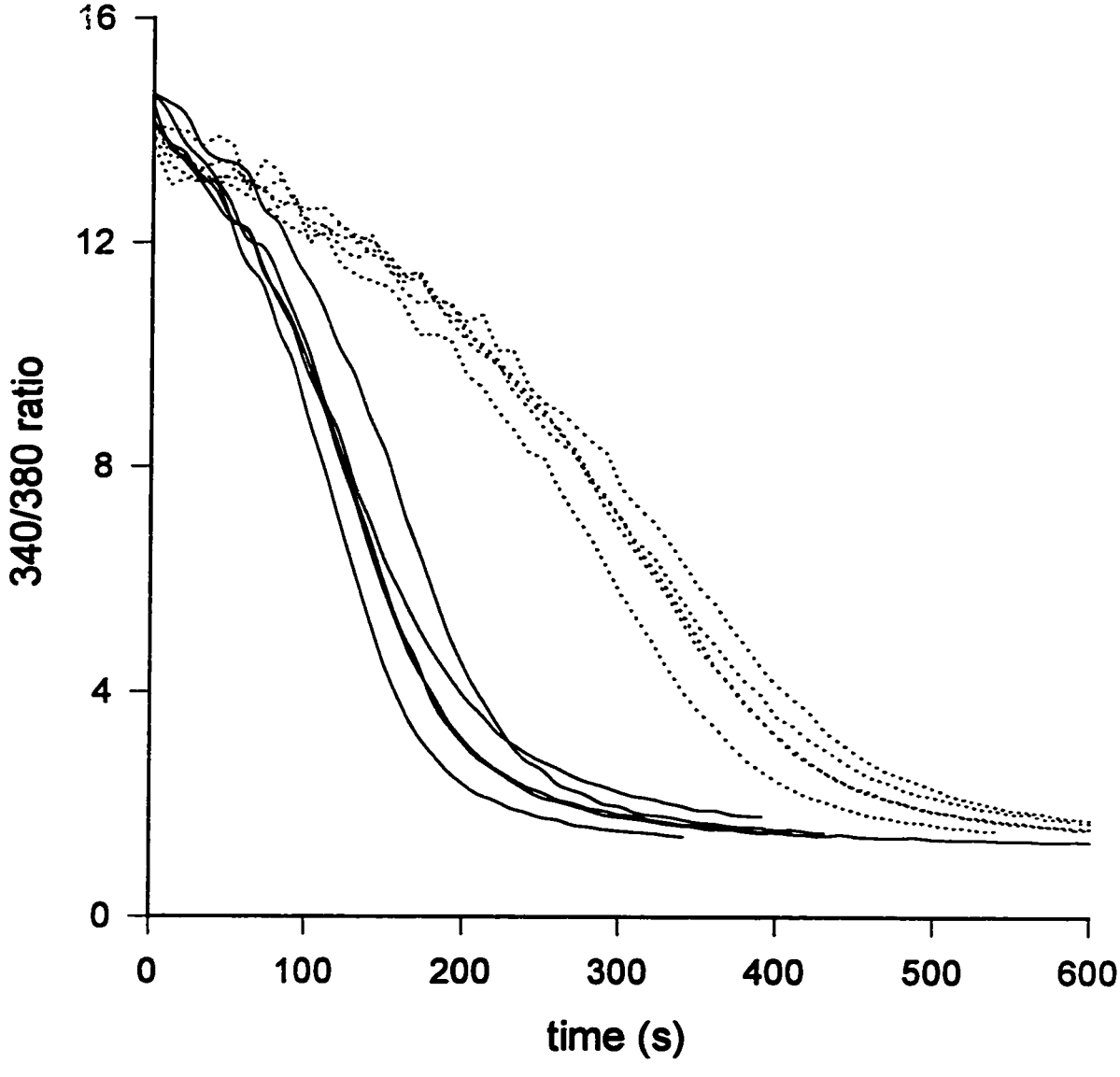
16
12
8
4
0
340/380 ratio
0
100
200
300
400
500
600
time (s)

Figure 32. V_{max} of Ca^{2+} uptake in cardiac SR vesicles in four buffers of different anionic composition. V_{max} is presented as percent of mean KCl V_{max} (100 $\pm$ 9.61%; n = 29). The V_{max} from vesicles in MeS buffer was higher (111.6 $\pm$ 4.8%; p = 0.003) compared to controls (n = 10). The V_{max} value was 76.1 $\pm$ 6.7% in KBr buffer (n = 8) and 47.1 $\pm$ 4.8% in KI buffer (n = 10). The reduced V_{max} values in KBr and KI were statistically significantly different with p-values of 1.0×10^{-7} and $< 1 \times 10^{-10}$, respectively. * indicates statistical significance at $p \leq 0.01$.

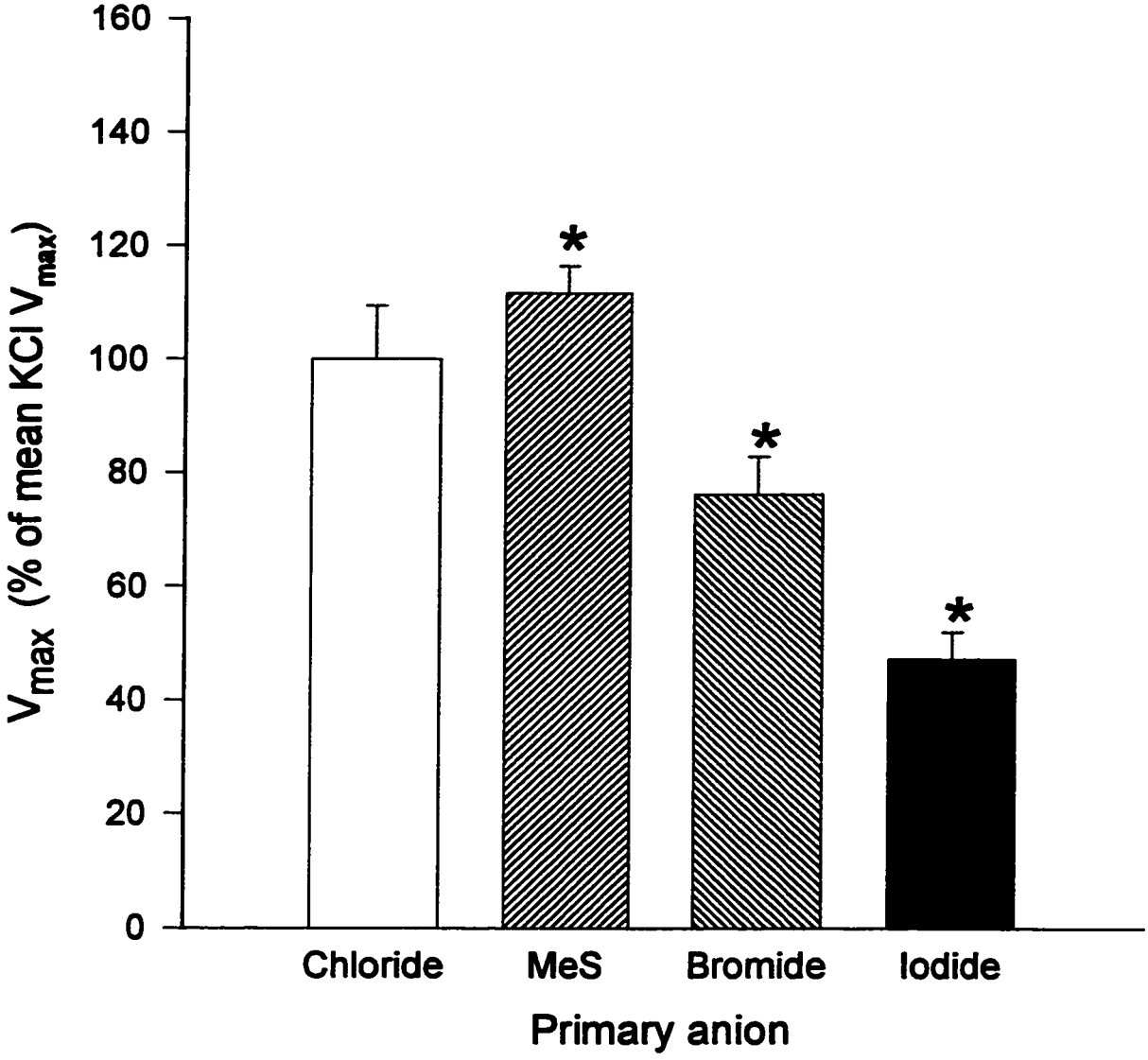
160
140
120
100
80
60
40
20
0
V_{max} (% of mean KCl V_{max})
*
*
*
Chloride
MeS
Bromide
Iodide
Primary anion

Figure 33. $Ca_{50\%}$ values from cardiac SR vesicles in four buffers with different primary anions. This figure shows how the Ca^{2+} sensitivity of the pump changes in the presence of different anions. Buffers comprised of MeS or Cl^- had similar Ca^{2+} sensitivities. $Ca_{50\%}$ in Br^- was significantly different than that in KCl ($p = 2.9 \times 10^{-4}$), The Ca^{2+} sensitivity in I^- buffer was also significantly different from the control ($p = 5.1 \times 10^{-9}$). * indicates statistical significance at $p = \leq 0.01$.

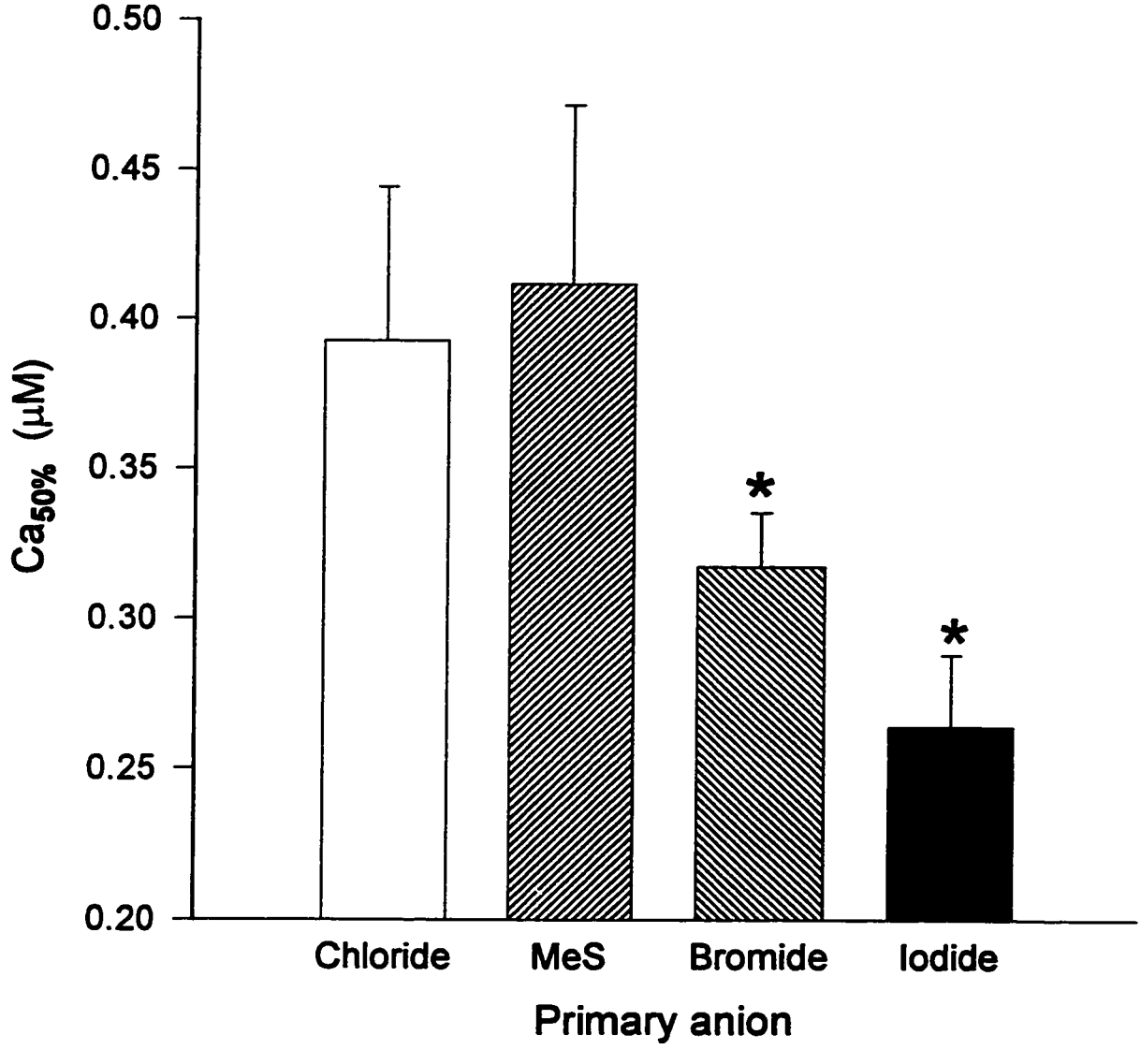
0.50
0.45
0.40
0.35
0.30
0.25
0.20
Ca50% (μM)
*
*
Chloride
MeS
Bromide
Iodide
Primary anion

Figure 34. Hill coefficient for cardiac SR uptake in four buffers with different anionic composition. The Hill coefficient indicates the cooperativity of the Ca^{2+} pump, and normally is close to 2.0. This figure shows that the Hill coefficients obtained from cardiac vesicles in KMeS ($p = 0.004$), KBr ($p = 1.47 \times 10^{-5}$) and KI ($p = 2.29 \times 10^{-5}$) are significantly greater than the control in KCl buffer. Statistical significance is indicated with an asterisk.

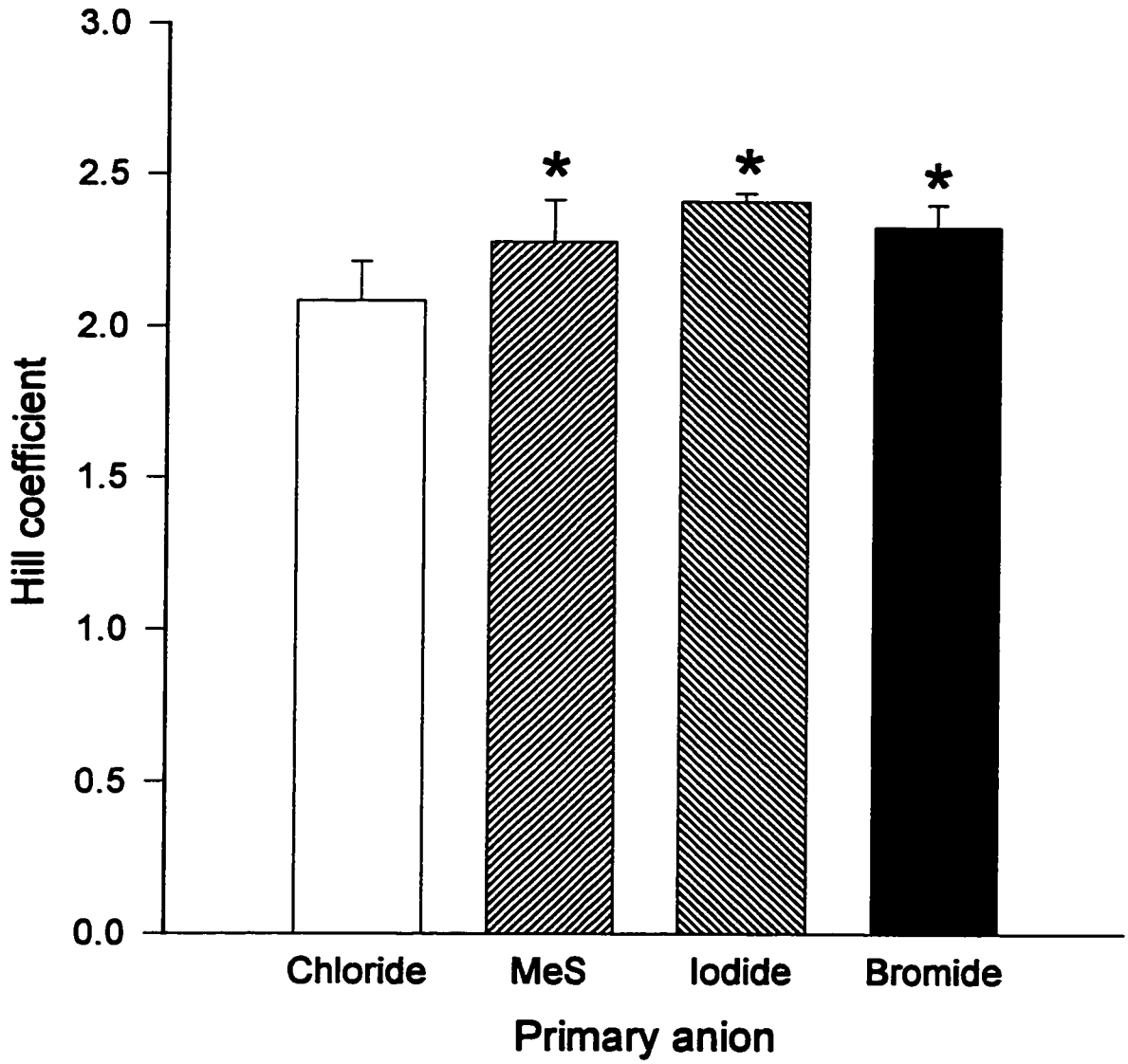
3.0
2.5
2.0
1.5
1.0
0.5
0.0
Hill coefficient
*
*
*
Chloride
MeS
Iodide
Bromide
Primary anion

uptake rates were found to be similar or slightly greater in the presence of MeS but somewhat slower when Br^- was substituted for Cl^-. I^- slowed down the rate of uptake considerably. Ca^{2+} uptake experiments in cardiac vesicles with oxalate were not performed with SO_4^{2-}.

The addition of oxalate to the uptake buffers also allows the kinetics (V_{max}, $Ca_{50\%}$, and Hill coefficient) of Ca^{2+} uptake to be determined. The kinetic parameters were determined as described in *Methods*. Figure 32 shows that the V_{max} was reduced in the presence of Br^- and I^-. The calculated V_{max} was greater in MeS than Cl^- ($p = 0.003$). V_{max} was significantly lower in KBr (76.1 $\pm$ 6.7% of control, significant at $p = 1.7 \times 10^{-7}$) and KI (47.1 $\pm$ 4.8% of control significant at $p = < 1 \times 10^{-10}$). $Ca_{50\%}$ (Figure 33) also appears to change in a pattern that mimicks the effect of anion substitution on V_{max}. MeS and Cl^- buffers had the highest $Ca_{50\%}$ values which were not significantly different from one another ($p = 0.340$), whereas Br^- ($p = 2.9 \times 10^{-4}$) and I^- ($p = 5.1 \times 10^{-9}$) had significantly lower Ca^{2+} sensitivities. The Hill coefficient was significantly higher (Figure 34) in MeS ($p = 0.004$), KI ($p = 2.29 \times 10^{-5}$) and KBr (1.47×10^{-5}).

DISCUSSION

Cl^- channel blockers

In isolated smooth muscle cells, low concentrations of either NPPB (17 μM) or (R)-IAA-94 (17 M) were found to inhibit Ca^{2+} uptake across the SR. These inhibitors were chosen because of their potency and their specificity for Cl^- channels at low concentrations. Three examples of less potent Cl^- channel blockers are described by Sorota (1994). DIDS (100 μM) and dinitrostilbene disulfonic acid (DNDS; 5 mM) only partially inhibited the swelling-induced Cl^- current in dog atrial myocytes. Anthracene-9-carboxylic acid (ACA) blocked the swelling-induced Cl^- current by 50% at a concentration of 1 mM (Sorota, 1994).

Since smooth muscle SR Cl^- channels have received relatively little experimental attention, no prior information was available to assess the action of NPPB or (R)-IAA-94 on SR Ca^{2+} uptake. However, these agents have been used in the study of other (primarily plasma membrane) Cl^- channels. Only Townsend and Rosenberg (1996) had previously used NPPB (0-50 μM) as a blocker of SR Cl^- channels of porcine cardiac myocytes. By applying NPPB to both the cytoplasmic and lumenal side of the SR membrane, they found that NPPB blocked the Cl^- channels only from the lumenal side of the membrane. They described a dose-dependent effect of this inhibitor and determined that lumenal NPPB decreased channel open probability with a K_i of 52.6 μM (Townsend and Rosenberg, 1996). Gekle et al. (1993) report an inhibitory concentration (IC_{50}) of plasma membrane anion conductance of 600 (+/- 50) nmol/l for NPPB in

Madin-Darby canine kidney cells in culture.

(R)-IAA-94 blocked plasma membrane Cl^- channels of kidney (Landry et al., 1989; Redhead et al., 1992), trachea (Landry et al., 1989), afferent arteriole (Takenaka et al., 1996) and canine atrial myocytes (Sorota, 1994). In these experiments, (R)-IAA-94 proved to be a highly specific and potent plasma membrane Cl^- channel blocker. Reeves et al. (1992) showed that (R)-IAA-94 reduced the open probability of a 116 pS endosomal Cl^- channel from rabbit kidney cortex with a K_i of 15 μM and Landry et al. (1989) reported a K_i for bovine kidney cortex microsomes of 1 μM. In fact, (R)-IAA-94 has been used to purify Cl^- channels from kidney (Redhead et al., 1992; Landry et al., 1989) and tracheal membranes (Landry et al., 1989). Interestingly, Weber-Schurholz et al. (1993) found that (R)-IAA-94-sensitive channels were present in the sarcolemmal fraction but were *not* present in the SR membranes of rabbit skeletal muscle. But Redhead et al. (1992), who purified a 64 kDa protein using (R)-IAA-94 as a high affinity ligand, concluded that the purified voltage-sensitive Cl^- channel from epithelial cells was a component of both the plasma membrane and intracellular membranes. This was determined by labelling kidney cortex membranes with both Na^+,K^+-ATPase and Golgi markers.

NPPB inhibited SR Ca^{2+} uptake by permeabilized smooth muscle cells with a concentration of 17 μM (Figure 12). NPPB likely exerted its effects on the cytoplasmic side of the SR membrane since in this preparation the sarcolemma, but not the SR, is permeabilized. It is improbable that either of the blockers are entering the SR through a channel and acting on the lumenal side of the Cl^- channels. However, Branchini et al.

(1995) explained the diverse cellular effects of NPPB based on its putative interaction with both membrane lipids and Cl^- channels. An *in vivo* study by Fryklund et al. (1993) provides evidence for an interaction of NPPB with plasma proteins. They found that the NPPB dose-response curve in the colonic cell line T84 was shifted to the right with increasing amounts of albumin added to the mucosal medium. Frylund et al. (1993) report an IC_{50} of 100 μM for NPPB in T84 cells.

Our results demonstrate an inhibitory effect of (R)-IAA-94 on SR Ca^{2+} uptake in smooth muscle cells. The fact that this inhibition was seen at (R)-IAA-94 concentrations (1 and 17 μM) similar to those used by other investigators to block Cl^- channels makes it unlikely that it acts non-specifically on other SR channels. This is supported by the work of Takenaka et al. (1996) who used (R)-IAA-94 to determine the role of plasmalemmal Cl^- channels in afferent arteriolar constriction in rats. They were able to fully constrict the arterioles with high K^+ in the presence of (R)-IAA-94 (30 μM). This indicates that (R)-IAA-94 does not interfere with plasmalemmal K^+ channels or voltage-operated Ca^{2+} channels (VOCC), since high K^+ could depolarize the plasma membrane and evoke a contractile response by activating VOCC.

The fact that NPPB and (R)-IAA-94 both inhibit SR Ca^{2+} uptake in smooth muscle cells provides further support that the agents act on SR Cl^- channels and that Cl^- movement occurs during Ca^{2+} uptake. Sorota et al. (1994) looked at the effects of NPPB and (R)-IAA-94 on swelling-induced Cl^- current in dog atrial cells. Both Cl^- channel blockers were equally efficacious at inhibiting Cl^- current in concentrations of 10-40 μM (NPPB) and 100 μM ((R)-IAA-94).

In contrast to the results on smooth muscle SR, we found that even high (96 μM) concentrations of either NPPB or (R)-IAA-94 had no significant effect on Ca^{2+} uptake in cardiac SR vesicles. This, again, provides support for the hypothesis that NPPB and (R)-IAA-94 do not act on the SR Ca^{2+}-ATPase of smooth muscle since smooth muscle and cardiac Ca^{2+}-ATPase isoforms are similar (Lytton et al., 1992), making it less likely that only one of the isoforms was non-specifically affected by both NPPB and (R)-IAA-94.

The lack of effect of Cl^- channel blockers on Ca^{2+} uptake in cardiac vesicles could be due to a variety of differences in the SR membrane between cardiac and smooth muscle cells. It is possible that cardiac Cl^- channels lack sensitivity to the blockers which were employed in the cardiac SR experiments or that K^+ conductivity is facilitated in cardiac vesicles (ie. a greater density of K^+ channels) relative to smooth muscle.

Preliminary experiments were also performed using the Cl^- ionophore TppMnIII. This agent appeared to re-initiate SR Ca^{2+} uptake by smooth muscle cells in the presence of inhibitory concentrations of NPPB (96 μM; not shown). Although this is preliminary data, it suggests that the Ca^{2+}-ATPase can operate with the Cl^- channel inhibitor present. If this is the case, then the inhibitor is not acting to block pump activity.

It is impossible to deduce the contribution of counter-ion movement during Ca^{2+} uptake when Cl^- channel blockers are present without employing experiments that directly measure cation efflux. The above experiments with TppMnIII offer some insight into the role of K^+ channels during Ca^{2+} uptake, however. Since we have not been able to completely eliminate Ca^{2+} uptake with the use of either high concentrations of Cl^-

channel blockers, or by complete substitution for Cl^- with impermeant anions, it appears that counter-ion movement is only sufficient to sustain minimal Ca^{2+} uptake in the absense of Cl^- conductance. Reinitiation of Ca^{2+} uptake with a Cl^- ionophore seems to suggest that it is Cl^- conductance in particular which facilitates Ca^{2+} uptake into the SR. However, studies have not examined the specificity of this ionophore, so any conclusions based on these results would be premature.

At this point, it is not possible to say whether the Cl^- channel inhibitors are acting on a class of Cl^- channels that are present in the smooth muscle but not in the cardiac SR. If the NPPB- and (R)-IAA-94-sensitive Cl^- channel density is less in cardiac SR compared to smooth muscle SR, or if cations such as K^+ or H^+ predominate in charge compensation during Ca^{2+} uptake in cardiac SR, the inhibition of Cl^- movement could have had little effect on net Ca^{2+} uptake. The results of the anion substitution experiments on cardiac SR vesicles would argue against this, however.

Ion substitution

Ion permeability sequences are a commonly employed data to differentiate between channel subtypes. Our results reveal no difference in the rate of Ca^{2+} uptake with complete substitution of K-methanesulfonate, KBr or KI for KCl in the smooth muscle cells. The results were presented so that the uptake rate in the experimental buffer could be compared to the average rate of Ca^{2+} uptake in KCl buffer at different $[Ca^{2+}]_{free}$. None of the uptake rates in the presence of experimental buffers (MeS, KBr

or KI) fell significantly above or below the mean of smooth muscle cells. When calculations of Ca^{2+} uptake in KI buffer were corrected for Ca^{2+}-ATPase quantity, the uptake rates were found to be very similar to those in KCl buffer (Figure 19). This suggests that the SR Cl^- channel of rabbit stomach may operate as a non-selective anion channel which is sensitive to Cl^- channel blockers.

Differences in Ca^{2+} uptake rates were observed when cardiac SR vesicles were suspended in KI buffer. Cl^- conductance appears to play an important role as co-ion during Ca^{2+} uptake in cardiac SR. Ca^{2+} uptake rate decreased when I^- served as the sole anion. Therefore, the Cl^- channel of canine cardiac SR may have a different selectivity for anions compared to smooth muscle SR Cl^- channels. The permeability sequence that we obtained with cardiac SR vesicles was: MeS $\approx$ Cl^- $\approx$ SO_4^{2-} $\approx$ Br^- > I^-. These results do not permit any conclusion regarding the similarity to previously described channels, but the data do suggest that different Cl^- permeant pathways function in the SR of canine versus porcine cardiac SR. This view is supported by the fact that the Cl^- channel of porcine cardiac SR described by Townsend and Rosenberg (1996) was more permeable to I^- (P=1.31) than to Cl^- (P=1.00). On the other hand, I^- has been reported to block the CFTR plasmalemmal Cl^- channel in the T84 colonic cell line (Tabcharani et al., 1992).

Anion substitution experiments in the presence of oxalate were plotted as changes in 340/380 ratio (background subtracted) with time. The superposition of 340/380 control traces compared with traces in MeS, KBr or KI buffer clearly showed how these substitutions affected uptake rate. Uptake in KBr buffer was slightly slower than in KCl.

In contrast, the uptake rate in KI was significantly slower than control traces in KCl. The experiments with oxalate verified the inhibitory effect of KI on Ca^{2+} uptake rate. This effect can be attributed to reduced conductance of I^- through a Cl^- permeant pathway that functions to compensate for the charge moved into the SR by Ca^{2+} during ATP-dependent Ca^{2+} uptake. Since our initial experiments with cardiac SR vesicles (without oxalate) were duplicated in the presense of oxalate, we concluded that oxalate was not interferring with anion conductance, or providing a secondary pathway for anions to enter the SR. If oxalate had an effect on Cl^- conductance, we would not have expected the same results with and without oxalate.

The Ca^{2+} uptake kinetics that were obtained from the vesicle experiments with oxalate supported the conclusions obtained from cardiac SR without oxalate. The V_{max} in MeS buffer was slightly greater than in the control. Compared to KCl, both KBr and KI resulted in slower V_{max} values. $Ca_{50\%}$ data further supports the permeability sequences, and demonstrates a decrease in Ca^{2+} sensitivity: KMeS = KCl > KBr > KI. The interpretation of these results is made complex by the fact that we are measuring net Ca^{2+} uptake. Lastly, our calculations of the Hill coefficient suggest that it may increase in MeS, KBr and KI buffers compared to KCl buffer, which further suggests that cooperativity of Ca^{2+} binding may also increase in these buffers.

The permeability sequence of only two SR Cl^- channels has been determined to date. Tanifuji et al. (1987) examined the conductances of a Cl^- channel in rabbit skeletal muscle SR with different anions and found the channel to have a permeability sequence of: $NO_3^- > Br^- = ClO_4^- > Cl^- >> SO_4^-$. Another channel of porcine cardiac SR lipid

bilayers was reported to have a sequence of SCN > I^- > NO_3^- = Br^- > Cl^- > F^- > $HCOO^-$ (Townsend and Rosenberg, 1995). Several skeletal muscle SR Cl^- channels from rabbit are inhibited by SO_4^{2-} on the cytoplasmic side of the membrane (Tanifuji et al., 1987; Kourie et al., 1996). Another SR Cl^- channel from canine cardiac SR described by Rousseau et al. (1989) was inhibited by 15 mM SO_4^{2-} on the cytoplasmic side of the membrane. These data are consistent with the present results (Figure 28) in which cardiac SR uptake appeared to be reduced in the presence of SO_4^{2-}. Others, however, have found SO_4^{2-} to be completely ineffective in reducing SR Cl^- current of rabbit skeletal muscle SR (Kourie et al., 1996b). Comparison of these results in cardiac SR with the present observations on smooth muscle suggests that the SR channel in this tissue may be unique in its ability to conduct anions non-selectively, while being quite sensitive to NPPB and (R)-IAA-94. As more complete information about Cl^- channels becomes available, additional support for this hypothesis may be obtained.

CONCLUSION and FUTURE DIRECTIONS

In conclusion, this study has identified two different SR Cl^- conductances; one in rabbit smooth muscle SR and the other in canine cardiac SR. Although mediated by different conductances, Cl^- movement seems to be necessary for charge compensation during Ca^{2+} uptake into the SR of both tissue types. The smooth muscle SR Cl^- channel may operate as a non-specific anion channel which is sensitive to both NPPB and (R)-IAA-94. Inhibition of Cl^- channels by these compounds is followed by a concomitant decrease in Ca^{2+} uptake rate, suggesting that Cl^- and Ca^{2+} movement into the SR may

be coupled. As these blockers have been tested primarily on plasma membrane Cl^- channels in the past, it is impossible to draw parallels between reported channels and the cardiac and smooth muscle SR channels examined here. However, it is important to note that there are differences between cardiac and smooth muscle SR Cl^- channels which may relate to the different rates of SR Ca^{2+} uptake in these tissues.

In cardiac SR vesicles, Ca^{2+} uptake was inhibited in the presence of I^--substituted buffer, both with and without oxalate. Presumably, this was due to minimal conductance of I^- through an SR Cl^- channel. Canine cardiac SR Cl^- channels were found to be insensitive to NPPB and (R)-IAA-94. However, due to the effect of KI substitution on Ca^{2+} uptake rate, Cl^- flux seems to play an important role in maintaining electroneutrality in cardiac SR.

Future work on SR Cl^- channels might employ fluorescent probes such as SPQ or MQAE to directly assess Cl^- flux during Ca^{2+} uptake. There are many other documented Cl^- channel blockers which could be used as well, including ochratoxin A, tamoxifen, DIDS and SITS. Although the latter two Cl^- channel blockers are commonly used as Cl^- channel inhibitors, they were not used in this study because of their fluorescent nature. Also, TppMnIII should be thoroughly exploited as a Cl^- ionophore (El-Etri and Cuppoletti, 1996). This should confirm the specificity of present Cl^- channel blockers. The present identification of a non-selective SR Cl^- channel in smooth muscle brings into question the validity of experiments which have used MeS to eliminate Cl^- channels from electrophysiological recordings.

Investigations into the normal function of the SR are important for providing a

knowledge base for the study of dysfunctional states. Two diseases which are being currently investigated as putative Cl^- channel mutations are cystic fibrosis and myotonia. The methodology employed in this study approximates physiological conditions and can be used to assess the effect of reduced Cl^- conductance on Ca^{2+} uptake in the SR. A change in conductance could occur in disease states in cardiac or smooth muscle and result in a reduced Ca^{2+} handling ability of these cells.

REFERENCES

Baksh, S., and M. Michalak. Expression of calreticulin in *Escherichia coli* and identification of its Ca^{2+} binding domains. *J. Biol. Chem.* **266**:21458-21465, 1991.

Berridge, M.J. Inositol trisphosphate and calcium signalling. *Nature* **361**:315-324, 1993.

Brown, A. Movements of molecules and ions across cell membranes *In* Medical Physiology. D.W. Stubbs, editor. John Wiley and Sons, Inc., USA. 2-25, 1983.

Burk, S.E., J. Lytton, D.H. MacLennan, and G.E. Shull. cDNA cloning, functional expression, and mRNA tissue distribution of a third organellar Ca^{2+} pump. *J. Biol. Chem.* **264**:18561-18568, 1989.

Cala, S.E., and L.R. Jones. Rapid purification of calsequestrin from cardiac and skeletal muscle sarcoplasmic reticulum vesicles by Ca^{2+}-dependent elution from phenyl-sepharose. *J. Biol. Chem.* **258**:11932-11936, 1983.

Campbell, A.M., P.D. Kessler, and D. M. Fambrough. The alternative carboxyl termini of avian cardiac and brain sarcoplasmic reticulum/endoplasmic reticulum Ca^{2+}-ATPases are on opposite sides of the membrane. *J. Biol. Chem.* **267**:9321-9325, 1992.

Carafoli, E. The Ca^{2+} pump of the plasma membrane. *J. Biol. Chem.* **267**:2115-2118, 1992.

Chamberlain, B.K., D.O. Levitsky, and S. Fleischer. Isolation and characterization of canine cardiac sarcoplasmic reticulum with improved Ca^{2+} transport properties. *J. Biol. Chem.* **258**:6602-6609, 1983.

Chen, Q., and C. van Breeman. Function of smooth muscle sarcoplasmic reticulum *In* Advances in Second Messenger and Phosphoprotein Research. J.W. Putney, editor. Raven Press, Ltd., NY, USA 335-350, 1992.

Chen, W., C. Steenbergen, L.A. Levy, J. Vance, R.E. London, and E. Murphy. Measurement of free Ca^{2+} in sarcoplasmic reticulum in perfused rabbit heart loaded with 1,2-bis(2-amino-5,6-difluorophenoxy)ethane-N,N,N',N'-tetraaceticacid by ^{19}F NMR. *J. Biol. Chem.* **271**:7398-7403, 1996.

Cole, W.C., and R.E. Garfield. Ultrastructure of the myometrium *In* Biology of the Uterus second edition). R.M. Wynn and W.P. Jollie, editors. Plenum Publishing Co. NY, USA 455-504, 1989.

Colyer J., and J.H. Wang. Dependence of cardiac sarcoplasmic reticulum calcium pump activity on the phosphorylation status of phospholamban. *J. Biol. Chem.* **266**:17386-

17493, 1991.

Decrouy, A., M. Juteau, S. Proteau, J. Teijiera, and E. Rousseau. Biochemical regulation of sarcoplasmic reticulum Cl^- channel from human atrial myocytes: involvement of phospholamban. *J. Mol. Cell. Cardiol.* **28**:767-780, 1996.

Decrouy, A., M. Juteau, and E. Rousseau. Examination of the role of phosphorylation and phospholamban in the regulation of the cardiac sarcoplasmic reticulum Cl^- channel. *J. Membrane Biol.* **146**:315-326, 1995.

Eggermont, J.A., F. Wuytack, and R. Casteels. Characterization of the mRNAs encoding the gene 2 sarcoplasmic/endoplasmic-reticulum Ca^{2+} pump in pig smooth muscle. *Biochem. J.* **266**:901-907, 1990.

Eggermont, J.A., F. Wuytack, J. Verbist and R. Casteels. Expression of endoplasmic-reticulum Ca^{2+}-pump isoforms and of phospholamban in pig smooth-muscle tissue. *Biochem. J.* **271**:649-653, 1990.

Ehrlich, B.E., and J.Watras. Inositol 1,4,5-trisphosphate activates a channel from smooth muscle sarcoplasmic reticulum. *Nature* **336**:583-586, 1988.

El-Etri, M., and J. Cuppoletti. Metalloporphyrin chloride ionophores: induction of

increased anion permeability in lung epithelial cells. *Am. J. Physiol.* **270**:L386-92, 1996.

Everitt, B.S. The Cambridge dictionary of statistics in the medical sciences, Cambridge University Press, N.Y. USA; 1995.

Feher, J.J., and A. Fabiato. Cardiac sarcoplasmic reticulum: calcium uptake and release *In Calcium and the Heart.* Glenn A. Langer, editor. Raven Press, Ltd., NY, USA 199-269, 1990.

Fink, R.H.A., and D.G. Stephenson. Ca^{2+}-movements in muscle modulated by the state of K^{+}-channels in the sarcoplasmic reticulum membranes. *Pflugers Arch.* **409**:374-380, 1987.

Gabella, G. Structure of smooth muscles *In* Smooth Muscle: an Assessment of Current

Garcia, A.M. and C. Miller. Channel-mediated monovalent cation fluxes in isolated sarcoplasmic reticulum vesicles. *J. Gen. Physiol.* **83**:819-839, 1984.

Grynkiewicz, G., M. Poenie, and R.Y. Tsien. A new generation of Ca^{2+} indicators with greatly improved fluorescence properties. *J. Biol. Chem.* **260**:3440-3450, 1985.

Gunteski-Hamblin, A-M., J. Greeb, and G.E. Shull. A novel Ca^{2+} pump expressed in brain, kidney, and stomach is encoded by an alternative transcript of the slow-twitch

muscle sarcoplasmic reticulum Ca-ATPase gene. *J. Biol. Chem.* **263**:15023-15040, 1988.

Hals, G.D., P.G. Stein and P.T. Palade. Single channel characteristics of a high conductance anion channel in "sarcoballs". *J. Gen. Physiol.* **93**:385-410, 1989.

Haynes, D.H. Relationship between H^+, anion, and monovalent cation movements and Ca^{2+} transport in sarcoplasmic reticulum: further proof of a cation exchange mechanism for the Ca^{2+}-Mg^{2+}-ATPase pump. *Arch. Biochem. Biophys.* **215**:444-461, 1982.

Herrmann-Frank, A., E. Darling, and G. Meissner. Functional characterization of the Ca^{2+}-gated Ca^{2+} release channel of vascular smooth muscle sarcoplasmic reticulum. *Pflugers Arch.* **418**:353-359, 1991.

Higashihara, M., Young Frado, L.L., Craig, R., and M. Ikebe. Inhibition of conformational changes in smooth muscle myosin by a monoclonal antibody against the 17-kDa light chain. *J. Biol. Chem.* **264**:5218-5225, 1989

Holmberg S.R.M., and A.J. Williams. Single channel recordings from human cardiac sarcoplasmic reticulum. *Circ. Res.* **65**:1445-1449, 1989.

Hove-Madsen, L., and D. M. Bers. Sarcoplasmic reticulum Ca^{2+} uptake and thapsigargin sensitivity in permeabilized rabbit and rat ventricular myocytes. *Circ. Res.* **73**:820-828,

1993.

Ide, T., H. Sakamoto, T. Morita, T. Taguchi, and M. Kasai. Purification of a Cl^- channel protein of sarcoplasmic reticulum by assaying the channel activity in the planar lipid bilayer system. *Biochem. Biophys. Res. Comm.* **176**:38-44, 1991.

Ikemoto, N., M. Ronjat, L.G. Meszaros, and M. Koshita. Postulated role of calsequestrin in the regulation of calcium release from sarcoplasmic reticulum. *Biochemistry* **28**:6764-6771, 1989.

Ikemoto, N., M. Yano, R. El-Hayek, B. Antoniu, and M. Morii. Chemical depolarization-induced SR calcium release in triads isolated from rabbit skeletal muscle. *Biochemistry* **33**:10961-10968, 1994.

Inesi, G., and L. de Meis. Regulation of steady state filling in sarcoplasmic reticulum. *J. Biol. Chem.* **264**:5929-5936, 1989.

James, P., M. Inui, M. Tada, M. Chiesi, and E. Carafoli. Nature and site of phospholamban regulation of the Ca^{2+} pump of sarcoplasmic reticulum. *Nature* **342**:90-92, 1989.

Jentsch, T.J., and W. Gunter. Chloride channels: an emerging molecular picture.

Bioessays **19**:117-126, 1997.

Jorgensen, A.O., and L.R. Jones. Localization of phospholamban in slow but not fast canine skeletal muscle fibres. *J. Biol. Chem.* **261**:3775-3781, 1986.

Kargacin, G.J., and F.S. Fay. Physiological and structural properties of saponin-skinned single smooth muscle cells. *J. Gen. Physiol.* **90**:49-73, 1987.

Kargacin, M.E., and G.J. Kargacin. Direct measurement of Ca^{2+} uptake and release by the sarcoplasmic reticulum of saponin permeabilized isolated smooth muscle cells. *J. Gen. Physiol.* **106**:1-18, 1995.

Kasai, M., and T. Kometani. Ionic permeability of sarcoplasmic reticulum membrane *In* Cation Flux Across Biomembranes. Academic Press, NY, USA; pp.166-177, 1979.

Kawano, S., and M. Hiraoka. Protein kinase A-activated chloride channel is inhibited by the Ca^{2+}-calmodulin complex in cardiac sarcoplasmic reticulum. *Circ. Res.* **73**:751-757, 1993.

Kawano, S., F. Nakamura, T. Tanaka, and M. Hiraoka. Cardiac sarcoplasmic reticulum chloride channels regulated by protein kinase A. *Circ. Res.* **71**:585-589, 1992.

Khan, I., and A.K. Grover. Abundance of heteronuclear and messenger RNA for internal Ca pump in stomach smooth muscle and myocardium. *Cell Calcium* **14**:17-23, 1993.

Khan, I., G.G. Spencer, S.E. Samson, P. Crine, G. Boileau, and A.K. Grover. Abundance of sarcoplasmic reticulum calcium pump isoforms in stomach and cardiac muscles. *Biochem. J.* **268**:415-419, 1990.

Knowledge. E. Bulbring, A. F. Brading, A.W. Jones, and T. Tomita, editors. University of Texas Press, Austin, TX.; 1-46, 1983.

Kourie, J.I., D.R. Laver, G.P. Ahern, and A.F. Dulhunty. A calcium-activated chloride channel in sarcoplasmic reticulum vesicles from rabbit skeletal muscle. *Am. J. Physiol.* **270**:C1675-C1686, 1996a.

Kourie, J.I., D.R. Laver, P.R. Junankar, P.W. Gage, and A.F. Dulhunty. Characteristics of two types of chloride channel in sarcoplasmic reticulum from rabbit skeletal muscle. *Biophys. J.* **70**:202-221, 1996b.

Kowarski, D., H. Shuman, A.P. Somlyo and A.V. Somlyo. Calcium release by noradrenaline from central sarcoplasmic reticulum in rabbit main pulmonary artery smooth muscle. *J. Physiol.* **366**:153-175, 1985.

Kremer, S.G., W. Zeng, R. Hurst, T. Ning, C. Whiteside, and K.L. Skorecki. Chloride is required for receptor-mediated divalent cation entry in mesangial cells. *J. Cell. Physiol.* **162**:15-25, 1995.

Laemmli, U.K. Cleavage of structural proteins during the assembly of the head of bacteriophage T4. *Nature* **227**:680-685, 1970.

Landry, D., M.H. Akabas, C. Redhead, A. Edelman, E.J. Cragoe, Jr., and Q. Al-Awqati. Purification and reconstitution of chloride channels from kidney and trachea. *Science* **244**:1469-1472, 1989.

Landry, D., S. Sullivan, M. Nicolaides, C. Redhead, A. Edelman, M. Field, Q. Al-Awqati, and J. Edwards. Molecular cloning and characterization of p64; a Cl^- channel protein from kidney microsomes. *J. Biol. Chem.* **268**:14948-14955, 1993.

Levy, D., M. Seigneuret, A. Bluzat, and J-L. Rigaud. Evidence for proton countertransport by the sarcoplasmic reticulum Ca^{2+}-ATPase during calcium transport in reconstituted proteoliposomes with low ionic permeability. *J. Biol. Chem.* **265**:19524-19534, 1990.

Lewis, T.M., M.L. Roberts, and A.H. Bretag. Immunolabelling for VDAC, the mitochondrial voltage-dependent anion channel, on sarcoplasmic reticulum from

amphibian skeletal muscle. *Neurosci. Lett.* **181**:83-86, 1994.

Lukacs, G.L., A. Nanda, O.D. Rotstein, and S. Grinstein. The chloride channel blocker 5-nitro-2-(3-phenylpropyl-amino) benzoic acid (NPPB) uncouples mitochondria and increases the proton permeability of the plasma membrane in phagocytic cells. *FEBS Lett.* **288**:17-20, 1991.

Lytton, J., and D.H. MacLennan. Molecular cloning of cDNAs from human kidney coding for two alternatively spliced products of the cardiac Ca^{2+}-ATPase gene. *J. Biol. Chem.* **263**:15024-15031, 1988.

Lytton, J., M. Westlin, S.E. Burk, G.E. Shull, and D.H. MacLennan. Functional comparisons between isoforms of the sarcoplasmic or endoplasmic reticulum family of calcium pumps. *J. Biol. Chem.* **267**:14483-14489, 1992.

Lytton, J., M. Westlin, and M.R. Levy. Thapsigargin inhibits the sarcoplasmic or endoplasmic reticulum Ca-ATPase family of calcium pumps. *J. Biol. Chem.* **266**:17067-17071, 1991.

McKinley, D., and G. Meissner. Evidence for a K^+,Na^+ permeable channel in sarcoplasmic reticulum. *J. Membrane Biol.* **44**:159-186, 1978.

Meissner, G., and R. Allen. Evidence for two types of rat liver microsomes with differing permeability to glucose and other small molecules. *J. Biol. Chem.* **266**:6413-6422, 1981.

Meissner, R., and D. McKinley. Permeability of canine cardiac sarcoplasmic reticulum vesicles to K^+, Na^+, H^+, and Cl^-. *J. Biol.Chem.* **257**:7704-7711, 1982.

Michalak, M., R.E. Milner, K. Burns, and M. Opas. Calreticulin. *Biochem. J.* **285**:681-692, 1992.

Milner, R.E., S. Baksh, C. Shemanko, M.R. Carpenter, L. Smillie, J.E. Vance, M. Opas, and M. Michalak. Calreticulin, and not calsequestrin is the major calcium binding protein of smooth muscle sarcoplasmic reticulum and liver endoplasmic reticulum. *J. Biol. Chem.* **266**:7155-7165, 1991.

Missiaen, L., H. De Smedt, G. Droogmans, B. Himpens and R. Casteels. Calcium ion homeostasis in smooth muscle. *Pharmac. Ther.* **56**:191-231, 1992.

Moore, E.W., and D. Gleeson. Pathogenesis of calcium-containing gallstones: the Gibbs-Donnan equilibrium is a potentially important factor governing ionized and total calcium in canalicular and whole bile. *Hepatology* **5**:993, 1985.

Moore, E.D.W., E.F. Etter, K.D. Philipson, W.A. Carrington, K.E. Fogarty, L.M. Lifshitz, and F.S. Fay. Coupling of the Na^+/K^+ pump and sarcoplasmic reticulum in smooth muscle. *Nature* **365**:657-660, 1993.

Morimoto T., and M. Kasai. Reconstitution of sarcoplasmic reticulum Ca^{2+}-ATPase vesicles lacking ion channels and demonstration of electrogenicity of Ca^{2+} -pump. *J. Biol. Chem.* **99**:1071-1080, 1986.

Morris, G.L., H-C. Cheng, J. Colyer, and J.H. Wang. Phospholamban regulation of cardiac sarcoplasmic reticulum (Ca^{2+}-Mg^{2+})-ATPase. *J. Biol. Chem.* **266**:11270-11275, 1991.

Moutin, M-J., and Y. Dupont. Rapid filtration studies of Ca^{2+}-induced Ca^{2+} release from skeletal sarcoplasmic reticulum. *J. Biol. Chem.* **263**:4228-4235, 1988.

Patel, J.R., M. Sukhareva, R. Coronado, and R. Moss. Chloride-induced Ca^{2+} release from the sarcoplasmic reticulum of chemically skinned rabbit psoas fibre and isolated vesicles of terminal cisternae. *J. Membrane. Biol.* **154**:81-89, 1996.

Pusch, M., K. Steinmeyer, M.C. Koch, and T.J. Jentsch. Mutations in dominant myotonia congenita drastically alter the voltage-dependence of the CLC-1 chloride channel. *Neuron* **15**: 1455-1463, 1995.

Raemaekers, L., and L.R. Jones. Evidence for the presence of phospholamban in the endoplasmic reticulum of smooth muscle. *Biochim. Biophys. Acta* **882**:258-265, 1986.

Raemaekers, L., and F. Wuytack. Calcium pumps *In* Biochemistry of Smooth Muscle Contraction. M. Barany, editor. Academic Press, Inc., 1996.

Ran, S., C. Fuller, M.P. Arrate, R. Latorre, and D.J. Benos. Functional reconstitution of a Cl^- channel protein from bovine trachea. *J. Biol. Chem.* **267**:20630-20637, 1992.

Redhead, C.R., A.E. Edelman, D. Brown, D.W. Landry, and Q. Al-Awqati. A ubiquitous 64-kDa protein is a component of a chloride channel of plasma and intracellular membranes. *Proc. Natl. Acad. Sci.* **89**:3716-3720, 1992.

Reeves, W.B., and R.W. Gurich. Calcium-dependent chloride channels in endosomes from rabbit kidney cortex. *Am. J. Physiol.* **266**:C741-C750, 1994.

Rousseau, E. Single chloride-selective channel from cardiac sarcoplasmic reticulum studied in planar lipid bilayers. *J. Membrane Biol.* **110**:39-47, 1989.

Seeman, P., D. Cheng, and G.H. Iles. Structure of membrane holes in osmotic and saponin hemolysis. *J. Cell Biol.* **56**:519-527, 1973.

Shoshan-Barmatz, V., N. Hadad, W. Feng, I. Shafir, I. Orr, M. Varsanyi, and L.M.G. Heilmeyer. VDAC/porin is present in sarcoplasmic reticulum from skeletal muscle. *FEBS Lett.* **386**:205-210, 1996.

Simmerman, H.K., J.H. Collins, J.L. Theiber, A.D. Wegener, and L.R. Jones. Sequence analysis of phospholamban. *J. Biol. Chem.* **261**:13333-13341, 1986.

Soler, F., P. Sanchez-Migallon, J.C. Gomez-Fernandez, and F. Fernandez-Belda. Interdependence of H^+ and K^+ fluxes during the Ca^{2+}-pumping activity of sarcoplasmic reticulum vesicles. *J. Bioenerg. Biomem.* **26**:127-136, 1994.

Somlyo, A.V., and C.F. Franzini-Armstrong. New views of smooth muscle structure using freezing, deep-etching and rotary shadowing. *Experientia* **41**:841-856, 1985.

Somlyo, A.P., and B. Himpens. Cell calcium and its regulation in smooth muscle. *FASEB J.* **3**:2266-2276, 1989.

Somlyo, A.P., and A.V. Somlyo. Signal transduction and regulation in smooth muscle. *Nature* **372**:231-236, 1994.

Somlyo, A.P., A.V. Somlyo, H. Shuman, and M. Endo. Calcium and monovalent ion in smooth muscle. *FASEB J.* **41**:2883-2890, 1982.

Sorota, S. Pharmacologic properties of the swelling-induced chloride current of dog atrial myocytes. *J. Cardiovasc. Electrophysiol.* **5**:1006-1016, 1994.

Sturek, M., K. Kunda, and Q. Hu. Sarcoplasmic reticulum buffering of myoplasmic calcium in bovine coronary artery smooth muscle. *J. Physiol.* **451**:25-48, 1992.

Sukhareva, M., J. Morrissette, and R. Coronado. Mechanism of chloride-dependent release of Ca^{2+} in the sarcoplasmic reticulum of rabbit skeletal muscle. *Biophys. J.* **67**:751-765, 1994.

Tada, M., M. Yamada, F. Ohmori, T. Kuzuya, M. Inui, and H. Abe. Transient state kinetic studies of Ca^{2+}-dependent ATPase and calcium transport by cardiac sarcoplasmic reticulum. *J. Biol. Chem.* **255**:1985-1992,1980.

Takenaka, T., Y. Kanno, Y. Kitamura, K. Hayashi, H. Suzuki, and T. Saruta. Role of chloride channels in afferent arteriolar constriction. *Kidney International* **50**:864-872, 1996.

Tanifuji, M., M. Sokabe and M. Kasai. An anion channel of sarcoplasmic reiculum incorporated into planar lipid bilayers: Single-channel behaviour and conductance properties. *J. Membrane Biol.* **99**:103-111, 1987.

Tharin, S., E. Dziak, M. Michalak, and M. Opas. Widespread tissue distribution of rabbit calreticulin, a non-muscle functional analogue of calsequestrin. *Cell Tissue Res.* **269**:29-37, 1992.

Townsend, C., and R.L. Rosenberg. Characterization of a chloride channel reconstituted from cardiac sarcoplasmic reticulum. *J. Membrane Biol.* **147**:121-136, 1995.

Verboomen, H., F. Wuytack, H. De Smedt, B. Himpens, and R. Casteels. Functional difference between SERCA2a and SERCA2b Ca^{2+} pumps and their modulation by phospholamban. *Biochem. J.* **286**:591-596, 1992.

Verboomen, H., F. Wuytack, L. van den Bosch, L. Mertens and R. Casteels. The functional importance of the extreme C-terminal tail in the gene 2 organellar Ca^{2+}-transport ATPase (SERCA2a/b). *Biochem. J.* **303**:979-984, 1994.

Weber-Schurholz, S., E. Wischmeyer, M. Laurien, H. Jockusch, T. Schurholz, D.W. Landry, and Q. Al-Awqati. Indanyloxyacetic acid-sensitive chloride channels from outer membranes of skeletal muscle. *J. Biol. Chem.* **268**:547-551, 1993.

Wuytack, F., L. Raemaekers, J. Verbist, L.R. Jones, and R. Casteels. Smooth-muscle endoplasmic reticulum contains a cardiac-like form of calsequestrin. *Biochim. Biophys. Acta* **899**:151-158, 1987.

Yu, X., S. Carroll, J-L. Rigaud, and G. Inesi. H^+ countertransport and electrogenicity of the sarcoplasmic reticulum Ca^{2+} pump in reconstituted proteoliposomes. *Biophys. J.* **64**:1232-1242, 1993.

Zimniak, P., and E. Racker. Electrogenicity of Ca^{2+} transport catalyzed by the Ca^{2+}-ATPase from sarcoplasmic reticulum. *J. Biol. Chem.* **253**:4631-4637, 1978.

SPEED BUMP By Dave Coverly

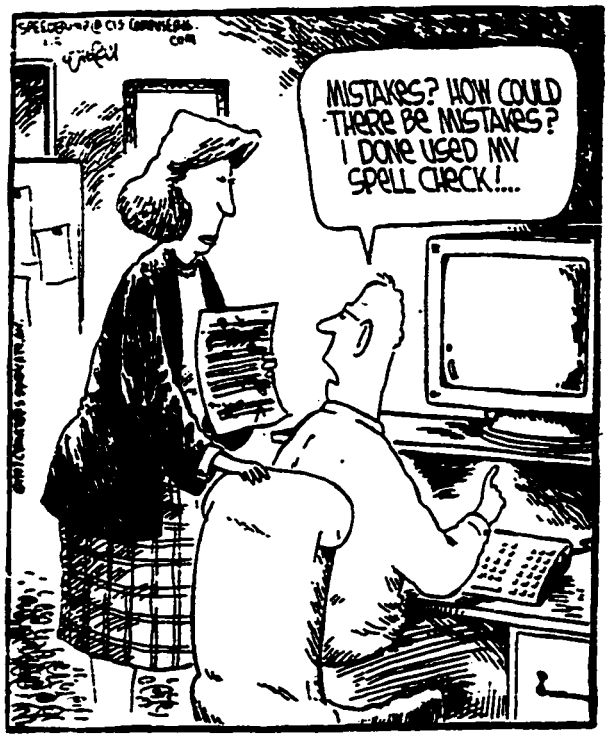

TEST TARGET (QA-3)

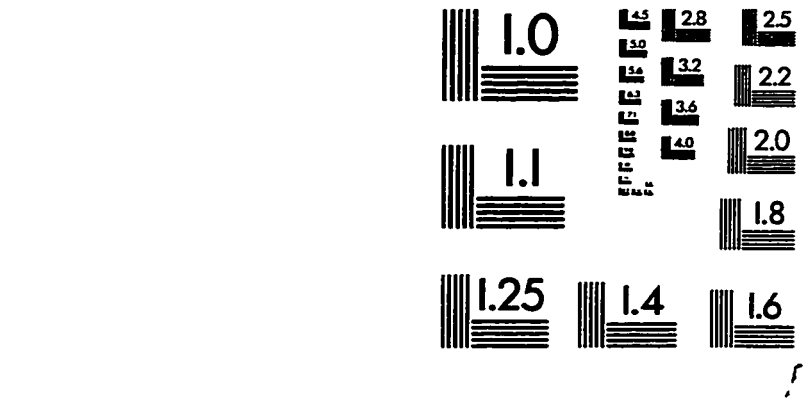

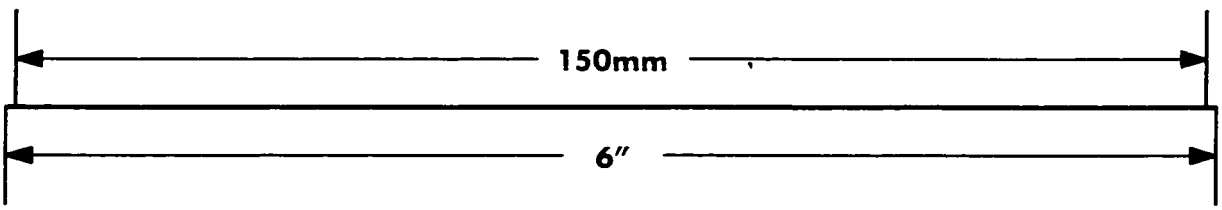

APPLIED IMAGE, Inc
1653 East Main Street
Rochester, NY 14609 USA
Phone: 716/482-0300
Fax: 716/288-5989